The reviewers' insightful comments are highly appreciated. Below we have listed the referees' comments in black and our response in blue.

We have made the following major revisions in the revised manuscript:

1. More descriptions of aerosol properties simulated in the model are added in the revised manuscript.
2. Two aerosol precursors (NO_2 and SO_2) observed by EPA are included to diagnose model biases in NO_3 and SO_4, respectively.
3. Analyses of meteorological variables, including temperature, relative humidity, wind speed and precipitation, are included.
4. Analysis of Ångström exponent is included to diagnose the model simulated aerosol particle size.
5. More quantitative information, including correlation and bias, is included in the discussion.
6. We have performed some sensitivity experiments to provide more in-depth analyses on model results, including changing the anthropogenic emission source (20km_NEI11), the chemical boundary conditions (20km_BC1) and the PBL scheme (20km_P7).
7. A bug in calculating equivalent potential temperature is fixed in the revised manuscript. The unit of relative humidity was wrong in previous version. The updated profiles of equivalent potential temperature do not change the conclusions of this study.
8. The OC (organic carbon) from observations are converted to OM (organic matter), which is simulated in the model, by multiplying by 1.4 to account for hydrogen, oxygen, etc.

Anonymous Referee #1

This paper examines the performance of a regional-scale chemical transport model in representing aerosol properties in the San Joaquin Valley over a one year period. The model is compared with surface measurements of composition and AOD as well as satellite measurements. The motivation for the paper is sufficient (although could be improved), but the main weakness is their approach and interpretation of the simulations. In addition, the paper is poorly written.

Major Comments:

The most important problem the manuscript has is how the model was configured to address the purpose of the study. WRF-Chem is a useful tool, but as with all models can only perform well when it is configured properly.

The following is a discussion of items the authors should consider to revise and/or address.

Domain and Dust Emissions: It is clear that the model domain is larger than the one shown in Figure 1. But it is hard for me to assess the importance of dust emissions since those are not shown. For local sources, dust is likely generated in the desert areas to the southwest of the SJV. It would be useful to show the emission regions from GOCART and DUSTRAN. My understanding is that the emission regions in DUSTRAN as implemented in WRF-Chem are rather ad hoc. They may depend on vegetation type. I suspect that dust is being generated locally in the SJV in DUSTRAN but not in GOCART.

Thanks for the suggestion. Dust emissions are included in Figure 7 in the revised manuscript (also in the following Figure 1). As the reviewer hinted, dust is being generated locally in the SJV in DUSTRAN but not in GOCART. Discussions about the differences between DUSTRAN and GOCART are included in the last two paragraphs of section 3 in the revised manuscript.

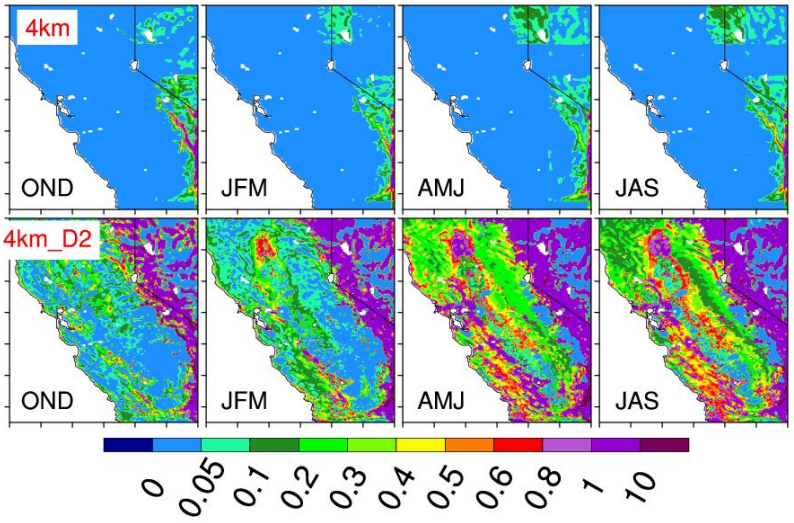

Figure 1. Seasonal mean of dust emission rate (μg m^{-2} s^{-1}) for (upper panel) GOCART; (lower panel) DUSTRAN.

The authors mention how many grid nodes are used in the vertical direction, but should give an idea of the vertical resolution near the surface that will affect dust emissions.

The vertical resolution from surface to 1 km gradually increases from 28 m to 250 m. It is clarified in Line 204 of the revised manuscript.

Dust emissions will depend in part on wind speed, and representing wind speed in California depends a lot on circulations affected by terrain. Both a fine horizontal and vertical resolution is needed to represent those winds that will affect dust emissions. It is not clear how well the model performed in winds – particularly over the dust emission regions. While some evaluation of the thermodynamic structure is given, there is nothing for the winds.
The evaluation of wind speed comparing to surface observations from CIMIS (California Irrigation Management Information System) is included in Figure 2b of the revised manuscript. The model simulations underestimate wind speed in the cold season. In the warm season, the 20km run underestimates wind speed except June while the 4km run overestimates wind speed, which indicates wind speed is not the main reason for AOD biases in the warm season. Discussions of wind speed impacts are included in the first paragraph of section 4.3 in the revised manuscript.

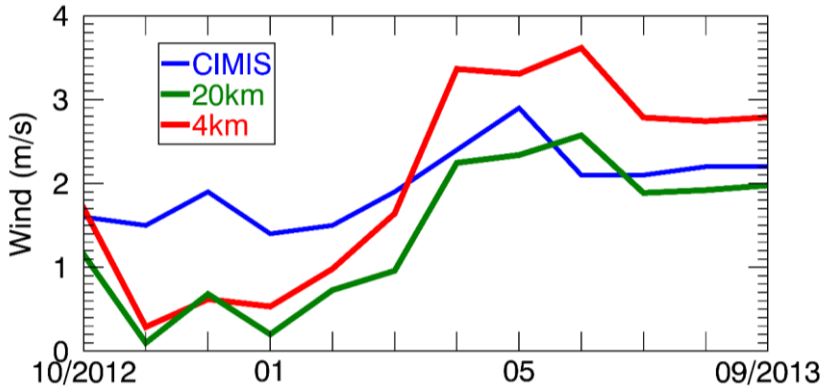

Figure 2. Simulated monthly 10-m wind speed (m/s) at Fresno, CA compared to CIMIS (California Irrigation Management Information System) observations.

Boundary Conditions: The authors half the amount of aerosols from MOZART following Fast et al. (2014). But the errors in a coarse global model, like MOZART, will likely change in time and depend on meteorological conditions. There is no sensitivity results or evidence whether such a change in boundary conditions is warranted in the present study. I believe the version of MOZART the authors use prescribes dust using climatology which would affect the simulations over California. The potential errors in MOZART that will contribute to AOD over California will likely vary over a year-long period.

We have run two sensitivity experiments with DUSTRAN at 20 km resolution, one with MOZART divided by 2 (20km_D2) and the other with original MOZART (20km_BC1). AOD maps are shown in the Supplementary Fig. 1 and the following figure. It is clear that the 20km_BC1 run overestimates AOD in the rural regions from OND to AMJ. Both the 20km_D2 (BC0.5) and 20km_BC1 (BC1) runs underestimate AOD in the rural regions in JAS, which indicates chemical boundary condition is not the main reason for the underestimation of JAS AOD in the simulations. Thus, we keep the setting of halving the amount of aerosols from MOZART in the simulations.

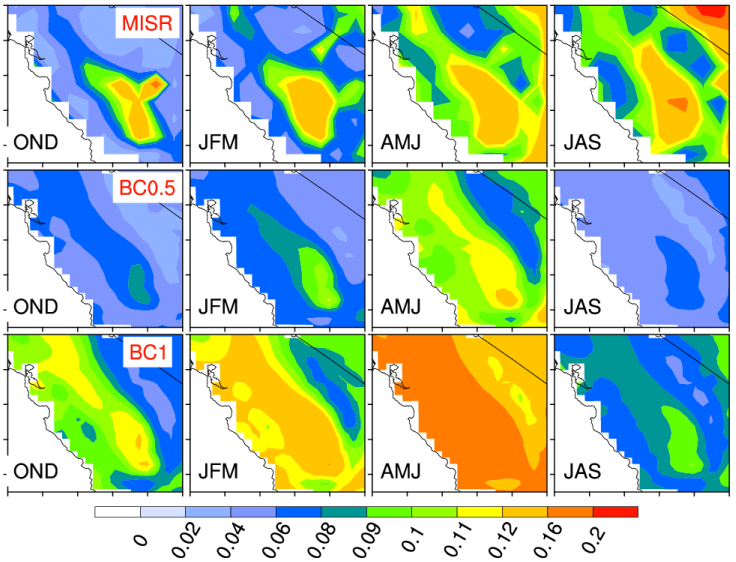

Figure 3. Spatial distribution of seasonal mean 550 nm AOD from MISR, the 20km_D2 (BC0.5) and 20km_BC1 (BC1) in WY2013.

Simulation Period: On line 167, the authors state that the simulation period is from 2012 to 2013. There is no rationale as to why this period is chosen. Perhaps it does not matter and they are only looking at seasonal variations. But this are these seasons "typical" or not?

We are only looking at seasonal variations. Similar results are also shown in our initial experiment in WY2012. For further investigation of model performance by comparing with the DISCOVER-AQ field campaign datasets in 2013 (a future study), we switched all our experiments to WY2013.

Anthropogenic Emissions: The authors use the 2005 NEI, but it would have been more appropriate to use this 2011 inventory which is closer to the time of

the simulation period. Even more ideal, would be to use emissions generated by CARB that are likely to have local emissions in California better represented. There are papers describing this inventory that at least be cited and the changes in SO2 and NH3 emissions in the SVJ valley (which are likely to be very different that the NEI 2005) will contribute to the nitrate and sulfate errors described in the paper. Since dust is an important factor over a large portion of the year, the differences in anthropogenic emissions are not likely to affect that conclusion. But it would affect the relative contribution of anthropogenic to natural sources over the year.

The 2011 NEI was not available in the WRF-Chem emission datasets when we initiated this study. We have run two sensitivity experiments with the 2011 NEI (20km_NEI11) and 2005 NEI (20km_D2) at 20 km resolution with the DUSTRAN dust scheme. Results are shown in the supplementary materials and the following figures. The differences between NEI11 and NEI05 are small comparing to the identified model biases in this study. As the reviewer pointed out, the differences in SO_4 and NH_4 are relatively large. However, SO_4 in NEI11 has larger biases than SO_4 in NEI05.

As shown in Fast et al. (2014), "reducing the default CARB emissions by 50% led to an overall improvement in many simulated trace gases and black carbon aerosol at most sites and along most aircraft flight paths; however, simulated organic aerosol was closer to observed when there were no adjustments to the primary organic aerosol emissions". We can see all the emission datasets (CARB, NEI11 and NEI05) have uncertainties in the aerosol emissions. We decide to keep our current model setup and include discussions of the uncertainty in the emission data sources in the revised manuscript.

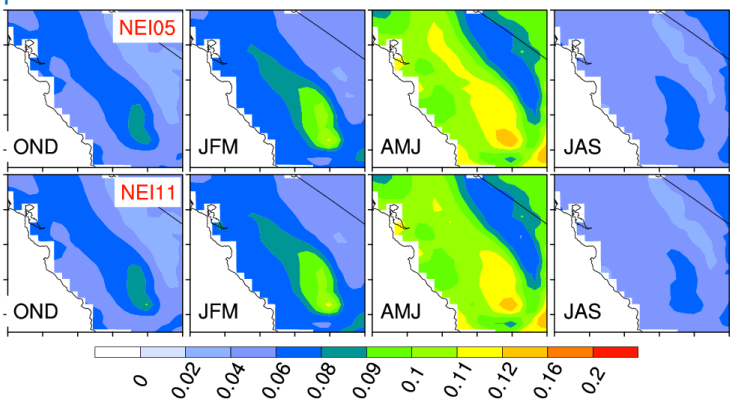

Figure 4. Spatial distribution of seasonal mean 550 nm AOD from the 20km_NEI11 (NEI11) and 20km_D2 (NEI05) runs in WY2013.

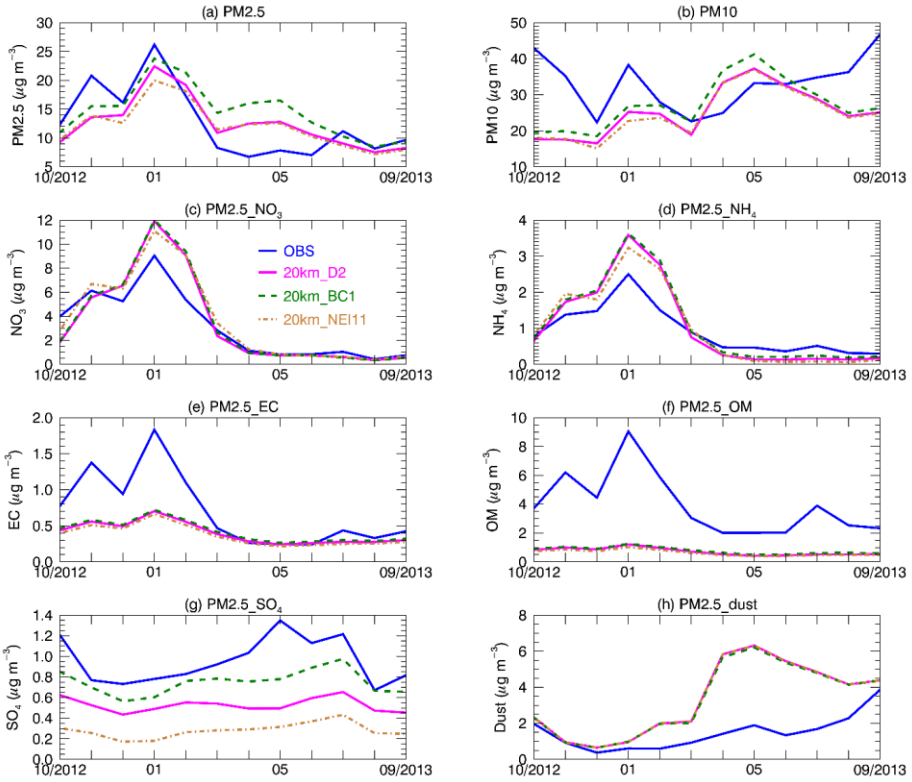

Figure 5. Aerosol mass (μg m^{-3}) for different species from EPA-CSN (OBS), the NEI05 (20km_D2) and NEI11 (20km_NEI11) runs at Fresno, CA. $PM2.5\_NO_3$ represents NO_3 with diameter ≤ 2.5 μm. Similar definition for SO_4, EC, OM, dust and NH_4 in the figures.

Model Evaluation: The authors used satellite equivalent potential temperature to evaluate the temperature profiles in the model. As seen in Figure 9, it seems that the vertical resolution is coarse so it is not the best source to examine near-surface temperature gradients. Two of the near-surface AIRS profiles look unrealistic to me. In addition it appears to have a 1 deg uncertainty (which is large for temperature) and is from a 1 degree grid – which will average out substantial temperature variations in areas affected by terrain. Using radiosondes would be a much better way to evaluate the model. The coarse vertical resolution of AIRS also leads to misinterpretations about boundary layer mixing. They claim that boundary layer mixing is too weak and explains why the simulated extinction profiles are wrong in AMJ and JAS.

There is simply not enough aerosols around, no matter what the vertical distribution.

Unfortunately, there is no routine radiosonde observation available in the SJV. AIRS data have been extensively evaluated using radiosondes in other regions. We agree that the coarse vertical resolution of AIRS data cannot fully resolve near-surface temperature gradients. However, AIRS is the best dataset currently available to evaluate seasonal variations of the vertical temperature/moisture profiles in the model simulations over the SJV. Evaluation of surface temperature/RH is conducted by comparing with surface observations in the revised manuscript. Results are consistent with evaluations of vertical profiles comparing to AIRS. More analyses of aerosol biases in the boundary layer are included in the revised manuscript.

We have found that the unit of RH is wrong in our code to calculate equivalent potential temperature. It is fixed in the revised manuscript. The profiles look reasonable now. It doesn't change the conclusions of this study.

Missing Aspects: While the authors have evaluated simulated aerosol composition and PM25/PM10 mass, they have not examined aerosol water. During dry conditions of the summer months, this may not be a large factor contributing to extinction. Aerosol water is likely to become more important aloft, where RH is likely to be higher. But one does not know unless it is examined. Is there significant aerosol water in the simulations? Aerosol water will be influenced by simulated RH, so an evaluation of simulated RH is in order.

Evaluation of simulated RH is included in the supplementary and discussed in the revised manuscript. As shown in following figures, there are dry biases in the model simulations. However, due to the relative dry environment (RH<50%) in the warm season, the dry bias may not be responsible for the underestimation of aerosol extinction in the boundary layer and column-integrated AOD through hygroscopic effects (Feingold and Morley, 2003).

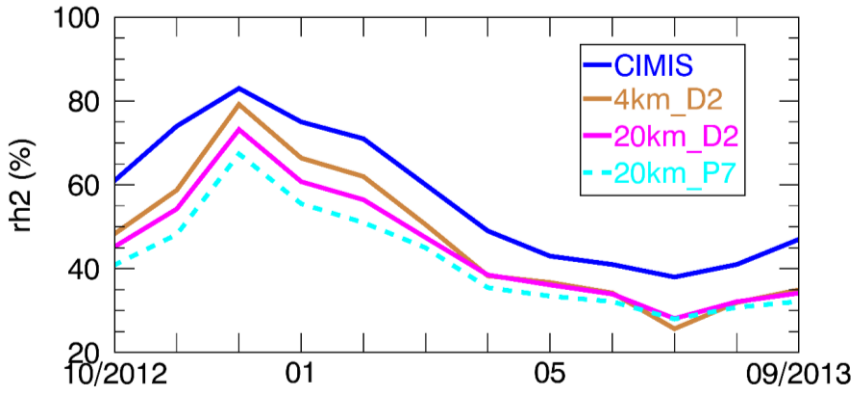

Figure 6. Monthly mean 2-m RH (%).

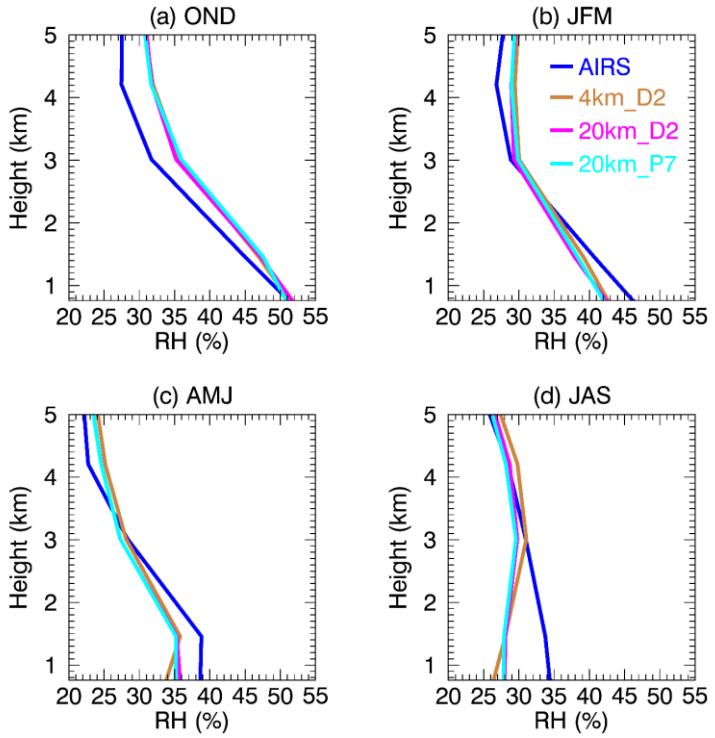

Figure 7. Vertical profile of seasonal mean relative humidity (%) in the WRF-Chem simulations comparing to AIRS. The 20km (not shown) run is similar to the 20km_D2 run while the 4km run (not shown) is similar to the 4km_D2 run.

A second missing aspect is SOA. I assume the version of MOSAIC they use does not include SOA. Yet SOA has been shown to be a major factor in PM25 for much of the year in California. While SOA concentrations will be lower than dust concentrations (when significant dust is present), it seems that omitting SOA is problem. One motivation factor in the study was related to using and air quality model (such as WRF-Chem) to guide emission control strategies. That would include OC emissions. But it seems that only primary OC is included, so that comparing simulated OC to observed OC is misleading.

SOA processes are not included in our simulation. Fast et al. (2014) used the simplified two-product volatility basis set parameterization to simulate equilibrium SOA partitioning in the WRF-Chem model. SOA is still underestimated in their simulation in May and June. We tried to run the WRF-Chem model at 20 km resolution (20km_VBS2) following the settings in Fast et al. (2014). However, our simulation can only produce comparable AOD in AMJ while AOD in other seasons are underestimated. Since it is challenging to correctly represent SOA processes in regional climate models, we keep our current settings and discuss the impact of SOA processes in the revised manuscript.

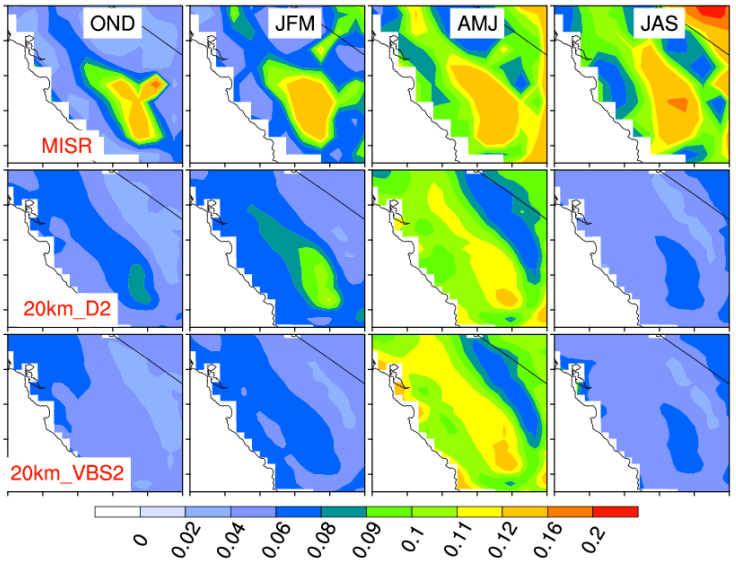

Figure 8. Spatial distribution of seasonal mean 550 nm AOD from MISR, 20km_D2 and 20km_VBS2 in WY2013.

Also, MOSAIC simulates organic matter (both carbon and oxygen), so do the authors account for the missing oxygen parts in the measurements that are labeled OC?

Thanks for your comment. The observed OC is converted to organic matter (multiply by 1.4) to compare with the simulated organic matter in the revised manuscript.

The authors also use a 4-bin version of the model which coarsely represents the aerosol size distribution. The authors should at a minimum discuss how this assumption affects their results and conclusions.

Discussion of the impacts of this assumption is provided in the revised manuscript as following:

"Zhao et al. (2013a) compared the impacts of aerosol size partition on dust simulations. It showed that the 4-bin approach reasonably produces dust mass loading and AOD comparing to the 8-bin approach. The size distribution of the 4-bin approach follows that of the 8-bin approach with coarser resolution, resulting in ±5% difference on the ratio of PM2.5-dust/PM10-dust in dusty regions. Dust number loading and absorptivity are biased high in the 4-bin approach comparing to the 8-bin approach."

It would have been useful to see some sort of evaluation of aerosol size distribution, since that also affects extinction and AOD. So the authors are really not probing all the aspects that affect uncertainties in simulated extinction and AOD.

Evaluation of Ångström exponent (AE), an indicator of aerosol particle size, is included in Fig. 4b of the revised manuscript. WRF-Chem captures the seasonal variability of the AE well, with a correlation of 0.90 in both the 20km and 4km simulations. The magnitude of AE is also approximately simulated in the cold season, with a mean of 1.15 (1.20) in the 20km (4km) runs compared to 1.33 in the observation. However, the simulated AE is underestimated by ~30% in the warm season, indicating that the simulated particle size is biased high during this period.

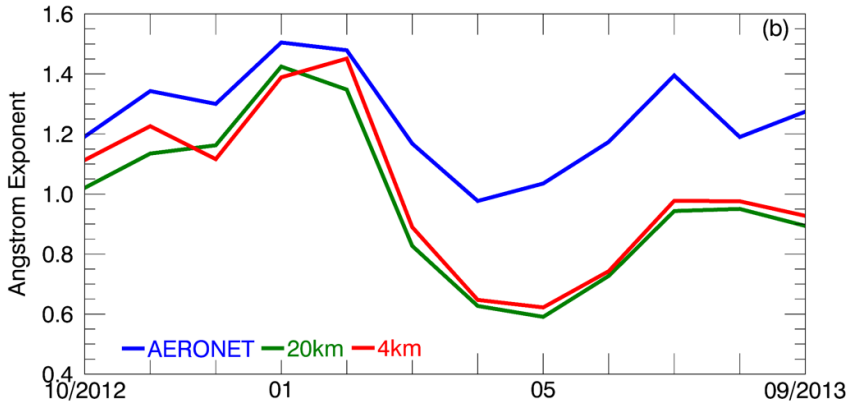

Figure 9. Monthly mean Ångström Exponent between 600 nm and 400 nm at Fresno, CA.

Model Interpretation: All of the above factors will affect the interpretation of the model results and whether local (due to WRF-Chem) or long-range transport (not WRF-Chem related) sources of dust contribute to the errors in simulated dust concentrations and the vertical distributions. As stated in the summary, the authors claim the errors are largely due to errors in the dust emissions (not clear whether they mean local emissions or those from long-range transport) and vertical mixing. Given how the model has been used, they have not provided sufficient evidence to convince me that is the case.

The simulated aerosol extinction in the free troposphere above the boundary layer is close to or larger than CALIOP, suggesting that aerosols transported from remote areas through chemical boundary conditions (e.g., the differences between the 20km_BC1 and 20km_D2 runs in Supplementary Fig. 3) may not be the major factor contributing to the underestimation of dust in the boundary layer in the SJV. It is clarified in the revised manuscript.

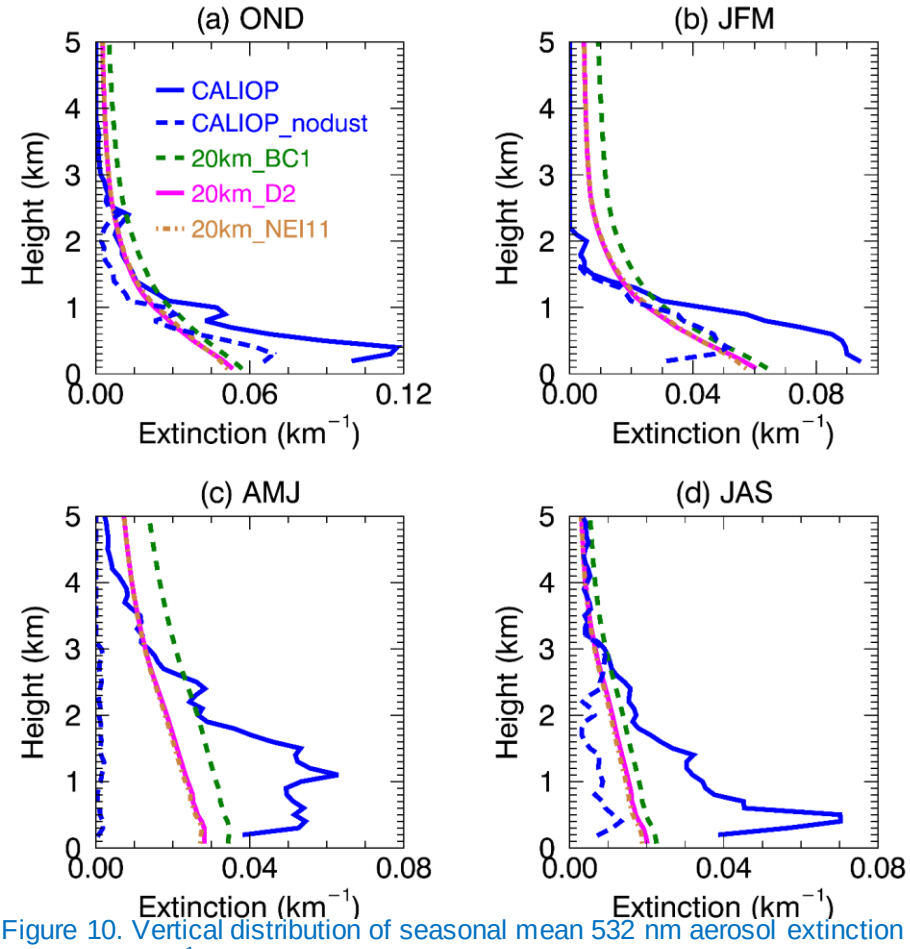

Figure 10. Vertical distribution of seasonal mean 532 nm aerosol extinction coefficient (km^{-1}) from CALIOP, CALIOP_nodust, and the WRF-Chem (20km_D2, 20km_BC1 and 20km_NEI11) simulations over the red box region in Fig. 1a in WY2013.

Specific Comments:

Lines30-31: Change "in cold season" to "in the cold season" and similarly "in warm season" to "in the warm season". This is the first instance of poor use of English in the text. I will not comment on other problems since I seem my role as commenting on the science, rather than correcting the grammar. The

authors should use an editor if the co-authors are not willing to help out with the English.
Careful proofreading is provided by the co-authors (James Campbell and Hui Su) for the revised manuscript.

Lines 43-45: This statement is an obvious one and I am not sure it is needed. The focus of the paper seems to be on dust, so this is a secondary issue.
Removed per your suggestion.

Lines 92-104. This paragraph provides an important motivation for the study, but could be strengthened. Many readers will not know why models, such as WRF-Chem, are needed to develop/verify/modify satellite retrievals. It would be useful to add a few sentences describing how such models are used to demonstrate the purpose.
The following sentences are added in the revised manuscript to describe how the WRF-Chem model will be used in the MAIA retrieval algorithm.

"A significant challenge for aerosol remote sensing in retrieving spatial information on specific aerosol types, especially near the surface, is due to the lack of information on the vertical distribution of aerosols in the atmospheric column and limited instrument sensitivity to aerosol types over land. The WRF-Chem model will be used to provide near-real-time estimation of particle properties, aerosol layer heights, and aerosol optical depths (AOD) to constrain the instrument-based PM retrievals."

Line 214: "averaging process" is a phrase that is not clear or specific enough. It is not clear how the authors apportion the NEI 2005 emissions to the WRF domain, and the procedure should be some sort of "reapportionment" rather than interpolation. Simple interpolation cannot be used since that would not conserve mass. Did they check to make sure the total mass emitted from NEI 2005 with the WRF domain was actually the same as what was used after the emissions were reapportioned to the WRF domains?
Reworded to "reapportionment process". We use the standard emission conversion program in the WRF-Chem (convert_emiss.exe) to reapportion the anthropogenic emission. The domain-averaged emission rates for the 20km and 4km simulations are quite similar, as listed in the updated Fig. 1.

Line 257: The sensitivity experiment mentioned does not contain sufficient details for the reader to know why or how it was performed.

Reworded as: “The underestimation also exists in a sensitivity experiment (not shown) with the same model setups except initialized in April, indicating that the identified model biases in the warm season are not caused by potential model drift after a relatively long simulation period.”

Line 264: The authors start discussion Figure 5c before 5a. Why not change the order of the panels then to match the progression of the discussion in the text?

Order changed as suggested.

Line 338: There are far more studies evaluation WRF-Chem in simulating biomass burning than simply the one the first author led.

Two more references (Grell et al., 2011; Archer-Nicholls et al., 2015) are included in the revised manuscript.

Anonymous Referee #2

In this study, the authors use the WRF-Chem model to simulate the seasonal variability of aerosol properties in the San Joaquin Valley. The authors investigate the roles of 1) horizontal resolution of model; 2) dust emission schemes; and 3) meteorology in modeling aerosol properties and compared the model results against ground-based (e.g. IMPROVE) and satellite (e.g. MISR and CALIPSO) observations. This paper has scientific merit to be published on ACP; however, some major revisions are needed.

General comments:

1. Uncertainties in dust schemes

First of all, the authors did not thoroughly describe the dust schemes in the paper, but only cited a paper by Zhao et al. (2010), in which the two dust schemes are used to simulate the dust emissions over Africa. The parameters "C", the empirical proportionality constants, in both schemes are tuned for the African dust emissions.Whether the authors use updated or original values for "C" is never discussed in the paper. Since the dust emission schemes are associated with such large uncertainties (in terms of values of C), the discussions in section 4.2 (sensitivity to dust scheme) makes not much sense to the reviewer, because both schemes need to be tuned before any new case studies with different domains, simulation periods, and re-analysis inputs.

In our study, we use the original "C" in Ginoux et al. (2001) and Shaw et al. (2008). It is clarified in the revised manuscript. More analyses about the two dust emissions are also included in the revised manuscript. The low emission in GOCART is due to the source function for potential wind erosion. We agree that "C" in DUSTRAN needs to be tuned for better agreement with observations. As our simulations show high biases of dust at the surface, the "C" value in DUSTRAN are not likely the main reason for low aerosols in the boundary layer in the warm season.

In addition, in Zhao et al. (2010), the dust emission schemes are coupled with 8-bin version of MOSIAC, while in Zhao et al. (2013) with MADE/SORGAM. In this paper, the dust emission schemes are coupled with 4-bin version of MOSAIC. Please mention how the dust masses are partitioned in these four bins.

The dust masses are partitioned into four size bins (0.039-0.156 μm, 0.156-0.625 μm, 0.625-2.5 μm, and 2.5-10.0 μm dry diameter), respectively. Aerosols are considered to be spherical and internally mixed in each bin (Barnard et al., 2006; Zhao et al., 2013b). The bulk refractive index for each particle is calculated by volume averaging in each bin. Mie calculations as

described by Ghan et al. (2001) are used to derive aerosol optical properties (such as extinction, single-scattering albedo, and the asymmetry parameter for scattering) as a function of wavelength. It is clarified in the revised manuscript. Discussion of the impacts of bin-size assumption is provided in the revised manuscript.

Please also discuss the relative importance of local dust vs. transported dust over SJV.

The simulated aerosol extinction in the free troposphere above the boundary layer is close to or larger than CALIOP, suggesting that aerosols transported from remote areas through chemical boundary conditions (e.g., the differences between the 20km_BC1 and 20km_D2 runs in Supplementary Fig. 3) may not be the major factor contributing to the underestimation of dust in the boundary layer in the SJV. It is clarified in the revised manuscript.

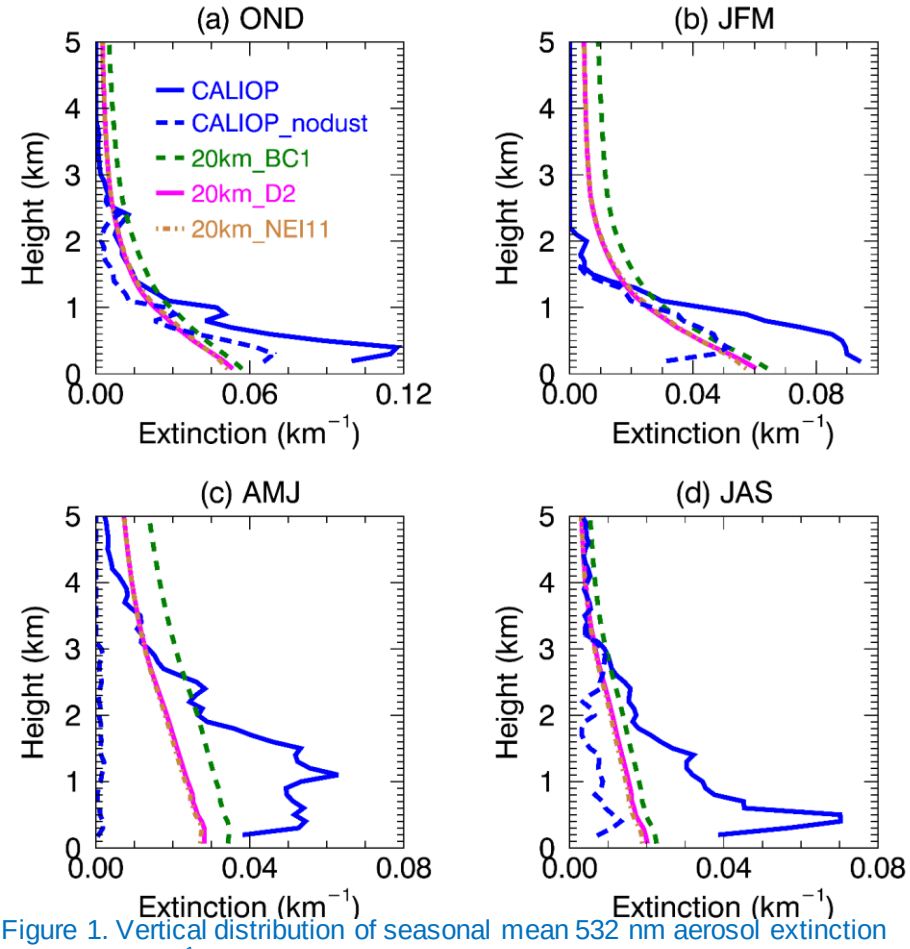

Figure 1. Vertical distribution of seasonal mean 532 nm aerosol extinction coefficient (km^{-1}) from CALIOP, CALIOP_nodust, and the WRF-Chem (20km_D2, 20km_BC1 and 20km_NEI11) simulations over the red box region in Fig. 1a in WY2013.

2. Lack of in-depth analyses

In the paper, the authors demonstrate differences in modeled and observed aerosol properties without giving in-depth analyses. The quality of the paper can be significantly improved if the authors can provide more in-depth

analyses other than just quoting conclusions from other papers. Here are three examples:

Following three reviewers' comments, more analyses on differences in modeled and observed aerosol properties are given in section 4 of the revised manuscript.

Lines 239-242: To explain the underestimations of OC in 4km and 20km simulation, the authors quote the explanation from Fast et al. (2014): "low bias in WRF-Chem simulation is primarily due to incomplete understanding of SOA processes." To my knowledge, a simple version of VBS SOA scheme is used in Fast et al. (2014) but not in this Wu et al. paper. If this is the case, then the authors' explanation is definitely wrong. If the VBS SOA scheme is also adopted in this Wu et al. paper, then "incomplete understanding of SOA processes" does not explain the differences between the OC loadings in two cases with different horizontal resolutions because SOA processes are treated the same way in two cases.

Thanks for the insightful comment. We have checked our setting and confirmed that SOA processes are not included in our current setting. We tried to run the WRF-Chem model at 20 km resolution (20km_VBS2) following the settings in Fast et al. (2014). However, that simulation produces reasonably AOD in AMJ while AOD in other seasons are underestimated. We keep our current settings and discuss the impacts of SOA processes in the revised manuscript. The statement of "incomplete understanding of SOA processes" is removed in the revised manuscript.

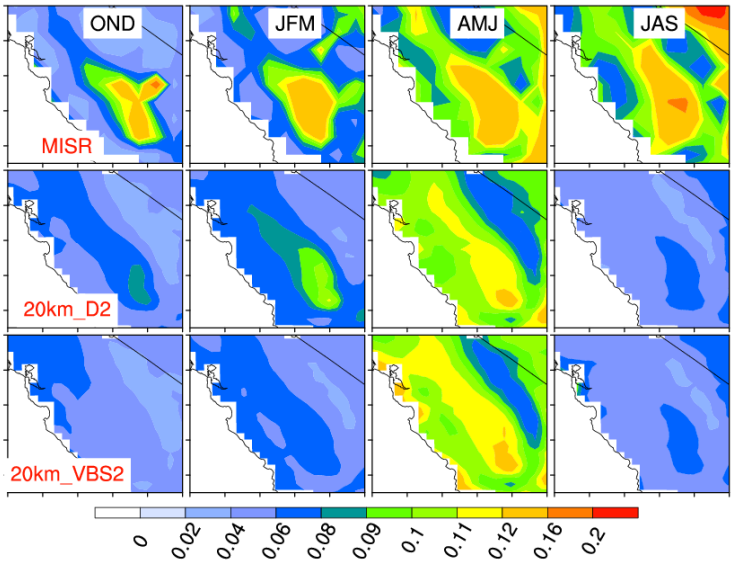

Figure 2. Spatial distribution of seasonal mean 550 nm AOD from MISR, the 20km_D2 and 20km_VBS2 simulations in WY2013.

Lines 245-248: To explain the low bias in modeled sulfate, the author mention that low bias in sulfate is also shown at one site Bakersfield in Fast et al. (2014). However, in Fast et al. (2014), the sulfate concentrations over some other sites are reasonable compared to observations. The authors are trying to explain their model results (domain integrated; one-year simulation) by comparing against model results over one site and two-month period from Fast et al. (2014). The authors claim, "it [Fast et al. (2014)] suggests that improvement in understanding the photochemical processes involving sulfate is needed to reproduce seasonal variability of sulfate in the SJV. "; However, Fast et al. (2014) never studies the seasonal variability of aerosol properties. We have removed this statement and include more discussions (precursor and marine intrusions) in the revised manuscript.

Section 4.3 The Role of Meteorology: In this section, the authors focus on the role of instability only other than "meteorology". The other meteorological fields also strongly control the aerosol properties, but are never discussed or mentioned in the study. For example, between 4km and 20km, the surface wind fields, which are important for dust emissions, are definitely very different. The precipitation fields, which are important for wet removal processes, are definitely very different between two cases too. The reviewer

455 strongly suggests the authors add these results, because they can also
456 partially explain the differences among three cases (4km, 4km_D2, 20km).
457 Evaluation of temperature, RH, wind speed and precipitation are included in
458 section 4.3 of the revised manuscript and the supplementary. More
459 discussions of meteorological impacts on aerosol simulations are also
460 included in the revised manuscript. Biases in surface wind speed and
461 precipitation may not be the main reasons for the identified aerosol biases in
462 the boundary layers during the warm season.
463
464 **Specific comments:**
465 Figure 1: Add domain-integrated values of daily anthropogenic emissions
466 (miug/day) in each sub figures. Similar to anthropogenic emissions, please
467 add dust emissions for three cases too (not necessarily in figure 1).
468 We add the domain-averaged PM2.5 emission rate in each sub figure. Dust
469 emissions are shown in Fig. 8 in the revised manuscript and the following
470 figure.

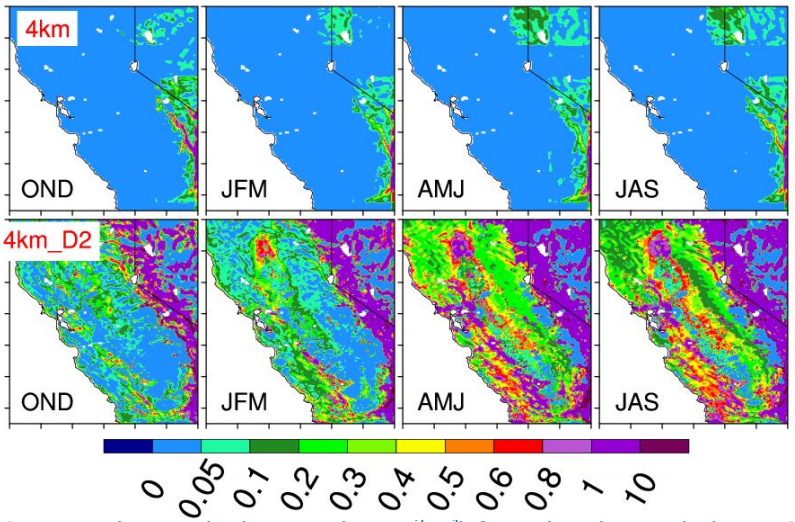

471
472 Figure 3. Mean dust emission rate (μg m^{-2} s^{-1}) from the 4km and 4km_D2
473 runs.
474
475 Table 2 and Figure 6: it seems that table 2 and Figure 6 provide some same
476 information. It may be better to merge table 2 and Figure 6.
477 Because some reader may be more interested in magnitude while other may
478 be more interested in relative contribution, we prefer to keep both Table 2

(Table 3 in the revised manuscript) and Fig. 6 (Fig. 10 in the revised manuscript).

Line 337: Please explain the reason to use climatological fire emissions from GFED instead of using daily fire emission from GFED. The fire emissions from GFED are available for 2013 as mentioned on the website (http://www.globalfiredata.org/).

We use the standard emission preparation program (prep_chem_sources_v1.5) for the WRF-Chem model to generate our fire emissions. Currently, only GFEDV2.1 is available in this program. Since fire emissions are not the major issues in our current simulations, we keep current settings.

Anonymous Referee #3

This paper shows the WRF-Chem simulation of aerosols in the SJV in California for one year and compares the results with observations of AOD from one AERONET site at Fresno and from MISR for a domain covering SJV, as well as measurements of aerosol mass concentrations of PM2.5, PM10, nitrate, sulfate, EC, OC, and dust from IMPROVE measurements. It tests the effects of using two different model resolution and two dust schemes, and attributes the model problems in matching observed AOD and PM10 to mainly the poor simulation of dust. It is stated in the "Introduction" that the paper a) "serves as the first step for future investigation of the aerosol impact on regional climate and water cycle in California" and b) provides a priori input for remote sensing retrievals for air quality for the MAIA mission.

While this paper has clearly shown the WRF-Chem performance over SJV that provides useful information, it lacks the vigor and thoroughness in the analysis and interpretation, and the information presented in the paper is insufficient in helping understand the problems of the model. Given the goal of using such a model for MAIA retrieval and for climate study, much more in-depth analysis and vigorous diagnostics is necessary in order for the model improvements to be useful for those purposes. Although the content is suitable for ACP, major revisions are necessary before the paper can be considered again for publication.

General comments:

1. Dust simulations: The authors have concluded that the dust simulation is the major problem for model to capture the observed aerosol amount and variability in the warm months. Switching from GOCART to DUSTRAN just shows different problems but does not resolve the issue. However, there is no any explanation on the differences between the two schemes in terms of emission strength, source location, parameterization of dust mobilization, and deposition in order to understand why the dust amount and seasonal cycles are so different between the two schemes and yet none can capture the observations. Without understanding the cause of the problem, future improvement is not possible.

More descriptions and analyses of the two dust schemes are provided in the revised manuscript for better understanding the cause of the problem. For details, please see the last two paragraphs of section 3 in the revised manuscript.

2. Non-dust aerosols: Figure 4 clearly shows that the model does not have much skill to simulate sulfate and OC, but the problem has not been investigated. The ammonium is completely left out, which is an important part

of total aerosol mass. Also, large fraction of aerosol is classified as "other", but it is not clear what the "other" aerosols are in both model and IMPROVE data.
Biases in simulated sulfate from precursor and marine intrusion are investigated in the revised manuscript.

The bias in OC is because SOA processes are not included in our simulation. It is still challenging to correctly represent SOA processes in regional climate models. We keep our current settings and discuss the impacts of SOA processes in the revised manuscript.

The ammonium is included in Fig. 4d of the revised manuscript. The performance of simulated ammonium is similar to nitrate.

"Other" refers to the difference of PM2.5 and the summation of specified PM2.5 (NO3, NH4, SO4, OM, EC, dust). It is clarified in the revised manuscript. In the model, it includes sea salt and other inorganic matter simulated in MOSAIC. In IMPROVE, it includes all other aerosols observed.

3. Optical properties: It is also not clear how AOD and aerosol extinction are computed from the simulated aerosol mass. Is aerosol microphysics package used for calculating particle sizes and mixing state? How is mass-based aerosol converted to extinction and AOD? Is the relative humidity considered in these calculations?
Description of how AOD and aerosol extinction are computed is added in the revised manuscript and attached as follows. More details can be found in Barnard et al. (2006, ACP).

"Aerosols are considered to be spherical and internally mixed in each bin (Barnard et al., 2006; Zhao et al., 2013b). The bulk refractive index for each particle is calculated by volume averaging in each bin. Mie calculation as described by Ghan et al. (2001) is used to derive aerosol optical properties (such as extinction, single-scattering albedo, and the asymmetry parameter for scattering) as a function of wavelength."

4. Chemistry: Nitrate, sulfate, and a significant fraction of OC are secondary aerosols that are produced by chemical reactions of their gaseous precursors in the atmosphere. The authors attribute the high bias of model-simulated nitrate to "high bias in nitrate emission", which is erroneous. The diagnostics should involve investigations of nitrate precursors such as NOx and HNO3, and also the formation of nitrate via heterogeneous reactions on dust and sea salt surfaces and homogeneous reactions in the sulfate-nitrate-ammonium

system. It is not clear how WRF-Chem deals with nitrate formations and which is the major reaction pathway for nitrate aerosol production.
Same as sulfate – it is formed via gas and aqueous phase reactions of SO2.
Better diagnostics of the problem is needed.
Thanks for the comments. Analyses of NO_2 and SO_2 are included in Fig. 6 of the revised manuscript. We also notice that switching the PBL scheme can produce better simulation of nitrate. More diagnostics of model biases are included in section 4 of the revised manuscript.

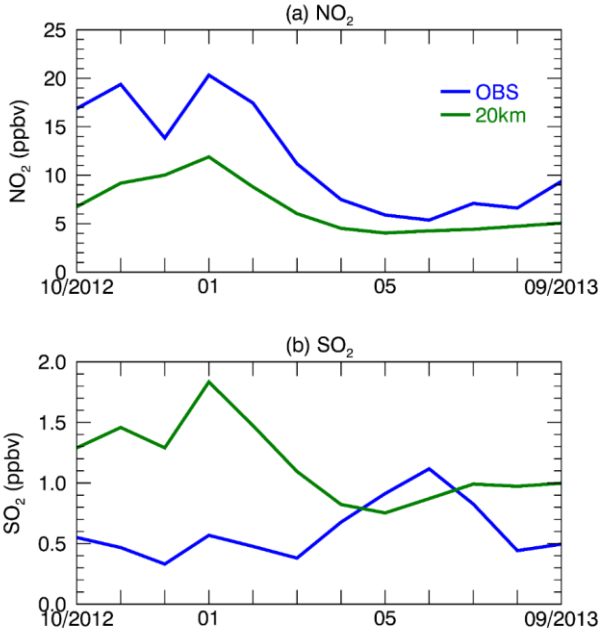

Figure 1. (a) NO_2 and (b) SO_2 from EPA (OBS) and the 20km run at Fresno, CA.

5. Other physical processes: Dry and wet depositions are the major removal processes for aerosols. The seasonal cycles of these processes also need to be investigated. For example, can the differences in seasonal variations between model and obs be partly explained by the differences in simulated and measured precipitation amount that determines the wet removal of aerosols? Or if the winds are realistically simulated in WRF-Chem that not only affect the dust emission, but also advection, both have profound effect on aerosol temporal and spatial distributions?

6. Meteorological fields: The only meteorological field compared in the paper is the equivalent potential temperature, which provides information on the atmospheric stability. Other important met fields, such as precipitation and wind speed/direction, as mentioned above, plays key roles in aerosol removal, transport, and wind-driven emissions of dust and sea salt but have not even mentioned in the paper. In addition, these fields and the physical processes driven by them are resolution-dependent, so the role of these met fields should be examined at different spatial resolutions.

The seasonal variability of precipitation is well captured in the simulations, while the magnitude of precipitation is smaller than the observations during the warm season (Supplementary Table 2). Wet removal processes are thus not likely the primary reason for the aerosol biases in the warm season.

The model simulations underestimate wind speed in the cold season (Figure 9 in the revised manuscript). In the warm season, the 20km run underestimates wind speed except June while the 4km run overestimates wind speed, which indicates wind speed is not likely the main reason for AOD biases in the warm season.

Discussions of the impacts from precipitation, wind speed and other factors are included in section 4.3 of the revised manuscript.

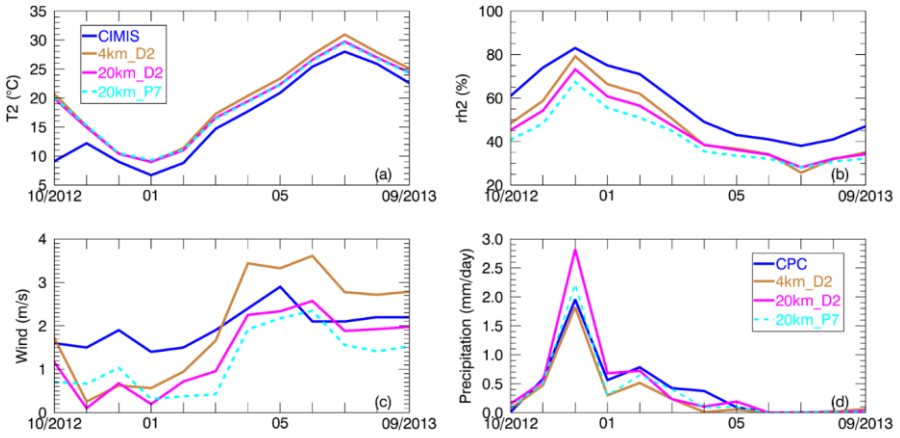

Figure 2. Monthly mean of (a) 2-m temperature (°C); (b) 2-m relative humidity (%); (c) 10-m wind speed (m/s); (d) precipitation (mm/day) at Fresno, CA. The 20km run (not shown) is similar to the 20km_D2 run while the 4km run (not shown) is similar to the 4km_D2 run.

7. Lateral boundary conditions: The effects of lateral boundary condition should be examined, or at lease discussed, particularly because of SJV's geophysical locations that is susceptible to the transpacific transport. How much of the aerosol species and their precursor gases are regionally/locally produced vs. imported from the lateral boundary, and how they affect the seasonal cycle? In other words, are the features/problems mainly produced by WRF-Chem? How important is the lateral boundary conditions to different aerosol species?

The simulated aerosol extinction in the free troposphere above the boundary layer is close to or larger than CALIOP, suggesting that aerosols transported from remote areas through chemical boundary conditions (e.g., the differences between the 20km_BC1 and 20km_D2 runs in Supplementary Fig. 3) may not be the major factor contributing to the underestimation of dust in the boundary layer in the SJV. It is clarified in the revised manuscript. The impacts of the lateral boundary conditions to different PM2.5 species are small except SO4 (as shown in the following figure).

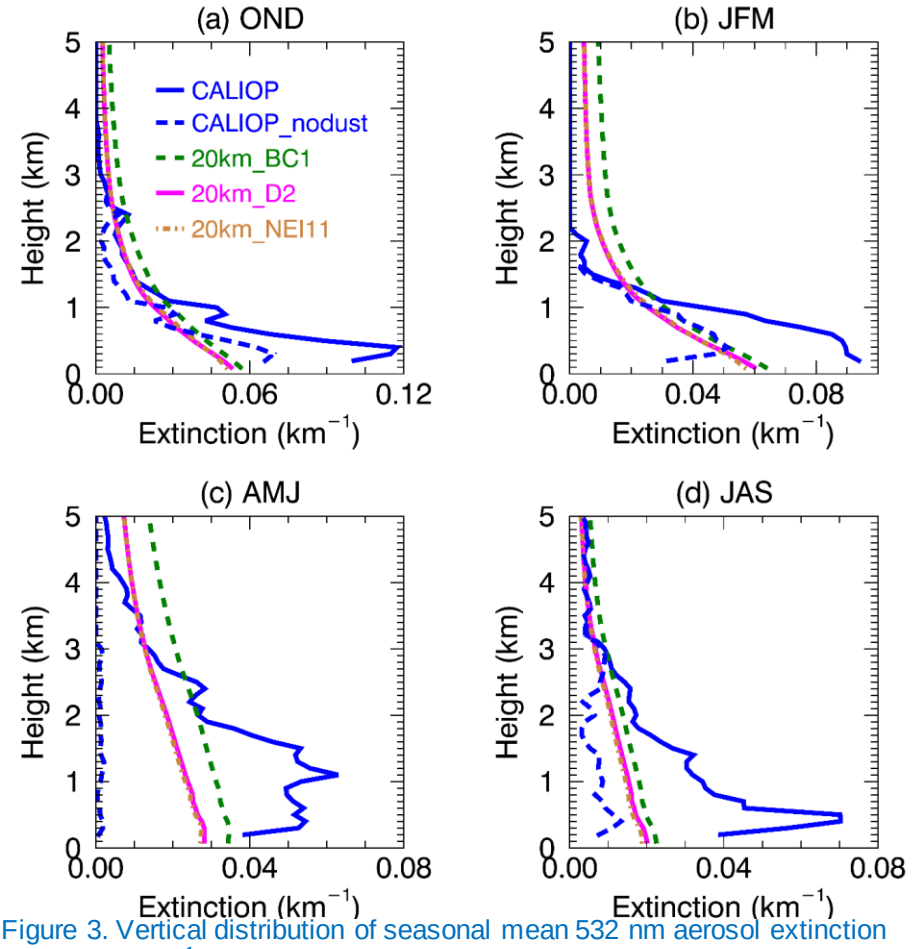

Figure 3. Vertical distribution of seasonal mean 532 nm aerosol extinction coefficient (km^{-1}) from CALIOP, CALIOP_nodust, and the WRF-Chem (20km_D2, 20km_BC1 and 20km_NEI11) simulations over the red box region in Fig. 1a in WY2013.

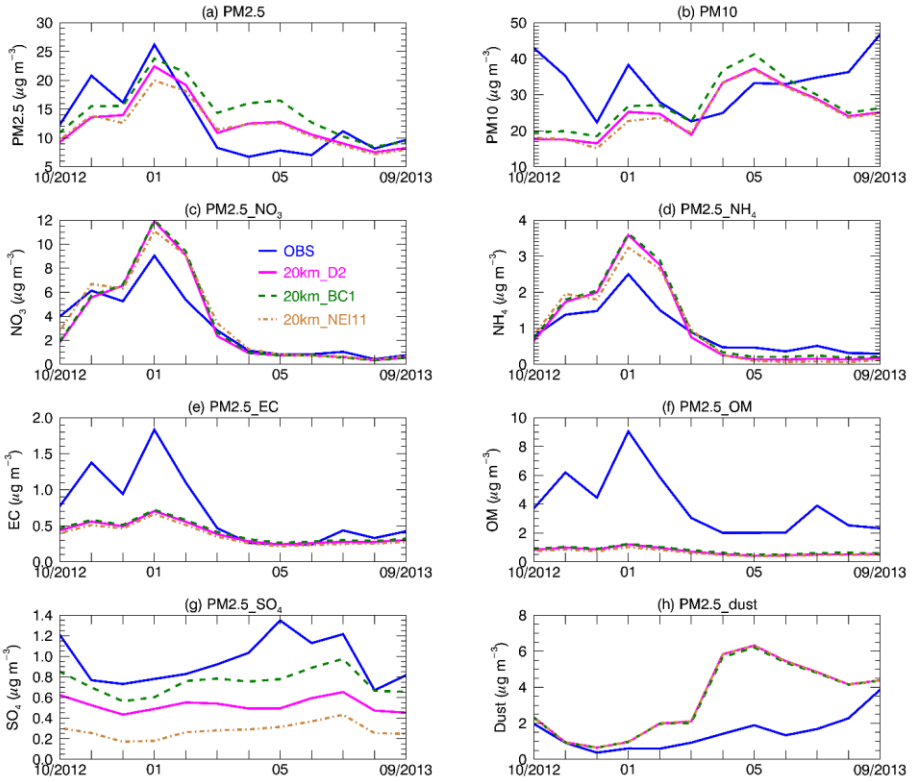

Figure 4. Aerosol mass (μg m-3) for different species from OBS, the 20km_D2, 20km_BC1 and 20km_NEI11 simulations at Fresno, CA. NH4 observations are from EPA; other observations are from IMPROVE. PM2.5_NO3 represents NO3 with diameter ≤ 2.5 μm. Similar definition for NH4, EC, OM, SO4 and dust in the figures.

8. Emissions: It seems the anthropogenic and biomass burning emissions used in this work are not up to date. For example, why the authors choose to use NEI05 emissions instead of more recent ones (e.g., NEI 2011 or NEI 2014) to better match the simulated time period (2012-2013)? Why GFEDv2 is preferred instead of GFEDv3 that was released a few years ago or GFEDv4 that has been available since 2015?

The 2011 NEI was not available in the WRF-Chem emission datasets when we initiated this study. We have run two sensitivity experiments with the 2011 NEI (20km_NEI11) and 2005 NEI (20km_D2) at 20 km resolution with the DUSTRAN dust scheme. As shown in Fig. 4 and 5 here, the differences

659 between NEI11 and NEI05 are small comparing to the identified model biases
660 in this study.

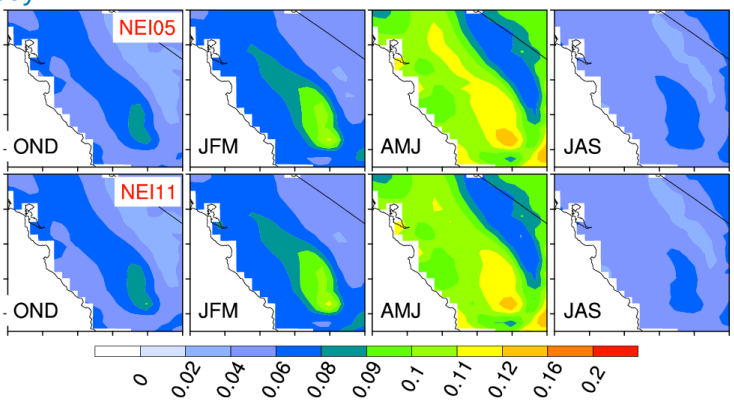

661
662 Figure 5. Spatial distribution of seasonal mean 550 nm AOD from
663 20km_NEI11 (NEI11) and 20km_D2 (NEI05) in WY2013.
664
665 We use the standard emission preparation program
666 (prep_chem_sources_v1.5) for the WRF-Chem model to generate our fire
667 emissions. Currently, only GFEDV2.1 is available in this program. Since fire
668 emissions are not the major issues in our current simulations, we keep current
669 settings.
670
671 9. Model-data comparison: 1) For AOD, there is only one AERONET site in
672 the study region, and MISR's spatial coverage is limited. Why not use MODIS,
673 which has a much better spatial coverage to have a better representation of
674 "monthly average", in addition or even instead of using MISR?
675 We have compared the MISR data with the MODIS dark target and deep blue
676 combined AOD V6 (as shown in the following figure). The MODIS data at
677 1°x1° cannot resolve the sharp gradient of aerosols in the SJV.

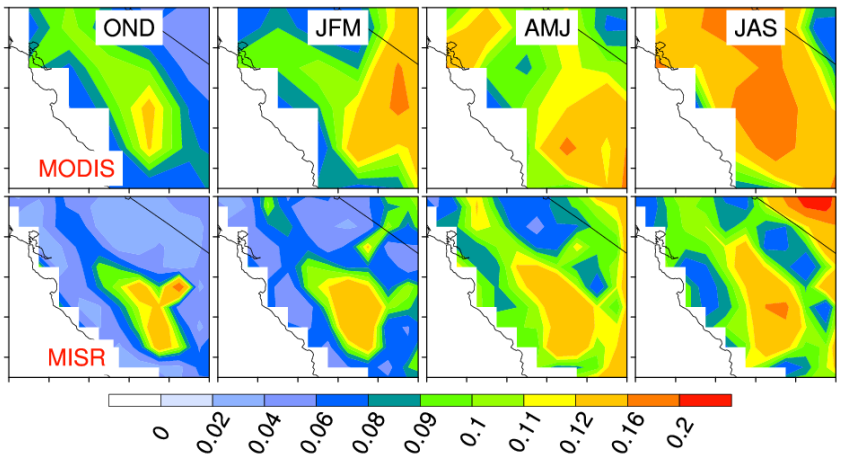

Figure 6. Seasonal mean AOD from MODIS and MISR.

2) Which months are defined as "cold" or "warm" months?
Cold months are from October to March; warm months are from April to September. The descriptions are in Line 277 and 282 in the revised manuscript.

3) More statistical quantities are needed to mark the agreement between model and observations, including correlation coefficients and seasonal/annual bias.
Correlation coefficients are included in the revised manuscript. More quantitative information are provided in the revised manuscript.

4) The authors should avoid using the subjective adjectives, such as "good agreement", "reasonably well", etc., to describe the comparisons between model and observations. More objective and quantitative methods and presentations are needed.
Following your suggestions, more objective and quantitative presentations are included in the revised manuscript.

5) Given that air quality changes quite a bit day to day and air quality forecasts are given on daily bases, why all the comparisons are done on monthly time scale instead of daily or sub-daily?
One of our goals is to evaluate model performances in simulating regional climate on the subseasonal-to-seasonable time scale. Many previous studies

have evaluated the performance of WRF-Chem in daily or sub-daily scale. It is not the focus of this study.

10. The most important step forward is to understand the causes of deficiencies in the model and suggest/incorporate improvements for better results. However, the current paper does not offer those aspects.
Following three reviewers' comments, more analyses about the causes of deficiencies in the model are included in section 4 of the revised manuscript. We summarize the model sensitivities in section 5 and indicate future directions for improvements.

Specific comments

Page 5, line 72-82: I wonder why Fast et al 2014 and Zhao et al 2013 were able to "reasonably" represent the observations with the same WRF-Chem model, either in the warm months (Fast) or on annual bases (Zhao), but this work has difficulties to do the same?
The WRF-Chem simulation is sensitive to various factors such as initial and boundary conditions, model parameterizations and emission sources. The performance of the WRF-Chem model are also different in different seasons and at different locations. Because we are focusing on different seasons and/or different locations, we can see different performances of the model simulations. Some sensitivity experiments are included in the revised manuscript to provide more in-depth analyses on model results.

Page 5, line 83: I don't think the word "extend" is appropriate – this study only focuses on SJV while Fast and Zhao showed large regions in CA.
Reworded as "we focus on simulating aerosol seasonal variability in the SJV, California using similar model configurations as that used in Fast et al. (2014) and Zhao et al. (2013b)."

Page 6, line 102-104: I don't get it – why simulation for SJV is critical to MAIA? Is MAIA only focuses on SJV?
SJV is a testbed for the MAIA retrieval algorithm development. It is clarified in the revised manuscript.

Page 7, line 116: Why are the original wavelength(s) from AEORNET that you used to interpolate to 550 nm?
AERONET AOD is interpolated to 0.55 μm from 0.50 μm and 0.675 μm. It is clarified in the revised manuscript.

Page 8, line 146: What does "speciated" mean here? There is no aerosol species information from the CALIOP data. Marine, polluted continental, etc. provided by CALIOP are aerosol types, not species.
Reworded as "Level 2 532 nm aerosol extinction data classify aerosols into 6 types" in the revised manuscript.

Page 9, line 179-180: How is convective transport (and removal) of aerosols simulated in 4-km resolution?
Convective transport (and removal) of aerosols are simulated at grid-scale in 4-km resolution. It is clarified in the revised manuscript.

Page 9-10, line 183-184: Was the overestimation by MOZART in the free troposphere a factor of 2 such that the concentrations had to be divided by 2? If the overestimation was only in the free troposphere, why the concentrations in the lower atmosphere and BL were also divided by 2?
The overestimation by MOZART is mainly in the free troposphere as shown in Fast et al. (2014) and our sensitivity experiment (20km_BC1). Lowering the boundary conditions of aerosols concentration by 50% greatly reduced the bias in simulated AOD for all regions of California. The impact of chemical boundary conditions at the surface is small in the SJV. For simplicity, all the boundary conditions by MOZART are divided by 2.

Page 10, line 198: Are the dust emissions in the GOCART and DUSTRAN also available in 20 and 4 km resolutions? What are the major differences between GOCART and DUSTRAN schemes?
Yes. More descriptions of GOCART and DUSTRAN schemes are included in last two paragraphs of section 3 in the revised manuscript.

Page 11, first paragraph in section 4.1: What PM2.5 species and precursor gases are emitted?
Nineteen gases (including SO2, NO, NH3 etc.) are emitted, while aerosol emissions include SO4, NO3, EC, organic aerosols, and total PM2.5 and PM10 masses. It is clarified in the revised manuscript.

Have you checked the domain budget between 4 and 20 km resolution to ensure the total emission for all species are identical with these different resolutions?
Yes, they are quite similar. Mean emission rates for the 4km and 20km runs are listed in Fig. 1 in the revised manuscript.

Page 11, line 215: How was AOD calculated without having information of PM2.5 composition? For example, dust and BC have very different mass to extinction conversion factor, known as mass extinction efficiency (MEE). There is no single MEE for a generic PM2.5 or PM10.
Aerosol composition is considered in AOD calculation. Different refractive index are assigned to different particles. Description of how AOD and aerosol extinction are included in the revised manuscript as the following.

"Aerosols are considered to be spherical and internally mixed in each bin (Barnard et al., 2006; Zhao et al., 2013b). The bulk refractive index for each particle is calculated by volume averaging in each bin. Mie calculation as described by Ghan et al. (2001) is used to derive aerosol optical properties (such as extinction, single-scattering albedo, and the asymmetry parameter for scattering) as a function of wavelength."

Page 12, line 237: As I said earlier, nitrate is not emitted but chemically produced. The precursor emission/concentration/transport/chemistry have to be examined to explain the nitrate.
NO_3 is included in PM2.5 emission dataset. NO_2, one precursor of NO_3, is evaluated in the revised manuscript.

Page 12, line 238: Why is simulation over Texas relevant here?
This discussion is removed.

Page 12, line 242: Be specific on what "SOA processes" is referred here.
This sentence is removed in the revised manuscript because SOA processes are not simulated in our settings.

Page 12, line 244 and 246: Be quantitative – what is the standard of "good agreement"?
Quantitative evaluations are provided in the revised manuscript.

Page 12, line 250: How large is the "large low bias"?
From 30% to 85%. It is clarified in the revised manuscript.

Page 13, line 253-254: "The 4km simulation has better agreement…", but only in the cold season.
It is clarified in the revised manuscript.

Page 13, line 254-255: "The 4km simulation captures seasonal variability of PM2.5 and its speciation": From Figure 4, the seasonal variability for the

PM2.5 species are very similar between the 4- and 20-km simulations, only the concentrations are higher from the 4km simulation. The seasonal variability of PM2.5 sulfate and OC are not capture by both 4 and 20 km simulations.
The seasonal variability of sulfate is not captured in the 4km simulation while 20km simulation has a correlation of 0.63. OM has a correlation of 0.93 for all the simulations. Reworded as "Both the 20km and 4km simulations approximately capture the seasonal variability of PM2.5 and most of its speciation" in the revised manuscript.

Page 13, line 267-268: The 4km_D2 overestimates PM2.5 by 52%, but it overestimates the PM2.5_dust by up to a factor of 4 in the warm season!
The quantitative information is provided in the revised manuscript.

Page 13, line 270-272: As I suggested earlier, please show correlation coefficients on all comparisons (in addition to the bias), which indicates how model and data agree on seasonal variations.
Correlations are provided in the revised manuscript.

Page 14, line 285-286: How much better does 4km_D2 agree with MISR than other simulations? Visually, JAS is still nowhere near MISR, and AMJ is higher than MISR. Please quantify the degree of agreement.
Quantitative information is provided in the revised manuscript.

Page 14, line 290-292: I don't understand the statement of "reasonably capture the vertical distribution", even though the model has "low biases in the boundary layer and high biases in the free troposphere". To me, this is rather "unreasonable".
Reworded as "roughly capture".

Page 15, line 298-299: "…suggesting relative good performance…": How good? Figure shows poor agreement between obs and model for sulfate and OC, so they are not "good" at all.
Reworded as "suggesting that dust is the primary factor contributing to the model biases in aerosol extinction" in the revised manuscript.

Page 15, line 303: How to explain that dust from 4km_D2 is way too high but the extinction in the boundary layer is still way too low?
The model doesn't simulate the unstable environment in the warm season. Although the dust emission at the surface is large in the 4km_D2 run, no

enough convective vertical mixing is produced in the simulations, resulting the low biases in the boundary layer. It is clarified in the revised manuscript.

Page 15, line 313 and 316: If the model has weak vertical mixing, the aerosols should be trapped within the BL and not transported to high altitudes. But the model actually overestimates the aerosol at high altitude – what is the source of high altitude aerosol?
High altitude aerosols are from horizontal transport primarily governed by chemical boundary conditions.

Page 16, line 321-322: This precisely indicates the need to quantify the role of chemical boundary conditions.
The role of chemical boundary conditions is discussed in the revised manuscript.

Page 16, line 323-324, "good performance…": But in JFM the model results are much higher (by a factor of infinity?) at above 1.5 km! How can that be evaluated as "good"?
Changed to "relatively good".

Page 16, line 330: "reasonable simulation", "good representation" – what are the measures of reasonable and good here?
Quantitative information are provided in Table 2 and 3 the revised manuscript.

Page 16, line 337: Please explain what "climatological fire emissions" mean.
Reworded as "monthly-varying fire emissions".

Page 16, line 339-340: Why can Wu et al do it right for South America fire but cannot do it for California? What are the major obstacles?
In our simulation for South America, it is a 7-day case. Daily satellite data are used to generate biomass burning emission. In this study, we are focusing on seasonal variations. Biomass burning emission is updated every month, which cannot capture the single fire event in this case.

Page 17, line 371-372: No need to spell out what GOCART and DUSTRAN stand for at the last part of the paper, since they have been introduced and used many times earlier in the text.
Most people don't read the whole paper, especially program managers. So we have all acronyms redefined to help them immediately understand what we are saying.

905 Page 17, line 383-385: Unfortunately, I cannot see how the evaluation in this
906 study can be apply to other regions to ensure that aerosols are simulated
907 correctly for the right reasons. This paper has shown the problems but has not
908 shown how to solve the problems with what approach.
909 This sentence is removed in the revised manuscript.

WRF-Chem simulation of aerosol seasonal variability in the San Joaquin Valley

Longtao Wu[1], Hui Su[1], Olga V. Kalashnikova[1], Jonathan H. Jiang[1], Chun Zhao[2], Michael J. Garay[1], James R. Campbell[3] and Nanpeng Yu[4]

1. Jet Propulsion Laboratory, California Institute of Technology, Pasadena, CA, USA

2. ~~Atmospheric Sciences and Global Change Division, Pacific Northwest National Laboratory, Richland, WA, USA~~School of Earth and Space Sciences, University of Science and Technology of China, Hefei, Anhui, China

3. Naval Research Laboratory, Monterey, CA, USA

4. University of California, Riverside, Riverside, CA, USA

Submitted to *Atmospheric Chemistry and Physics*

~~November~~March, ~~2016~~2017

Corresponding author address: Longtao Wu, 4800 Oak Grove Dr., Pasadena, CA 91109
E-mail: Longtao.Wu@jpl.nasa.gov

Highlights:

1. The WRF-Chem simulation successfully captures aerosol variations in the cold season in the San Joaquin Valley (SJV), but has poor performance in the warm season.
2. High resolution model simulation can better resolve inhomogeneous distribution of anthropogenic emissions in urban areas, resulting in better simulation of aerosols in the cold season in the SJV.
3. Observations show that dust is a major component of aerosols in the SJV, especially in the warm season. Poor performance of the WRF-Chem model in the warm season ~~in the SJV~~ is mainly due to misrepresentation of dust emission and vertical mixing.

Abstract

WRF-Chem simulations of aerosol seasonal variability in the San Joaquin Valley (SJV), California are evaluated by satellite and in-situ observations. Results show that the WRF-Chem model successfully captures the distribution, magnitude and variation of SJV aerosols ~~in~~ during the cold season. However, ~~the~~ aerosols are not well represented in the warm season. Aerosol simulations in urban areas during the cold season are sensitive to model horizontal resolution, with better simulations at 4 km resolution than at 20 km resolution, mainly due to inhomogeneous distribution of anthropogenic emissions and better represented precipitation in the 4 km simulation. In rural areas, the model sensitivity to grid size is rather small. Our observational analysis ~~show~~ reveals that dust is a primary contributor to aerosols in the SJV, especially ~~in~~ during the warm season. Aerosol simulations in the warm season are sensitive to parameterization of dust emission in ~~the~~ WRF-Chem ~~model~~. The GOCART (Goddard Global Ozone Chemistry Aerosol Radiation and Transport) dust scheme produces very little dust in the SJV while the DUSTRAN (DUST TRANsport model) scheme overestimates dust emission. Vertical mixing of aerosols is not adequately represented in the model ~~comparing to~~based on CALIPSO (Cloud-Aerosol Lidar and Infrared pathfinder Satellite Observation) aerosol extinction profiles. Improved representation of dust emission and vertical mixing in the boundary layer are needed for better simulations of aerosols during~~in~~ the warm season in the SJV. ~~Aerosols generated by wild fires are not captured in the simulations with climatological fire emissions, underscoring the need of fire emission observations for operational usage.~~

1. Introduction

The San Joaquin Valley (SJV) in the southern portion of the California Central Valley is surrounded by coastal mountain range to the west and the Sierra Nevada range to the east. With cool wet winters and hot dry summers, the unique natural environment makes SJV one of the most productive agricultural regions in the world (SJV APCD, 2012 and references therein). However, SJV is also one of the most polluted regions in US due to its unique geographical location. Frequent stagnant weather systems are conducive to air pollution formation, while the surrounding mountains block air flow and trap pollutions. Large seasonal and spatial variations of aerosol occurrence and distributions are observed in the SJV. Although significant progress at made to improving local air quality in past decades has been made achieved through strong emission controls, the PM2.5 (particulate matter with diameter ≤ 2.5 μm) concentrations in the SJV remain well above the national ambient air quality standards (NAAQS) threshold of 12 μg m^{-3} on an annual basis and 35 μg m^{-3} on daily basis, occurring mainly during the cold season. Improved understanding of the aerosol variabilityies and their impacts are is needed to provide further guidance for emission control strategies in the SJV.

Air quality models are a critical useful tool to understanding the formation and evolution of aerosols and their impacts on air quality, weather and climate. However, it is still quite a challengingge to accurately simulate aerosol properties (Fast et al., 2014). Fast et al. (2014) summarized the factors contributing to the errors in regional-scale modeling of aerosol properties,. They includeing 1) emission sources; 2) meteorological parameterizations; 3) representation of aerosol chemistry; 4) limited understanding of the formation processes of secondary organic aerosol (SOA); 5) spatial resolution; and 6) boundary conditions.

As one of the advanced regional air quality models available presently to the community, the Weather Research and Forecasting model with Chemistry (WRF-Chem) has been widely used to study aerosols and their impacts on regional air quality, weather and climate (e.g., Misenis and Zhang, 2010; Zhang et al., 2010; Zhao et al., 2010; 2013a, 2013b; 2014; Wu et al., 2011a, 2011b, 2013; Fast et al., 2012, 2014; Scarino et al., 2014; Tessum et al., 2015; Campbell et al., 2016; Hu et al., 2016). For example, Fast et al. (2014) showed that WRF-Chem simulations at 4 km horizontal resolution captured the observed meteorology and boundary layer structure over California in May and June of 2010. The model reasonably simulated and the spatial and temporal variations of aerosols were reasonably simulated. Aerosol simulations by WRF-Chem are usually sensitive to both local emission and long-range transport of aerosols from the boundary conditions provided by the global Model for Ozone and Related chemical Tracers, version 4 (MOZART-4). SimilarlyWith a similar model set-up, in a one-year simulation at 12 km horizontal resolution, Zhao et al. (2013b) conducted a one-year simulation at 12 km horizontal resolution and showed found that the WRF-Chem model represented the observed seasonal and spatial variation of surface particulate matter (PM) concentration over California. However, underestimation of elemental carbon (EC) and organic matter (OM) were noticed in the model simulation, with weakno sensitivity to horizontal model resolution.

In this study, we extend focus on simulating aerosol seasonal variability in the SJV, California using similar model configurations as that used inthe studies by Zhao et al. (2013b)Fast et al. (2014) and Fast et al. (2014) Zhao et al. (2013) by focusing on simulating aerosol seasonal variability in the most polluted SJV in California. This paper serves as the first step for future investigation of the aerosol impact on regional climate and the the water cycle in California. Previous studies have demonstrated that aerosols are better simulated at higher model resolution

(Misenis and Zhang et al., 2010; Qian et al., 2010; Stround et al., 2011; Fountoukis et al., 2013). However, most regional climate studies are still ~~limited to~~performed with coarse model resolutions (on the order of 10 km) due to the availability of computational resources. This study will investigate the sensitivity of aerosol simulations to horizontal resolution and identify ~~suitable~~ optimal model ~~resolution~~ physical choices for ~~regional climate study~~reasonable representation of aerosol variabilities in the SJV.

Another application of air quality modeling is to provide initial *a priori* ~~input~~ fields for remote sensing retrievals. The WRF-Chem model has been proposed as an input for retrieval algorithms to be developed for the ~~-~~recently-selected NASA (National Aeronautics and Space Administration) MAIA (Multi-Angle Imager for Aerosols) mission, which aims to map PM component concentrations in major urban areas (including the SJV, a testbed for the MAIA retrieval algorithm development). A significant challenge for aerosol remote sensing in retrieving spatial information on specific aerosol types, especially near the surface, is caused by the lack of information on the vertical distribution of aerosols in the atmospheric column and limited instrument sensitivity to aerosol types over land. The WRF-Chem model will be used to provide near-real-time estimation of particle properties, aerosol layer heights, and aerosol optical depths (AOD) to constrain the instrument-based PM retrievals. -A~~A~~ reasonable ~~initial~~ estimate of aerosol ~~speciation~~ properties from WRF-Chem is critical to ensuringe ~~the~~ retrieval speed and quality. Considering the sensitivity of WRF-Chem simulations to various factors such as initial and boundary conditions, model parameterizations and emission sources (e.g., Wu and Petty, 2010; Zhao et al., 2010, 2013a, 2013b; Wu et al., 2011a, 2015; Fast et al., 2014; Campbell et al., 2016; Morabito et al., 2016), careful model evaluations are needed before the simulations can be used operationally for remote sensing retrievals. ~~This study also serves as an evaluation for WRF-Chem~~

~~aerosol simulations in the SJV, which will provide important information for utilizing WRF-Chem for~~Thus, this study is important for the development of MAIA retrieval algorithms, critical to the success of the MAIA mission.

This paper is organized as follows. Section 2 describes observational datasets used for model evaluation. Section 3 provides the description of the WRF-Chem model and experiment setup. Model simulations and their comparison with observations are discussed in section 4. Section 5 presents the conclusions.

2. Observations

2.1 Column-integrated Aerosol Optical ~~Depth~~Properties

~~Aerosol optical depth (AOD)~~AOD is a measure of column-integrated light extinction by aerosols and a proxy for total aerosol loading in the atmospheric column. The Aerosol Robotic Network (AERONET) provides ground measurements of AOD every 15 minutes during daytime under clear skies (Holben et al., 1998), with an accuracy ~~of~~ approaching ±0.01 (Eck et al., 1999; Holben et al., 2001; Chew et al., 2011). The monthly level 2.0 AOD product with cloud screening and quality control is used in this study. ~~AERONET AOD is interpolated to 0.55μm using the~~ Ångström exponent (AE) ~~.~~ is an indicator of aerosol particle size. Small (large) AE values are generally associated with large (small) aerosol particles (Ångström, 1929; Schuster et al., 2006). The AE between 0.4 μm and 0.6 μm is derived from AERONET observed AODs, and is used to evaluate the model-simulated AE. For comparison with simulated AOD, AERONET AOD is interpolated to 0.55 μm from 0.50 μm and 0.675 μm using the AE. In the SJV, only one AERONET station at Fresno, CA (36.79°N, 119.77°W) has regular observations throughout the California water year 2013 (WY2013~~; i.e.,~~) from October 2012 to September 2013~~)~~.

The Multiangle Imaging Spectroradiometer (MISR) (Diner et al., 1998) instrument onboard the Terra satellite has provided global coverage of AOD once a week since December 1999. The standard MISR retrieval algorithm provides AOD observations at 17.6 km resolution using 16-x-16 pixels of 1.1 km x 1.1 km each. About 70% of MISR AOD retrievals are within 20% of the paired AERONET AOD, and about 50% of MISR AOD falls within 10% of the AERONET AOD, except in ~~the~~ dusty and hybrid (smoke+dust) sites (Kahn et al., 2010). We use version 22 of Level 3 monthly AOD product at 0.5° resolution in this study.

2.2 Surface Mass Concentration

Surface $PM_{2.5}$ speciation and PM_{10} (particulate matter with diameter ≤ 10 μm) data are routinely collected by two national chemical speciation monitoring networks: Interagency Monitoring of Protected Visual Environments (IMPROVE) and the ~~PM2.5~~$PM_{2.5}$ National Chemical Speciation Network (CSN) operated by Environmental Protection Agency (EPA) (Hand et al. 2011; Solomon et al., 2014). IMPROVE collects 24-h aerosol speciation every third day at mostly rural sites since 1988. The same frequency of aerosol speciation dataset was collected at EPA CSN sites in urban and suburban areas since 2000. The observed organic carbon is converted to OM by multiplying by 1.4 (Zhao et al., 2013b; Hu et al., 2016). Some precursors of aerosol pollutions (such as NO_2 and SO_2) are observed hourly by EPA (data available at: https://aqsdr1.epa.gov/aqsweb/aqstmp/airdata/download_files.html) and are used in this study. Selected IMPROVE and EPA CSN sites used in this study are shown in Figure 1a.

2.3 Aerosol Extinction Profile

The aerosol extinction coefficient profile reflects the attenuation of the light passing through the atmosphere due to the scattering and absorption by aerosol particles as a function of range. ~~-~~Version 3 Level 2 532 nm aerosol extinction profiles derived from Cloud-Aerosol Lidar

with Orthogonal Polarization (CALIOP) backscatter profiles collected onboard the Cloud-Aerosol Lidar and Infrared pathfinder Satellite Observation (CALIPSO) satellite are used (Omar et al., 2009; Young and Vaughan, 2009). Seasonal mean profiles are derived for WY2013 based on the methodology outlined in Campbell et al. (2012), whereby quality-assurance protocols are applied to individual profiles before aggregating and averaging the data. We highlight that no individual profiles are included in the averages if the CALIOP Level 2 retrieval failed to resolve any extinction within the column, a potential ~~biasing~~ issue to create bias that has recently been described by Toth et al. (~~2016~~2017). Level 2 532 nm aerosol extinction data classify ~~is speciated, with algorithms resolving~~ aerosols into 6 types ~~present for~~: clean marine, dust, polluted continental, clean continental, polluted dust and smoke. ~~-~~Dust and polluted dust are ~~specifically~~ distinguished in the averages ~~applied below~~in this study for their contribution to total extinction and the vertical profile seasonally in the SJV.

2.4 ~~Equivalent Potential Temperature~~Meteorology

AIRS ~~Equivalent potential temperature (θ_e) is a quantity relevant to the stability of the air. The θ_e profiles used in this study are derived from temperature and moisture profiles observed by AIRS~~ (Atmospheric Infrared Sounder) onboard the Aqua satellite (Susskind et al., 2003; Divakarla et al., 2006). ~~AIRS~~ has provided global coverage of the tropospheric ~~atmosphere~~ temperature and moisture at approximately 01:30 and 13:30 local time since 2002. AIRS retrievals have root-mean-squared (RMS) ~~difference~~ error of ~1 K for temperature and ~15% for water vapor (Divakarla et al., 2006). Level 3 monthly temperature and moisture retrievals (version 6) at 1° x 1° grid are used in this study. Vertical gradient of e~~E~~quivalent potential temperature (θ_e) ~~is a quantity relevant to the stability of the air. The θ_e profiles used in this study are~~marks atmospheric stability and is ~~derived~~computed from temperature and moisture profiles observed by AIRS. Surface

observations, including air temperature, relative humidity (RH) and wind speed, are routinely collected at the California Irrigation Management Information System (CIMIS; http://www.cimis.water.ca.gov/). Precipitation used in this study is the Climate Prediction Center (CPC) Unified Gauge-Based Analysis of Daily Precipitation product at 0.25° x 0.25° resolution.

3. Model Description and Experiment Setup

The WRF-Chem model Version 3.5.1 (Grell et al., 2005) updated by Pacific Northwest National Laboratory (PNNL) is used in this study (Zhao et al., 2014). ~~Similar to the chemical parameterizations used in the Zhao et al. (2014), t~~This study uses the CBM-Z (carbon bond mechanism) photochemical mechanism (Zaveri and Peters, 1999) coupled with the ~~four-~~sectional-bin MOSAIC (Model for Simulating Aerosol Interactions and Chemistry) aerosol scheme (Zaveri et al., 2008) as the chemical driver. The major components of aerosols (nitrate, ammonium, EC, primary ~~organic carbon~~OM, sulfate, sea salt, dust, water and~~, etc.~~ other inorganic matter) as well as their physical and chemical processes are simulated in the model. For computational efficiency, aerosol particles in this study are partitioned into four-sectional bins with dry diameter within 0.039-0.156 μm, 0.156-0.625 μm, 0.625-2.5 μm, and 2.5-10.0 μm. Zhao et al. (2013a) compared the impact of aerosol size partition on dust simulations. It showed that the 4-bin approach reasonably produces dust mass loading and AOD compared with the 8-bin approach. The size distribution of the 4-bin approach follows that of the 8-bin approach with coarser resolution, resulting in ±5% difference on the ratio of $PM_{2.5}$-dust/PM_{10}-dust in dusty regions (more large particles and less small particles). Dust number loading and absorptivity are biased high in the 4-bin approach compared with the 8-bin approach.

Aerosols are considered to be spherical and internally mixed in each bin (Barnard et al., 2006; Zhao et al., 2013b). The bulk refractive index for each particle is calculated by volume

averaging in each bin. Mie calculations as described by Ghan et al. (2001) are used to derive aerosol optical properties (such as extinction, single-scattering albedo, and the asymmetry parameter for scattering) as a function of wavelength. Aerosol radiation interaction is included in the shortwave and longwave radiation schemes (Fast et al., 2006; Zhao et al., 2011). By linking simulated cloud droplet number with shortwave radiation and microphysics schemes, aerosol cloud interaction is effectively simulated in WRF-Chem (Chapman et al., 2009). Aerosol snow interaction is implemented in this version of WRF-Chem (Zhao et al., 2014) by considering aerosol deposition on snow and the subsequent radiative impacts through the SNICAR (SNow, ICe, and Aerosol Radiative) model (Flanner and Zender, 2005, 2006). ~~More details of the chemical settings used in this study can be found in Zhao et al. (2014) and references therein.~~

The model simulations start on 1 September 2012 and run continuously for 13 months. With the first month ~~as~~ used for the model spin-up, our analysis focuses on WY2013 from October 2012 to September 2013. The model is configured with 40 vertical levels ~~,~~ and a model top at 50 hPa. The vertical resolution from the surface to 1 km gradually increases from 28 m to 250 m. The model center is placed at 38°N, 121°W, with 250 x 350 grid points~~s~~ at 4 km horizontal resolution (referred to as "4km" hereafter; Table 1), covering California and the surrounding area. To test the sensitivity of the aerosol simulations ~~on~~ to horizontal resolution, one simulation with the same model settings and domain coverage is conducted at 20 km horizontal resolution (referred to as "20km" hereafter).

The physics parameterizations used in the simulations include the Morrison double-moment microphysics scheme (Morrison et al., 2009), Rapid Radiative Transfer Model for General circulation model (RRTMG) shortwave and longwave radiation schemes (Iacono et al., 2008),

~~Yonsei University (YSU) planetary boundary layer scheme (Hong et al., 2006),~~ Community Land Model (CLM) Version 4 land surface scheme (Lawrence et al., 2011). The Yonsei University (YSU) planetary boundary layer (PBL) scheme (Hong et al., 2006) is used in all of the simulations, except one sensitivity experiment that uses the ACM2 (Asymmetric Convective Model with non-local upward mixing and local downward mixing; Pleim, 2007) PBL scheme (referred to as "20km_P7" hereafter, Table 1). Subgrid convection, convective transport of chemical constituents and aerosols, and wet deposition from subgrid convection are parameterized using the Grell 3D ensemble cumulus scheme (Grell and Devenyi, 2002) ~~is used~~ in the 20 km simulations while convective processes are resolved in the 4 km simulations ~~does not use cumulus parameterization~~. The ~~ERA-Interim~~Interim European Center for Medium-Range Weather Forecasts Re-Analysis ~~reanalysis data~~ (ERA-Interim; Dee et al., 2011) ~~provides~~ serves as~~meteorological~~ initial and boundary meteorological conditions for ~~the~~ WRF-Chem. The MOZART-4 global chemical transport model (Emmons et al., 2010) is used for ~~the chemical~~ initial and boundary chemical conditions. Fast et al. (2014) found that the MOZART-4 model ~~has overestimation of~~overestimates aerosols in the free troposphere over California, which is also found in one of our sensitivity experiments ("20km_BC1" in the supplementary). Following Fast et al. (2014), the chemical initial and boundary conditions from MOZART-4 are divided by two in all simulations except 20km_BC1.

Anthropogenic emissions are provided by US EPA 2005 National Emissions Inventory (NEI05), with area-type emissions on a structured 4-km grid and point-type emissions at specific latitude and longitude locations (US EPA, 2010). Nineteen gases (including SO_2, NO, NH_3 etc.) are emitted, and aerosol emissions include SO_4, NO_3, EC, organic aerosols, and total $PM_{2.5}$ and PM_{10} masses. Anthropogenic emissions are updated every hour to account for diurnal variability,

while its seasonal variation is not considered in the simulations. A sensitivity experiment with 2011 NEI emissions ("20km_NEI11" in the supplementary) does not produce significantly different results from the 2005 NEI emissions. ~~-~~Biogenic emissions are calculated online using the Model of Emissions of Gases and Aerosols from Nature (MEGAN) model (Guenther et al., 2006). Biomass burning emissions are obtained from the Global Fire Emissions Database~~,~~ version 2.1, with eight-day temporal resolution (Randerson et al., 2007) and updated monthly. Sea salt emissions ~~use~~ are derived from the PNNL-updated sea salt emission scheme that includes the correction of particles with radius less than 0.2 μm (Gong et al., 2003) and dependence on sea surface temperature (Jaeglé et al., 2011).

Following Zhao et al. (2013b), dust emission is computed from the GOCART (Goddard Global Ozone Chemistry Aerosol Radiation and Transport) dust scheme (Ginoux et al., 2001) in the 20km and 4km simulations. The GOCART dust scheme estimates the dust emission flux F as

$$F = CSs_p u_{10m}^2 (u_{10m} - u_t) \quad (1),$$

where C is an empirical proportionality constant, S is a source function for potential wind erosion that is derived from 1° x 1° GOCART database (Freitas et al., 2011), s_p is a fraction of each size class dust in emission, u_{10m} is 10-m wind speed and u_t is a threshold speed for dust emission.

As shown later, a significant amount of dust is observed in the SJV, ~~while~~ whereas the GOCART dust scheme produces little dust. ~~One~~ Two sensitivity experiments at 20 km and 4 km horizontal resolution (hereafter referred to as "20km_D2" and "4km_D2", respectively ~~hereafter~~) ~~is~~ are conducted by switching the dust emission scheme to the DUST TRANsport model (DUSTRAN) scheme (Shaw et al., 2008). ~~Detailed descriptions of the two dust emission schemes can be found in Zhao et al. (2010).~~ The DUSTRAN scheme estimates F as

$$F = \alpha C u_*^4 \left(1 - \frac{f_w u_{*t}}{u_*}\right) \quad (2),$$

where C is an empirical proportionality constant, α is the vegetation mask, u_* is the friction velocity, u_{*t} is a threshold friction velocity and f_w is the soil wetness factor. The C value in both GOCART and DUSTRAN is highly tunable for different regions. The original C values, 1.0 $\mu g\ s^2\ m^{-5}$ in GOCART (Ginoux et al., 2001) and $1.0\times10^{-14}\ g\ cm^{-6}\ s^{-3}$ in DUSTRAN (Shaw et al., 2008), are used in this study.

4. Model Simulation Results

Shown in Fig. 1a, our model domain includes three urban sites (Fresno, Bakersfield and Modesto) and two rural sites (Pinnacles and Kaiser) where surface measurements of aerosols are available. ~~WRF-Chem model simulation results and their evaluations are in this section. We start the discussions with a focus on the polluted urban areas.~~ Because aerosols properties and model performance are similar at all urban sites, our discussion is focused on the results at Fresno~~, CA while those at~~ and the simulations for other urban sites are provided in the supplementary materials. Model simulations in the rural areas are presented in the last subsection.

4.1 Sensitivity to Horizontal Resolution

Figure 1 ~~shows~~ features daily mean anthropogenic $PM_{2.5}$ emission rates used in the 20km and 4km simulations, respectively. Although both ~~of the PM2.5~~ emission rates are derived from the 4 km NEI05 dataset, localized high emission rates with sharp gradients are evident ~~at~~ in urban areas ~~in~~ from the 4km simulation (~~Figure~~Fig. 1b). The 20km simulation ~~has~~ exhibits lower emission rates at the urban areas with ~~smoother features~~weaker gradients due to the ~~averaging~~ reapportionment process (~~Figure~~Fig. 1a). As precipitation is an important process that removes aerosols, we examine the simulated precipitation for the 20km and 4km runs and find that the 20km simulation produces 51% more precipitation, although the domain averaged precipitation is lower in the 20km run than the 4km run (Fig. 2a).

Consistent with ~~the~~ higher emission rates and lower precipitation at Fresno ~~differences~~, the 4km run simulates higher AOD ~~is simulated at 4km~~ than the 20km run ~~, mainly~~ in the cold season (October-November-December and January-February-March; OND and JFM in ~~Figure~~Fig. ~~2~~3). Averaged over a broad area encompassing Fresno and Bakersfield, the most polluted region in the SJV (red box in Fig. 1a), the AOD is 0.090 in the 4km and 0.073 in the 20km, a 23% difference. Compared to the MISR observations, t~~T~~he 4km simulation reproduces the spatial distribution and magnitude of AOD ~~observed by MISR well~~ in the cold season. However, t~~T~~he AOD difference between the 20km and 4km runs ~~is~~ small in the warm season (April-May-June and July-August-September; AMJ and JAS in ~~Figure~~Fig. ~~2~~3~~).~~), and b~~B~~oth ~~the 20km and 4km~~ runs underestimate AOD by ~50% with respect to the MISR observations.

Comparing the point values at Fresno in the 4km and 20km simulations (Fig. 4a), we find similar results: the 4km AOD is closer to the AERONET measurements and is about 23% higher than that in the 20km run during the cold season, while both runs are biased low in AOD during the warm season ~~in the warm season compared with MISR. Model performance identified in Figure 2, including the sensitivity to horizontal resolution in cold season and underestimation of AOD in warm season, are further confirmed by comparing to AERONET observations at Fresno, CA (Figure 3). In cold season at Fresno, the AOD in the 20km simulation is 23% lower than the AOD in the 4km simulation.~~ The different model sensitivities to horizontal resolution ~~from~~ between the cold ~~to the~~and warm seasons suggest that the dominant aerosol sources ~~are~~ may be different ~~through~~ for the two seasons. We will elaborate upon the aerosol composition in the following section. MISR and AERONE~~N~~T ~~shows~~ observations display weak ~~small~~ seasonal AOD variation ~~of AOD~~ in the SJV and at Fresno, respectively, which is not well represented in the 20km and 4km simulations (~~Figure~~Fig. ~~2~~ 3 and ~~3~~4a).

Aside from AOD, significant seasonal variability of AE (Fig. 4b) is shown at Fresno. AE exhibits a maximum about 1.50 in January and a minimum of 0.98 in April, suggesting relatively small particles in the winter and large particles in the spring. A relatively large AE value of 1.40 (corresponding to small particles) is observed in July, possibly related to the wild fires in late July in the SJV. WRF-Chem captures the seasonal variability of the AE well, with a correlation of 0.90 in both the 20km and 4km simulations. The magnitude of AE is also approximately simulated in the cold season, with a mean of 1.15 (1.20) in the 20km (4km) runs compared to 1.33 in the observation. However, the simulated AE is underestimated by ~30% in the warm season, indicating that the simulated particle size is biased high during this period.

Significant seasonal variability of $PM_{2.5}$ is observed in the SJV urban areas (~~Figure~~Fig. ~~4a~~ 5a and Supplementary ~~Figure~~Fig. ~~1a~~ 4a and ~~5~~2~~a~~). $PM_{2.5}$ at Fresno peaks in January (26.18 μg m^{-3}) and ~~has~~ reaches a minimum of 7.03 μg m^{-3} in June, with an annual nonattainment value of 12.64 μg m^{-3} ~~in total~~ (~~Figure~~Fig. ~~4a~~5a). ~~All WRF-Chem simulations~~Both the 20km and 4km runs ~~successfully~~ approximately capture the observed seasonal variability of $PM_{2.5}$~~, observed in the SJV~~with a correlation around 0.90 (Table 2).

In the cold season, the 4km simulation overestimates $PM_{2.5}$ by 27% while the 20km simulation exhibits a low bias of 19% compared with IMPROVE observations at Fresno (Table ~~2~~3). The 4km simulation of PM_{10} ~~has~~is in good agreement with IMPROVE in the winter (December, January and February), but ~~a large~~has significant low biases of between 30% and 85% ~~is found~~ in other months (~~Figure~~Fig. ~~4~~5b). ~~The~~ 20km simulation underestimates PM_{10} throughout WY2013.

Formatted: Subscript

Formatted: Subscript

Formatted: Subscript

Formatted: Subscript

Formatted: Subscript

Formatted: Subscript

$PM_{2.5}$ is a mixture of nitrate (NO_3), ammonia (NH_4), OM, EC, sulfate (SO_4), dust and other aerosols. High ~~PM2.5~~ concentrations of $PM_{2.5}$ are ~~primarily~~primarily the result of ~~nitrate~~NO_3 at Fresno (Fig. 5c). Both simulations produce the seasonal variability of ~~nitrate~~ NO_3 with a correlation of 0.94, but ~~with~~ high bias of 17% (75%) ~~high biases~~is found ~~of 17%~~ in the 20km ~~and 75% in~~ (4km) simulations ~~in~~ during the cold season ~~(Figure 4c)~~. As one precursor of NO_3, NO_2 is underestimated by 43% in the 20km run (Fig. 6a). The overestimation in NO_3 and underestimation in NO_2 suggest that the precursor emissions may not the reason for the high biases in NO_3. NH_4 shows a similar performance to NO_3, with an overestimation by 38% (111%) in the 20km (4km) runs during the cold seasons (Fig. 5d). As shown later in section 4.3, both NO_3 and NH_4 simulations are quite sensitive to the PBL scheme applied. ~~It suggests that the NEI05 dataset may have a high bias in nitrate emissions, which was also found in Texas (Kim et al., 2011).~~

OM~~C~~, the second largest ~~contributor~~ contributing species ~~of~~ to cold season $PM_{2.5}$ in the SJV (Table 3), is significantly underestimated by 82~~76~~% in the 20km simulation (~~Figure~~Fig. ~~4~~5f). The 4km simulation produces ~~more~~ higher OM~~C than the 20km simulation~~, but it is still lower than the IMPROVE observations by ~~46~~63%. The underestimation of OM is expected, because SOA processes are not included in our model infrastructure. Fast et al. (2014) used the simplified two-product volatility basis set parameterization to simulate equilibrium SOA partitioning in WRF-Chem although SOA was still underestimated in their simulation. It remains ongoing research how to correctly represent SOA processes in regional climate models. ~~suggested that the low bias in the WRF-Chem simulation is primarily due to incomplete understanding of SOA processes.~~

Both the 20km and 4km simulations reproduce the seasonal variability of EC, with a correlation of 0.98 between the modeled and observed time series (Table 2). The 20km simulation

Formatted: Subscript

Formatted: Subscript

Formatted: Subscript

underestimates ~~Significant underestimation of~~ EC by 52% (16%) ~~and sulfate~~ in the cold (warm) season (Fig. 5e and Table 3). ~~are also shown in the 20km simulation, while t~~The 4km simulated EC~~ion~~ (1.12 μg m^{-3}) exhibits good agreement with IMPROVE (1.08 μg m^{-3}) ~~(Figure 4d and 4e)~~in the cold season, but overestimates EC by 53% in the warm season.

The seasonal variability of SO_4 at Fresno is very different from other $PM_{2.5}$ species. It peaks in May at 1.35 μg m^{-3} and reaches the minimum of 0.67 μg m^{-3} in August (Fig. 5g). The 20km simulated SO_4 exhibits good correlation of 0.63 with the observation (Table 2), but is biased low by 28% to 63% throughout WY2013 (Fig. 5g). Although the observed SO_2, the precursor of SO_4, has approximately similar seasonal variation to the observed SO_4 (Fig. 6b), the 20km simulated seasonal variability of SO_2 resembles other anthropogenic emissions, with high values in the cold season and low values in the warm season, out of phase with the simulated SO_4 and the observed SO_2. The 4km simulation produces higher SO_4 than the 20km run, resulting in better agreement with the observation (0.82 μg m^{-3} vs. 0.87 μg m^{-3}) during the cold season (Fig. 5g and Table 3). However, the 4km run produces an increase of SO_4 by only 13% comparing to the 20km run in the warm season, resulting in a correlation of -0.16 between the 4km simulation and the observation.

To explore the possible cause for the underestimation of SO_4 and SO_2 in the warm season in both the 20km and 4km simulations, we conduct a sensitivity experiment with different chemical boundary conditions from the baseline runs (20km_BC1 in the supplementary). We find that SO_4 in the SJV is partly contributed to by marine intrusions (the different chemical boundary conditions between 20km_BC1 and 20km_D2) throughout the year (supplementary Fig. 2g), as pointed out by Fast et al. (2014). Including the marine intrusions, the 20km_BC1 simulated SO_4 tracks the observation at a correlation of 0.78. Doubled chemical boundary conditions in the 20km simulation

Formatted: Subscript

Formatted: Subscript

results in 41% increase in SO_4 at Fresno, with a stronger increase in the warm season. Compared to the observed SO_4 of 1.04 μg m^{-3} in the warm season, the simulated SO_4 of 0.79 μg m^{-3} in the 20km_BC1 run is closer to the observation than that simulated in the 20km_D2 run (0.53 μg m^{-3}). The relative contributions of local emissions and remote transports (as well as other emission sources, such as wild fires) to SO_4 concentrations in different seasons of the SJV require further investigation.

~~Sulfate in both simulations exhibits a low bias of ~45% in the warm season. Low bias of simulated sulfate, with a failure of capturing the peaks during late afternoon, was also shown at Bakersfield in Fast et al. (2014). It suggests that improvement in understanding the photochemical processes involving sulfate is needed to reproduce seasonal variability of sulfate in the SJV. The 4km simulation of PM10 has good agreement with IMPROVE in winter (December, January and February), but a large low bias is found in other months (Figure 4b). The 20km simulation underestimates PM10 throughout WY2013.~~

Overall, the 4km simulation produces higher AOD and surface PM than the 20km simulation in urban areas of the SJV, especially ~~in~~ during the cold season~~., The 4km simulation has~~resulting in better agreement with satellite and surface ~~observ~~observations~~ations~~ than the 20km simulation. Both the ~~The~~ 20km and 4km simulations approximately capture~~s~~ the seasonal variability of $PM_{2.5}$ and most of its speciation. However, significant ~~underestimation~~ low biases of AOD and PM_{10} are ~~shown~~ found during the warm season in both ~~4km and 20 km~~ simulations. The underestimation also exists in a sensitivity experiment (not shown) with the same model setups except initialized in April ~~(not shown)~~, indicating that the identified model biases during the warm season are not caused by potential model drift after a relatively long simulation period. The relatively good performance in simulating $PM_{2.5}$ but not PM_{10} during the warm season suggests

Formatted: Subscript
Formatted: Subscript
Formatted: Subscript
Formatted: Subscript
Formatted: Subscript
Formatted: Subscript

that coarse aerosol particle mass (CM; 10 μm ≥ particulate matter with diameter > 2.5 μm), mainly dust in the SJV, is ~~-~~not properly represented ~~well~~ in the ~~simulations~~model. The impact of dust parameterizations is investigated in the 4km_D2 experiment.

4.2 Sensitivity to Dust Scheme

Limited amounts of $PM_{2.5}$ dust (dust with diameter ≤ 2.5 μm) are observed in the SJV cold season, with a minimum of 0.37 μg m^{-3} in December (~~Figure~~Fig. ~~5c~~7a). The amount of $PM_{2.5}$ dust increases in the warm season, with a peak of 3.86 μg m^{-3} in September. The 4km simulation produces comparable $PM_{2.5}$ dust relative to IMPROVE in the winter, but almost no dust in other months (Fig. 7 and upper panel in Fig. 8). On the other hand, the dust emission rate in the 4km_D2 run is significantly higher than the 4km run. We have found that the source function, *S*, for potential wind erosion in the SJV is set to zero in the 1°x1° GOCART dataset used for the 4km simulation (Fig. 9). An updated source function, *S*, at higher resolution is needed for the GOCART dust scheme to correctly represent dust emissions in the SJV.

The 4km_D2 simulation ~~represents well~~reproduces the ~~magnitude~~ amount of $PM_{2.5}$ dust in OND~~cold season~~ (Fig. 7a). However, ~~too much~~it overestimates $PM_{2.5}$ dust by up to a factor of 3 ~~is simulated~~ in the warm season, resulting in an overestimation of $PM_{2.5}$ by 52% (~~Figure~~Fig. ~~5b~~ 7b and Table ~~2~~3). $PM_{2.5}$ dust is not sensitive to long-range transport (from chemical boundary conditions in the model simulation; Supplementary Fig. 2h). Both the 4km and 4km_D2 simulations capture the seasonal variability of $PM_{2.5}$, but not ~~that of~~for PM_{10} (~~Figure~~Fig. ~~5a~~7c). The magnitude of PM_{10} in the 4km_D2 run is larger than the 4km simulation. PM_{10} in the 4km_D2 run is overestimated in April-May-June (AMJ) but underestimated in July-August-September (JAS), leading to a comparable season mean of 38.12 μg m^{-3} with IMPROVE observed 34.82 μg

Formatted: Subscript
Formatted: Subscript
Formatted: Subscript
Formatted: Subscript
Formatted: Subscript
Formatted: Subscript
Formatted: Subscript
Formatted: Subscript
Formatted: Subscript
Formatted: Subscript

1345 m^{-3}~~ations~~. The overestimation of AMJ PM_{10} and $PM_{2.5}$ dust in the 4km_D2 run is likely associated
1346 with the high bias in the simulated wind speed (Fig. 2b).

1347 On the relative contribution of different aerosol species, IMPROVE observations at Fresno
1348 show that ~~nitrate~~ NO_3 is the primary contributor (32.3%) to $PM_{2.5}$ while only 5.3% of $PM_{2.5}$ is dust
1349 in the cold season (panel 1 of ~~Figure~~Fig. ~~6~~10). Both the 4km and 4km_D2 runs roughly reproduce
1350 the relative contributions to $PM_{2.5}$ in the cold season, with an overestimation of ~~nitrate~~ NO_3 and
1351 NH_4 and an underestimation of ~~OC~~ OM, ~~found in~~consistent with the time series in ~~Figure~~Fig. ~~4~~5.
1352 Relative contributions of dust to $PM_{2.5}$ are better simulated in the 4km_D2 run (7.3%) than ~~in~~ the
1353 4km one (<1.0%). IMPROVE shows that 46.6% of PM_{10} is CM in the cold season (panel 2 of
1354 ~~Figure~~Fig. ~~6~~10). Both the 4km (6.3%) and 4km_D2 (20.6%) runs underestimate the contribution
1355 of CM to PM_{10}, mainly in October and November. In the warm season, dust (24.6%) becomes the
1356 primary contributor to $PM_{2.5}$ while the contribution from ~~nitrate~~ NO_3 decreases to 9.9% ~~as~~
1357 ~~observed by~~in IMPROVE observations (panel 3 of ~~Figure~~Fig. ~~6~~10). Almost no $PM_{2.5}$ dust is
1358 simulated in the 4km run while too much $PM_{2.5}$ dust is produced in the 4km_D2 (50.5%) run ~~in~~
1359 during the warm season. The relative contribution of CM to PM_{10} is too small (27.6%) in the 4km
1360 run, while the 4km_D2 run ~~has~~ reflects an better relative contribution of 66.3% as compared~~ing~~
1361 to an IMPROVE observed 75.8% (panel 4 of ~~Figure~~Fig. ~~6~~10).

1362 AOD simulations are improved in the 4km_D2 experiment (~~Figure~~Fig. ~~7~~11), with better
1363 agreement ~~with~~ found from MISR (~~Figure~~Fig. ~~2~~3) in AMJ. AOD (0.114) in the 4km_D2 run is
1364 comparable to observations (0.131) in AMJ, but still underestimated by 53% in JAS. Consistent
1365 with AOD, the vertical distribution of aerosol extinction is reasonably simulated ~~in~~ during the cold
1366 season in the WRF-Chem simulations, while large discrepancies are ~~shown~~ found in the warm
1367 season (~~Figure~~Fig. ~~8~~12). As observed by CALIOP at 532 nm, aerosols are mainly confined below

Formatted: Subscript
Formatted: Subscript
Formatted: Subscript
Formatted: Subscript
Formatted: Subscript
Formatted: Subscript
Formatted: Subscript
Formatted: Subscript
Formatted: Subscript
Formatted: Subscript
Formatted: Subscript

1 km above the surface in the cold season. Model simulations ~~reasonably~~ roughly capture the vertical distribution of aerosol extinction observed by CALIOP, with low biases in the boundary layer and high biases in the free atmosphere. Similar discrepancy between the model simulations and CALIOP is shown in other studies (Wu et al., 2011a; Hu et al., 2016). The difference between the 4km and 4km_D2 runs is small ~~in~~ during the cold season.

Dust in the boundary layer is a primary factor contributing to aerosol extinction in the SJV, as illustrated by the differences between the bulk seasonal CALIOP mean profile and those excluding the contributions of the dust and polluted dust ~~species~~ (CALIOP_nodust) profiles (~~Figure~~Fig. ~~8~~12). ~~The s~~Simulated aerosol extinction~~s~~ falls between the two in all seasons, suggesting ~~relatively good performance of simulating aerosols except for dust~~that dust is the primary factor contributing to the model biases in aerosol extinction. Although a small portion of $PM_{2.5}$ is dust in the cold season, ~~dust~~ it contributes to about 50% of total aerosol extinction (~~Figure~~Fig. ~~8a~~ 12a and ~~8b~~12b). ~~-~~A predominant~~te~~ portion of aerosol extinction in the boundary layer is contributed ~~to~~ by dust in the warm season (~~Figure~~Fig. ~~8c~~ 12c and ~~8d~~12d). There, the 4km_D2 simulation produces higher aerosol extinction in the boundary layer than the 4km simulation, although it is still lower than CALIOP. The simulated aerosol extinction in the free troposphere above the boundary layer is close to or larger than CALIOP, suggesting that aerosols transported from remote areas through chemical boundary conditions (e.g., the differences between the 20km_BC1 and 20km_D2 runs in Supplementary Fig. 3) may not be the major factor contributing to the underestimation of dust in the boundary layer in the SJV.

Overall, the poor simulations of dust in the boundary layer play ~~the~~ a dominant role in the low bias of aerosols during~~, especially in~~ the warm season. Both the GOCART and DUSTRAN dust emission schemes used in this study have ~~problems~~ difficulties in reproducing dust emissions

Formatted: Subscript

in the SJV, with an underestimation in GOCART and an overestimation in DUSTRAN (~~Figure~~Fig. ~~5c~~7). Improvement on the dust emission schemes is needed ~~is required~~ for ~~correctly~~ capturing ~~simulating~~ the seasonal variability of aerosols in the SJV.

4.3 The Role of Meteorology

The WRF-Chem simulations approximately reproduce the seasonal variations of meteorological variables near the surface (correlations > 0.80), including temperature, RH, wind speed and precipitation (Supplementary Fig. 6 and Supplementary Table 1). All of the model simulations exhibit warm and dry biases near surface and in the boundary layer, with cold and wet biases in the free atmosphere (Supplementary Fig. 6-8 and Supplementary Table 2). The dry bias in the 4km_D2 run is about 10% near the surface throughout WY2013. Due to the relative dry environment (RH<50%) in the warm season, the dry bias is likely not responsible for the underestimation of boundary layer aerosol extinctions and column-integrated AOD through hygroscopic effects (Feingold and Morley, 2003). In the cold season, the surface wind speed is underestimated by 0.67 m/s (1.00 m/s) in the 4km_D2 (20km_D2) runs. In the warm season, the 4km_D2 run overestimates wind speed by 0.78 m/s, while the 20km_D2 run has an underestimation of 0.16 m/s. These results suggest that wind speed is also not the primary factor contributing to low biases in the boundary layer aerosols. The seasonal variability of precipitation is well captured in the simulations, while the magnitude of precipitation is smaller than the observations during the warm season (Supplementary Table 2). Wet removal processes are thus not likely the primary reason for the aerosol biases in the warm season.

In the warm season, more aerosols are observed at higher altitude than during the cold season (~~Figure~~Fig. ~~8~~12). A well-mixed layer of aerosols is observed below 1.5 km in AMJ (~~Figure~~Fig. ~~8c~~12c), consistent with the ~~the large i~~unstable layers~~ility~~ below 1.5 km observed by

AIRS (~~Figure~~Fig. ~~9c~~13c). However, the WRF-Chem ~~Both~~ model simulates neutral (or weakly stable) layers below 1.5 km (Fig. 13c), which may lead to a ~~ions~~ failure in~~to~~ capturing~~e~~ the well-~~is~~ mixed layer of aerosols (~~Figure~~Fig. ~~8c~~12c) ~~due to weak vertical mixing as evidenced by relatively small instability in the simulations (Figure 9c)~~. Although the dust emission at the surface is large in the 4km_D2 run, not enough convective vertical mixing is produced in the simulations, plausibly resulting in the low biases found in the boundary layer. Aerosol extinction gradually decreases with height in the simulations ~~(Figure 8c)~~. Similar biases of aerosol and instability in the boundary layer are also shown in JAS (~~Figure~~Fig. ~~8d~~ 12d and ~~9d~~13d). ~~Weak instability~~Relative static stability in the simulations, which limits convective vertical mixing of aerosols, likely enhances the low bias of ~~JAS~~ column-integrated AOD in JAS (~~Figure~~Fig. ~~7~~11). Although the 4km_D2 experiment produces comparable AOD and surface PM mass in AMJ (~~Figure~~Fig. ~~5~~ 6 and ~~Figure~~Fig. ~~7~~11), the vertical distribution of aerosols is not well represented (~~Figure~~Fig. ~~8~~12). The comparable AOD in the 4km_D2 run results from the low bias in the boundary layer and the high bias in the free atmosphere. In JAS (Fig. 12d), ~~The high bias~~comparable aerosol extinction to CALIOP is simulated in the free atmosphere, suggesting~~s~~ that the low bias in AOD ~~are~~ is not due to the halved chemical boundary conditions from MOZART-4. Albeit some discrepancies in the magnitude of atmospheric stability, ~~The stability biases in cold season are relatively small~~all of the simulations capture the stable environment in the cold season (~~Figure~~Fig. ~~9a~~ 13a and ~~9b~~13b), consistent with relatively good performance of aerosol simulations in the cold season.

As biases in the model simulations are found mainly within the boundary layer, a sensitivity experiment is conducted at 20 km resolution using the ACM2 PBL scheme (20km_P7). Although the changes in the meteorological variables (Supplementary Fig. 6-8) and atmospheric static stability (Fig. 13) are rather small, the simulated surface NO_3 and NH_4 in the 20km_P7 run

decrease by 50% compared to the 20km_D2 run (Fig. 14c, 14d and Table 3). Considering that more NO_3 and NH_4 are simulated at 4 km resolution than at 20 km resolution as shown in section 4.1, the use of the ACM2 PBL scheme at 4 km simulation would largely resolve the high biases of NO_3 and NH_4 in the 4km_D2 simulation. The decrease of NO_3 and NH_4 at the surface is because more aerosols are transported to the layers above 0.5 km (Fig. 15a and 15b), resulting from different convective vertical mixing in the PBL schemes. However, $PM_{2.5}$ dust is significantly overestimated by a factor of 4 in the 20km_P7 simulation (Fig. 14h), leading to a small decrease of $PM_{2.5}$ by only 8% compared with the 20km_D2 run in the cold season. In the warm season, $PM_{2.5}$ dust in the 20km_P7 run is overestimated by a factor of 5, causing an overestimation of $PM_{2.5}$ and PM_{10} (Fig. 14a and 14b). Aerosol extinctions in the boundary layer increase in the warm season (Fig. 15c and 15d), possibly related to overestimation of dust emissions and more conducive convective vertical transport in the PBL scheme.

Formatted: Subscript

Formatted: Subscript

Formatted: Subscript

Formatted: Subscript

Formatted: Subscript

In summary, the WRF-Chem model captures the seasonal variations of meteorological variables (temperature, RH, wind speed and precipitation), despite some deviations in magnitude. The low biases in aerosol optical properties of the warm season likely do not originate from hygroscopic effects, wet removal processes or dust emissions associated with the wind speed bias. The model simulates a stable environment in the warm season, which is opposite to the observed unstable environment. The simulated stable environment may be most likely responsible for low biases in the aerosol extinction in the boundary layer and the column-integrated AOD in the warm season. Switching to the ACM2 PBL scheme leads to improved vertical mixing in the boundary layer, thus an improvement in the simulations of NO_3 and NH_4 in the cold season. However, dust emissions are significantly overestimated with the ACM2 PBL scheme, which contributes partly to the better simulation of aerosol extinction in the boundary layer and AOD in the column. These

results highlight that ~~the vertical mixing of dust must be correctly represented in order to resolve the aerosol extinction profile correctly. I~~improving the~~ed~~ simulation of boundary layer structure and processes are critical for~~physics and dynamics during the warm season in the SJV warrants future investigation.~~ capturing the vertical profiles of aerosol extinction.

4.4 Results in Rural Areas

In general, low values of PM concentration are observed in the rural areas, Pinnacles and Kaiser (~~Figure~~Fig. ~~10~~16 and ~~11~~17). The rural areas share some similar model performance ~~with~~ to the urban areas, such as the overestimation of ~~nitrate~~NO_3, reasonable simulation of EC, good representation of ~~sulfate~~ SO_4 in the cold season and underestimation of ~~sulfate~~ SO_4 in the warm season. However, the results are not sensitive~~ity~~ to model resolution ~~is not significant~~. It suggests that high ~~model~~ resolution is particularly important for heavily polluted areas due to the inhomogeneity of emission sources, but less important for relatively lightly polluted areas.

In late July/early August, MODIS (Moderate Resolution Imaging Spectroradiometer) fire data (not shown) ~~observed~~ showed active wild fires close to Kaiser, which resulted in high concentration of aerosols ~~at Kaiser~~locally (~~Figure~~Fig. ~~11~~17). Our model simulations with ~~climatological~~ monthly-varying fire emissions fail to reproduce these fire events. ~~Based on fire locations from satellite observations~~ Previous s~~,~~tudies (e.g., Grell et al., 2011; Wu et al. ~~(~~2011a; Archer-Nicholls et al., 2015) ~~has~~ demonstrated that the WRF-Chem model can capture aerosols distributions from wild fires based on fire locations from satellite observations ~~over South America~~. Campbell et al. (2016) further described the difficulties in ~~both~~ constraining total aerosol mass from operational satellite fire observations and the time ~~necessary within~~needed by the model for diffusion within the near-surface layers to render both reasonable AOD and vertical profiles of

aerosol extinction. For operational application of the WRF-Chem model in MAIA retrievals, the observations of daily fire events need to be more appropriately considered.

5. Summary

The WRF-Chem (Weather Research and Forecasting model with Chemistry) model is ~~applied~~ employed to simulate the seasonal variability of aerosols in WY2013 (water year 2013) in the SJV (San Joaquin Valley). Model simulations are evaluated using satellite and in-situ observations. In general, the model simulations conducted at 4 km resolution reproduce the spatial and temporal variations of regional aerosols in the cold season, when aerosols are mainly contributed to by anthropogenic emissions in the SJV. The magnitude of simulated aerosols in the cold season however, especially in ~~the~~ relatively dense urban areas, is sensitive to model horizontal resolution. The 4km simulation has comparable magnitude to ~~the~~ available observations, while the 20km simulation underestimates aerosols. ~~The d~~Differences ~~of~~ in aerosol ~~simulations~~ simulation fidelity ~~between different model~~as a function of variable resolutions are mainly due to the difference in aerosol emissions and simulated precipitation. Emissions at higher resolution can better resolve the inhomogeneity of anthropogenic emissions in the SJV than at lower resolution. The sensitivity to horizontal resolution is small in ~~the~~ rural areas and ~~in~~ during warm season, where/when the relative contribution of anthropogenic emissions is small.

Previous studies in the SJV are mainly focused on $PM_{2.5}$ (particulate matter with diameter ≤ 2.5 μm) and during cold season (e.g. Chow et al., 2006; Herner et al., 2006; Pun et al., 2009; Ying and Kleeman, 2009; Zhang et al., 2010; Chen et al., 2014; Hasheminassab et al., 2014; Kelly et al., 2014; Baker et al., 2015; Brown et al., 2016). CALIOP (Cloud-Aerosol Lidar with Orthogonal Polarization) and IMPROVE (Interagency Monitoring of Protected Visual Environments) observations show that dust is a primary contributor to the aerosols in the SJV,

Formatted: Subscript

especially in the warm season. Dust contributes 24.6% to $PM_{2.5}$ while more than 75.8% to PM_{10} ~~(particulate matter with diameter ≤ 10 μm)~~ in the warm season. For all seasons, the major component of aerosol extinction in the boundary layer is dust as observed by CALIOP, consistent with Kassianov et al. (2012). For a complete understanding of aerosol impacts on air quality, weather and ~~and regional~~ climate, the full spectrum of aerosols should be considered during all seasons.

All the model simulations conducted fail to capture aerosol vertical distribution and variability in the SJV warm season, largely due to the misrepresentation of dust emissions, static stability and vertical mixing in the boundary layer. The GOCART (Goddard Global Ozone Chemistry Aerosol Radiation and Transport) dust emission scheme significantly underestimates dust due to the non-active source function, S, for potential wind erosion used in this study while the DUSTRAN (DUST TRANsport model) scheme may overestimate dust emission in the SJV. Along with the bias in dust emissions, our simulations produce a relatively ~~weak atmospheric instability~~stable boundary layer in the warm season, in contrast with observations suggesting a more unstable environment, leading to a weak vertical mixing of aerosols in the boundary layer. Improved dust emission and better simulations of the boundary layer properties are needed for ~~correct~~ accurate simulation of aerosols in the SJV warm season ~~in the SJV~~.

Other biases are also identified in the model simulations. ~~Nitrate~~ NO_3 and NH_4 in the cold season ~~is~~ are overestimated in the model, ~~possibly due to the overestimation of emissions~~but the results are sensitive to the choice of the PBL (planetary boundary layer) scheme. The ~~Incomplete understanding of~~ SOA (secondary organic aerosol) ~~could~~processes contribute to the underestimation of OM~~C~~ (organic ~~carbon~~matter) in this study. The u~~U~~nderestimation of sulfate in the warm season may be ~~due to~~caused by the ~~incorrect photochemical processes of sulfate in~~

Formatted: Subscript
Formatted: Subscript
Formatted: Font: Not Italic

~~the model~~misrepresentation of emissions and the chemical boundary conditions related to marine intrusions. Aerosols from wild fires are not captured in the simulations with ~~climatological~~ monthly updated fire ~~emissions~~data. Further investigations are needed to improve model simulations in the SJV for both scientific and operational applications. ~~The evaluation framework used in this study can be used to other polluted regions to ensure that aerosols are simulated correctly for the right reasons.~~

Acknowledgements

Th~~is study~~e ~~research described in this paper~~ was carried out at the Jet Propulsion Laboratory, California Institute of Technology, under a contract with the National Aeronautics and Space Administration. The authors thank the funding support from the NASA ACMAP program and JPL PDF program. This work is partially sponsored by California Energy Commission under grant #EPC-14-064. Author JRC acknowledges the support of the NASA ACCDAM program and its manager Hal Maring. The authors thank the three anonymous reviewers for their helpful comments.

References

Archer-Nicholls, S., Lowe, D., Darbyshire, E., Morgan, W. T., Bela, M. M., Pereira, G., Trembath, J., Kaiser, J. W., Longo, K. M., Freitas, S. R., Coe, H., and McFiggans, G.: Characterising Brazilian biomass burning emissions using WRF-Chem with MOSAIC sectional aerosol, Geosci. Model Dev., 8, 549-577, doi:10.5194/gmd-8-549-2015, 2015.

Ångström, A.: On the atmospheric transmission of Sun radiation and on dust in the air, Geogr. Ann., 11, 156–166, 1929.

Baker, K. R., Carlton, A. G., Kleindienst, T. E., Offenberg, J. H., Beaver, M. R., Gentner, D. R., Goldstein, A. H., Hayes, P. L., Jimenez, J. L., Gilman, J. B., de Gouw, J. A., Woody, M. C., Pye, H. O. T., Kelly, J. T., Lewandowski, M., Jaoui, M., Stevens, P. S., Brune, W. H., Lin, Y.-H., Rubitschun, C. L., and Surratt, J. D.: Gas and aerosol carbon in California: comparison of

measurements and model predictions in Pasadena and Bakersfield, Atmos. Chem. Phys., 15, 5243-5258, doi:10.5194/acp-15-5243-2015, 2015.

Barnard, J. C., Fast, J. D., Paredes-Miranda, G., Arnott, W. P., and Laskin, A.: Technical Note: Evaluation of the WRF-Chem "Aerosol Chemical to Aerosol Optical Properties" Module using data from the MILAGRO campaign, Atmos. Chem. Phys., 10, 7325–7340, doi:10.5194/acp-10-7325-2010, 2010.

Brown, S. G., Hyslop, N. P., Roberts, P. T., McCarthy, M. C., and Lurmann, F. W.: Wintertime vertical variations in particulate matter (PM) and precursor concentrations in the San Joaquin Valley during the California Regional Coarse PM/Fine PM Air Quality Study, J. Air Waste Manage., 56, 1267–1277, 2006.

Campbell, J. R., Tackett, J. L., Reid, J. S., Zhang, J., Curtis, C. A., Hyer, E. J., Sessions, W. R., Westphal, D. L., Prospero, J. M., Welton, E. J., Omar, A. H., Vaughan, M. A., and Winker, D. M.: Evaluating nighttime CALIOP 0.532 μm aerosol optical depth and extinction coefficient retrievals, Atmos. Meas. Tech., 5, 2143-2160, doi:10.5194/amtd-5-2143-2012, 2012.

Campbell., J. R., Ge, C., Wang, J., Welton, E. J., Bucholtz, A., Hyer, E. J., Reid, E. A., Chew, B. N., Liew, S.-C., Salinas, S. V., Lolli, S., Kaku, K. C., Lynch, P., Mahmud, M., Mohamad, M., and Holben, B. N.: Applying Advanced Ground-Based Remote Sensing in the Southeast Asian Maritime Continent to Characterize Regional Proficiencies in Smoke Transport Modeling, J. Appl. Meteorol. Climatol., 55, 3-22, doi: http://dx.doi.org/10.1175/JAMC-D-15-0083.1, 2016.

Chapman, E. G., Gustafson Jr., W. I., Easter, R. C., Barnard, J. C., Ghan, S. J., Pekour, M. S., and Fast, J. D.: Coupling aerosolcloud-radiative processes in the WRF-Chem model: Investigating the radiative impact of elevated point sources, Atmos. Chem. Phys., 9, 945–964, doi:10.5194/acp-9-945-2009, 2009.

Chen, J., Lu, J., Avise, J. C., DaMassa, J. A., Kleeman, M. J., and Kaduwela, A. P.: Seasonal modeling of PM2.5 in California's San Joaquin Valley, Atmos. Environ., 92, 182–190, 2014.

Chew, B. N., J. R. Campbell, J. S. Reid, D. M. Giles, E. J. Welton, S. V. Salinas and S. C. Liew: Tropical cirrus cloud contamination in sun photometer data, Atmos. Env., 45, 6724-6731, doi:10.1016/j.atmosenv.2011.08.017, 2011.

1581 Chow, J. C., Chen, L. W. A., Watson, J. G., Lowenthal, D. H., Magliano, K. A., Turkiewicz, K.,
1582 Lehrman, D. E.: PM2.5 chemical composition and spatiotemporal variability during the
1583 California regional PM10/PM2.5 air quality study (CRPAQS), J. Geophys. Res.-Atmos., 111,
1584 D10S04, doi:10.1029/2005JD006457, 2006.

1585 Dee, D. P., Uppala, S. M., Simmons, A. J., Berrisford, P., Poli, P, Kobayashi, S., Andrae, U.,
1586 Balmaseda, M. A., Balsamo, G., Bauer, P., Bechtold, P., Beljaars, A. C. M., van de Berg, L.,
1587 Bidlot, J., Bormann, N., Delsol, C., Dragani, R., Fuentes, M., Geer, A. J., Haimberger, L.,
1588 Healy, S. B., Hersbach, H., Hólm, E. V., Isaksen, L., Kallberg, P., Köhler, M., Matricardi, M.,
1589 McNally, A. P., Monge-Sanz, B. M., Morcrette, J.-J., Park, B.-K., Peubey, C., de Rosnay, P.,
1590 Tavolato, C., Thépaut, J.-N., and Vitart, F.: The ERA-Interim reanalysis: configuration and
1591 performance of the data assimilation system, Q. J. R. Meteorol. Soc., 137, 553–597, 2011.

1592 Diner, D. J., Beckert, J. C., Reilly, T. H., Bruegge, C. J., Conel, J. E., Kahn, R. A., Martonchik, J.
1593 V., Ackerman, T. P., Davies, R., Gerstl, S. A. W., Gordon, H. R., Muller, J. P., Myneni, R. B.,
1594 Sellers, P. J., Pinty, B., and Verstraete, M. M.: Multi-angle Imaging SpectroRadiometer
1595 (MISR) Instrument Description and Experiment Overview, IEEE T. Geosci. Remote, 36,
1596 1072–1087, 1998.

1597 Divakarla, M. G., Barnet, C. D., Goldberg, M. D., McMillin, L. M., Maddy, E., Wolf, W., Zhou,
1598 L., and Liu, X.: Validation of Atmospheric Infrared Sounder temperature and water vapor
1599 retrievals with matched radiosonde measurements and forecasts, J. Geophys. Res., 111,
1600 D09S15, doi:10.1029/2005JD006116, 2006.

1601 Eck, T. F., Holben, B. N., Reid, J. S., Dubovik, O., Smirnov, A., O'Neill, N. T., Slutsker, I., and
1602 Kinn, S.: Wavelength dependence of the optical depth of biomass burning urban, and desert
1603 dust aerosols, J. Geophys. Res., 104, 31333–31349, 1999.

1604 Emmons, L. K., Walters, S., Hess, P. G., Lamarque, J.-F., Pfister, G. G., Fillmore, D., Granier, C.,
1605 Guenther, A., Kinnison, D., Laepple, T., Orlando, J., Tie, X., Tyndall, G., Wiedinmyer, C.,
1606 Baughcum, S. L., and Kloster, S.: Description and evaluation of the Model for Ozone and
1607 Related chemical Tracers, version 4 (MOZART-4), Geosci. Model Dev., 3, 43–67, doi:
1608 10.5194/gmd-3-43-2010, 2010.

Fast, J. D., Gustafson Jr., W. I., Easter, R. C., Zaveri, R. A., Barnard, J. C., Chapman, E. G., Grell, G. A. and Peckham, S. E.: Evolution of ozone, particulates, and aerosol direct radiative forcing in the vicinity of Houston using a fully coupled meteorology-chemistry-aerosol model, J. Geophys. Res., 111, D21305, doi:10.1029/2005JD006721, 2006.

Fast, J. D., Gustafson Jr., W. I., Berg, L. K., Shaw, W. J., Pekour, M., Shrivastava, M., Barnard, J. C., Ferrare, R. A., Hostetler, C. A., Hair, J. A., Erickson, M., Jobson, B. T., Flowers, B., Dubey, M. K., Springston, S., Pierce, R. B., Dolislager, L., Pederson, J., and Zaveri, R. A.: Transport and mixing patterns over Central California during the carbonaceous aerosol and radiative effects study (CARES), Atmos. Chem. Phys., 12, 1759-1783, doi:10.5194/acp-12-1759-2012, 2012.

Fast, J. D., Allan, J., Bahreini, R., Craven, J., Emmons, L., Ferrare, R., Hayes, P. L., Hodzic, A., Holloway, J., Hostetler, C., Jimenez, J. L., Jonsson, H., Liu, S., Liu, Y., Metcalf, A., Middlebrook, A., Nowak, J., Pekour, M., Perring, A., Russell, L., Sedlacek, A., Seinfeld, J., Setyan, A., Shilling, J., Shrivastava, M., Springston, S., Song, C., Subramanian, R., Taylor, J. W., Vinoj, V., Yang, Q., Zaveri, R. A., and Zhang, Q.: Modeling regional aerosol and aerosol precursor variability over California and its sensitivity to emissions and long-range transport during the 2010 CalNex and CARES campaigns, Atmos. Chem. Phys., 14, 10013-10060, doi:10.5194/acp-14-10013-2014, 2014.

Feingold, G., and Morley, B.: Aerosol hygroscopic properties as measured by lidar and comparison with in situ measurements, J. Geophys. Res., 108(D11), 4327, doi:10.1029/2002JD002842, 2003.

Flanner, M. G., and Zender, C. S.: Snowpack radiative heating: Influence on Tibetan Plateau climate, Geophys. Res. Lett., 32, L06501, doi:10.1029/2004GL022076, 2005.

Flanner, M. G., and Zender, C. S.: Linking snowpack microphysics and albedo evolution, J. Geophys. Res., 111, D12208, doi:10.1029/2005JD006834, 2006.

Fountoukis, C., Koraj, D., Denier van der Gon, H. A. C., Charalampidis, P. E., Pilinis, C., and Pandis, S. N.: Impact of grid resolution on the predicted fine PM by a regional 3-D chemical transport model, Atmos. Environ., 68, 24–32, 2013.

Freitas, S. R., Longo, K. M., Alonso, M. F., Pirre, M., Marecal, V., Grell, G., Stockler, R., Mello, R. F., and Sánchez Gácita, M.: PREP-CHEM-SRC – 1.0: a preprocessor of trace gas and aerosol emission fields for regional and global atmospheric chemistry models, Geosci. Model Dev., 4, 419-433, doi:10.5194/gmd-4-419-2011, 2011.

Ghan, S., Laulainen, N., Easter, R., Wagener, R., Nemesure, S., Chapman, E., Zhang, Y., and Leung, R.: Evaluation of aerosol direct radiative forcing in MIRAGE, J. Geophys. Res., 106(D6), 5295–5316, doi:10.1029/2000JD900502, 2001.

Ginoux, P., Chin, M., Tegen, I., Prospero, J. M., Holben, B., Dubovik, O., and Lin, S.: Sources and distributions of dust aerosols simulated with the GOCART model, J. Geophys. Res., 106, 20225–20273, 2001.

Gong, S. L.: A parameterization of sea-salt aerosol source function for sub- and super-micron particles, Global Biogeochem. Cy., 17, 1097, doi:10.1029/2003GB002079, 2003.

Grell, G. and Devenyi, D.: A generalized approach to parameterizing convection combining ensemble and data assimilation techniques, Geophys. Res. Lett., 29(14), doi:10.1029/2002GL015311, 2002.

Grell, G., Peckham, S., Schmitz, R., et al.: Fully coupled "online" chemistry within the WRF model, Atmos. Environ., 39(37), 6957–6975, 2005.

Grell, G., Freitas, S. R., Stuefer, M., and Fast, J.: Inclusion of biomass burning in WRF-Chem: impact of wildfires on weather forecasts, Atmos. Chem. Phys., 11, 5289-5303, doi:10.5194/acp-11-5289-2011, 2011.

Guenther, A., Karl, T., Harley, P., Wiedinmyer, C., Palmer, P. I., and Geron, C.: Estimates of global terrestrial isoprene emissions using MEGAN (Model of Emissions of Gases and Aerosols from Nature), Atmos. Chem. Phys., 6, 3181–3210, doi: 10.5194/acp-6-3181-2006, 2006.

Hand, J., Copeland, S. A., Day, D. E., Dillner, A. M., Indresand, H., Malm, W. C., McDade, C. E., Moore Jr., C. T., Pitchford, M. L., Schichtel, B. A., and Watson, J. G.: Spatial and seasonal patterns and temporal variability of haze and its constituents in the United States: Report V, June 2011, available at: http://vista.cira.colostate.edu/Improve/spatial-and-seasonal-patterns-

1665 and-temporal-variability-of-haze-and-its-constituents-in-the-united-states-report-v-june-
1666 2011/, 2011.

1667 Hasheminassab, S., Daher, N., Saffari, A., Wang, D., Ostro, B. D., and Sioutas, C.: Spatial and
1668 temporal variability of sources of ambient fine particulate matter ($PM_{2.5}$) in California, Atmos.
1669 Chem. Phys., 14, 12085-12097, doi:10.5194/acp-14-12085-2014, 2014.

1670 Herner, J. D., Ying, Q., Aw, J., Gao, O., Chang, D. P. Y., and Kleeman, M.: Dominant mechanisms
1671 that shape the airborne particle size and composition in central California, Aerosol Sci.
1672 Technol., 40, 827–844, 2006.

1673 Holben, B. N., Eck, T. F., Slutsker, I., Tanre ì, D., Buis, J. P., Setzer, A., Vermote, E., Reagan, J.
1674 A., Kaufman, Y. J., Nakajima, T., Lavenu, F., Jankowiak, I., and Smirnov, A.: AERONET –
1675 A Federated Instrument Network and Data Archive for Aerosol Characterization, Remote
1676 Sens. Environ., 66, 1–16, 1998.

1677 Holben, B. N., Tanr, D., Smirnov, A., Eck, T. F., Slutsker, I., Abuhassan, N., Newcomb, W. W.,
1678 Schafer, J. S., Chatenet, B., Lavenu, F., Kaufman, Y. J., Castle, J. V., Setzer, A., Markham,
1679 B., Clark, D., Frouin, R., Halthore, R., Karneli, A., O'Neill, N. T., Pietras, C., Pinker, R. T.,
1680 Voss, K., and Zibordi, G.: An emerging ground-based aerosol climatology: Aerosol optical
1681 depth from AERONET, J. Geophys. Res., 106, 12067–12097, 2001.

1682 Hong, S., Noh, Y., and Dudhia, J.: A new vertical diffusion package with an explicit treatment of
1683 entrainment processes, Mon. Weather Rev., 134, 2318–2341, 2006.

1684 Hu, Z., Zhao, C., Huang, J., Leung, L. R., Qian, Y., Yu, H., Huang, L., and Kalashnikova, O. V.:
1685 Trans-Pacific transport and evolution of aerosols: evaluation of quasi-global WRF-Chem
1686 simulation with multiple observations, Geosci. Model Dev., 9, 1725-1746, doi:10.5194/gmd-
1687 9-1725-2016, 2016.

1688 Iacono, M. J., Delamere, J. S., Mlawer, E. J., Shephard, M. W., Clough, S. A., and Collins, W. D.:
1689 Radiative forcing by long-lived greenhouse gases: calculations with the AER radiative transfer
1690 models, J. Geophys. Res., 113, D13103, doi:10.1029/2008JD009944, 2008.

1691 Jaeglé, L., Quinn, P. K., Bates, T. S., Alexander, B., and Lin, J.-T.: Global distribution of sea salt
1692 aerosols: new constraints from in situ and remote sensing observations, Atmos. Chem. Phys.,
1693 11, 3137–3157, doi:10.5194/acp-11-3137-2011, 2011.

Kahn, R. A., Gaitley, B. J., Garay, M. J., Diner, D. J., Eck, T. F., Smirnov, A., and Holben, B. N.: Multiangle Imaging SpectroRadiometer global aerosol product assessment by comparison with the Aerosol Robotic Network, J. Geophys. Res., 115, D23209, doi:10.1029/2010JD014601, 2010.

Kassianov, E., Pekour, M., and Barnard, J.: Aerosols in central California: Unexpectedly large contribution of coarse mode to aerosol radiative forcing, Geophys. Res. Lett., 39, L20806, doi: 10.1029/2012GL053469, 2012.

Kelly, J. T., Baker, K. R., Nowak, J. B., Murphy, J. G., Markovic, M. Z., VandenBoer, T. C., Ellis, R. A., Neuman, J. A., Weber, R. J., and Roberts, J. M.: Fine-scale simulation of ammonium and nitrate over the South Coast Air Basin and San Joaquin Valley of California during CalNex-2010, J. Geophys. Res.-Atmos., 119, 3600–3614, 2014.

~~Kim, S. W., McKeen, S. A., Frost, G. J., Lee, S. H., Trainer, M., Richter, A., Angevine, W. M., Atlas, E., Bianco, L., Boersma, K. F., Brioude, J., Burrows, J. P., de Gouw, J., Fried, A., Gleason, J., Hilboll, A., Mellqvist, J., Peischl, J., Richter, D., Rivera, C., Ryerson, T., te Lintel Hekkert, S., Walega, J., Warneke, C., Weibring, P., and Williams, E.: Evaluations of NO_x and highly reactive VOC emission inventories in Texas and their implications for ozone plume simulations during the Texas Air Quality Study 2006, Atmos. Chem. Phys., 11, 11361-11386, doi:10.5194/acp-11-11361-2011, 2011.~~

Lawrence, D. M., Oleson, K. W., Flanner, M. G., Thornton, P. E., Swenson, S. C., Lawrence, P. J., Zeng, X., Yang, Z.-L., Levis, S., Sakaguchi, K., Bonan, G. B., and Slater, A. G.: Parameterization improvements and functional and structural advances in version 4 of the Community Land Model, J. Adv. Model. Earth Sys., 3, M03001, doi: 10.1029/2011MS000045, 2011.

Misenis, C. and Zhang, Y.: An examination of sensitivity of WRF/Chem predictions to physical parameterizations, horizontal grid spacing, and nesting options, Atmos. Res., 97, 315–334, doi:10.1016/j.atmosres.2010.04.005, 2010.

Morabito, D., Wu, L., and Slobin, S.: Weather Forecasting for Ka-band Operations: Initial Study Results, IPN PR 42-206, pp. 1-24, August 15, 2016. Available at: http://ipnpr.jpl.nasa.gov/progress_report/42-206/206C.pdf, 2016.

1723 Morrison, H., Thompson, G., and Tatarskii, V.: Impact of cloud microphysics on the development
1724 of trailing stratiform precipitation in a simulated squall line: comparison of one- and two-
1725 moment schemes, Mon. Weather Rev., 137, 991–1007, 2009.

1726 Omar, A.H., Winker, D.M., Kittaka, C., Vaughan, M.A., Liu, Z., Hu, Y., Trepte, C.R., Rogers,
1727 R.R., Ferrare, R.A., Lee, K.P., Kuehn, R.E., Hostetler, C.A.: The CALIPSO automated aerosol
1728 classification and lidar ratio selection algorithm. J. Atmos. Ocean. Technol. 26, 1994–2014,
1729 2009.

1730 Pleim, J. E.: A combined local and nonlocal closure model for the atmospheric boundary layer.
1731 Part I: Model description and testing, J. Appl. Meteorol. Clim., 46, 1383–1395, 2007.

1732 Pun, B. K., Balmori, R. T. F., and Seigneur, C.: Modeling wintertime particulate matter formation
1733 in central California, Atmos. Environ., 43, 402–409, 2009.

1734 Qian, Y., Gustafson Jr., W. I., and Fast, J. D.: An investigation of the sub-grid variability of trace
1735 gases and aerosols for global climate modeling, Atmos. Chem. Phys., 10, 6917-6946,
1736 doi:10.5194/acp-10-6917-2010, 2010.

1737 Randerson, J. T., van der Werf, G. R., Giglio, L., Collatz, G. J., and Kasibhatla, P. S.: Global Fire
1738 Emissions Database, Version 2 (GFEDv2.1). Data set. Available on-line [http://daac.ornl.gov/]
1739 from Oak Ridge National Laboratory Distributed Active Archive Center, Oak Ridge,
1740 Tennessee, U.S.A. doi:10.3334/ORNLDAAC/849, 2007.

1741 San Joaquin Valley Air Pollution Control District: 2012 PM2.5 plan. Available from:
1742 http://www.valleyair.org/Air_Quality_Plans/PM25Plans2012.htm, 2012.

1743 Scarino, A. J., Obland, M. D., Fast, J. D., Burton, S. P., Ferrare, R. A., Hostetler, C. A., Berg, L.
1744 K., Lefer, B., Haman, C., Hair, J. W., Rogers, R. R., Butler, C., Cook, A. L., and Harper, D.
1745 B.: Comparison of mixed layer heights from airborne high spectral resolution lidar, ground-
1746 based measurements, and the WRF-Chem model during CalNex and CARES, Atmos. Chem.
1747 Phys., 14, 5547-5560, doi:10.5194/acp-14-5547-2014, 2014.

1748 Shaw, W., Allwine, K. J., Fritz, B. G., Rutz, F. C., Rishel, J. P., and Chapman, E. G.: An evaluation
1749 of the wind erosion module in DUSTRAN, Atmos. Environ., 42, 1907–1921, 2008.

1750 Solomon, P. A., Crumpler, D., Flanagan, J. B., Jayanty, R. K. M., Rickman, E. E., and McDade C.
1751 E.: U.S. National PM 2.5 Chemical Speciation Monitoring Networks – CSN and IMPROVE:

Description of Networks, J. Air Waste Manage., 64, 1410–1438, doi:10.1080/10962247.2014.956904, 2014.

Susskind, J., Barnet, C. D., and Blaisdell, J.: Retrieval of atmospheric and surface parameters from AIRS/AMSU/HSB data under cloudy conditions, IEEE Trans. Geosci. Remote Sens., 41(2), 390–409, doi:10.1109/TGRS.2002.808236, 2003.

Schuster, G. L., Dubovik, O., and Holben, B. N.: Angström exponent and bimodal aerosol size distributions, J. Geophys. Res., 111, D07207, doi:10.1029/2005JD006328, 2006.

Tessum, C. W., Hill, J. D., and Marshall, J. D.: Twelve-month, 12 km resolution North American WRF-Chem v3.4 air quality simulation: performance evaluation, Geosci. Model Dev., 8, 957-973, doi:10.5194/gmd-8-957-2015, 2015.

Toth, T. D., Campbell, J. R., Reid, J. S., Tackett, J. L., Vaughan, M. A. and Zhang, J.: Lower daytime threshold sensitivities to aerosol optical thickness in CALIPSO Level 2 products, J. ~~Atmos. Oceanic. Technol.~~Geophys. Res., in review, 2017~~6~~.

US Environmental Protection Agency, 2010: Technical Support Document: Preparation of Emissions Inventories for the Version 4, 2005-based Platform, 73 pp., Office of Air Quality Planning and Standards, Air Quality Assessment Division, available at: https://www3.epa.gov/crossstaterule/pdfs/2005_emissions_tsd_07jul2010.pdf, 2010.

Wu, L., and Petty, G. W. : Intercomparison of Bulk Microphysics Schemes in Simulations of Polar lows. Mon. Wea. Rev., 138, 2211-2228. doi: 10.1175/2010MWR3122.1, 2010.

Wu, L., Su, H. and Jiang, J. H.: Regional simulations of deep convection and biomass burning over South America: 1. Model evaluations using multiple satellite data sets, J. Geophys. Res., 116, D17208, doi:10.1029/2011JD016105, 2011a.

Wu, L., Su, H. and Jiang, J. H.: Regional simulations of deep convection and biomass burning over South America: 2. Biomass burning aerosol effects on clouds and precipitation, J. Geophys. Res., 116, D17209, doi:10.1029/2011JD016106, 2011b.

Wu, L., Su, H. and Jiang, J. H.: Regional simulations of aerosol impacts on precipitation during the East Asian summer monsoon. J. Geophys. Res. Atmos., 118, doi: 10.1002/jgrd.50527, 2013.

1780 Wu, L., Li, J.-L. F., Pi, C.-J., Yu, J.-Y., and Chen, J.-P.: An observationally based evaluation of
1781 WRF seasonal simulations over the Central and Eastern Pacific, J. Geophys. Res. Atmos., 120,
1782 doi:10.1002/2015JD023561, 2015.

1783 Ying, Q. and Kleeman, M. J.: Regional contributions to airborne particulate matter in central
1784 California during a severe pollution episode, Atmos. Environ., 43, 1218–1228, 2009.

1785 Young, S.A. and Vaughan, M.A.: The retrieval of profiles of particulate extinction from Cloud–
1786 Aerosol Lidar Infrared Pathfinder Satellite Observations (CALIPSO) data: algorithm
1787 description. J. Atmos. Ocean. Technol. 26, 1105–1119, 2009.

1788 Zaveri, R. A. and Peters, L. K.: A new lumped structure photochemical mechanism for large-scale
1789 applications, J. Geophys. Res., 104, 30387–30415, 1999.

1790 Zaveri, R. A., Easter, R. C., Fast, J. D., and Peters, L. K.: Model for Simulating Aerosol
1791 Interactions and Chemistry (MOSAIC), J. Geophys. Res., 113, D13204,
1792 doi:10.1029/2007JD008782, 2008.

1793 Zhang, Y., Liu, P., Liu, X.-H., Pun, B., Seigneur, C., Jacobson, M. Z., and Wang, W.-X.: Fine
1794 scale modeling of wintertime aerosol mass, number, and size distributions in central California,
1795 J. Geophys. Res.-Atmos., 115, D15207, doi:10.1029/2009jd012950, 2010.

1796 Zhao, C., Liu, X., Leung, L. R., Johnson, B., McFarlane, S. A., Gustafson Jr., W. I., Fast, J. D.,
1797 and Easter, R.: The spatial distribution of mineral dust and its shortwave radiative forcing over
1798 North Africa: modeling sensitivities to dust emissions and aerosol size treatments, Atmos.
1799 Chem. Phys., 10, 8821–8838, doi: 10.5194/acp-10-8821-2010, 2010.

1800 Zhao, C., Liu, X., Ruby Leung, L., and Hagos, S.: Radiative impact of mineral dust on monsoon
1801 precipitation variability over West Africa, Atmos. Chem. Phys., 11, 1879–1893,
1802 doi:10.5194/acp-11-1879-2011, 2011.

1803 Zhao, C., Chen, S., Leung, L. R., Qian, Y., Kok, J. F., Zaveri, R. A., and Huang, J.: Uncertainty in
1804 modeling dust mass balance and radiative forcing from size parameterization, Atmos. Chem.
1805 Phys., 13, 10733-10753, doi:10.5194/acp-13-10733-2013, 2013a.

1806 Zhao, C., Leung, L. R., Easter, R., Hand, J., and Avise, J.: Characterization of speciated aerosol
1807 direct radiative forcing over California, J. Geophys. Res., 118, 2372–2388, doi:
1808 10.1029/2012JD018364, 2013b.

1809 Zhao, C., Hu, Z., Qian, Y., Ruby Leung, L., Huang, J., Huang, M., Jin, J., Flanner, M. G., Zhang,
1810 R., Wang, H., Yan, H., Lu, Z., and Streets, D. G.: Simulating black carbon and dust and their
1811 radiative forcing in seasonal snow: a case study over North China with field campaign
1812 measurements, Atmos. Chem. Phys., 14, 11475-11491, doi:10.5194/acp-14-11475-2014,
1813 2014.

List of Table

Table 1. Experiment description

Experiment ID	Experiment description
20km	Simulation with the GOCART dust scheme at 20 km horizontal resolution.
20km_D2	Same as 20km, but with the DUSTRAN dust scheme.
20km_P7	Same as 20km_D2, but with the ACM2 PBL scheme.
4km	Same as 20km, but at 4 km horizontal resolution.
4km_D2	Same as 4km, but with the DUSTRAN dust scheme.

Table 2. Correlation with observations for different species at Fresno, CA

Species	20km	4km	4km_D2	20km_D2	20km_P7
$PM_{2.5}$	0.89	0.90	0.86	0.78	0.03
$PM_{2.5}\_NO_3$	0.94	0.95	0.94	0.94	0.91
$PM_{2.5}\_NH_4$	0.97	0.96	0.96	0.98	0.96
$PM_{2.5}\_OM$	0.93	0.93	0.94	0.93	0.91
$PM_{2.5}\_EC$	0.98	0.98	0.98	0.98	0.96
$PM_{2.5}\_SO_4$	0.63	-0.16	-0.14	0.61	0.63
$PM_{2.5}\_dust$	-0.55	-0.50	0.48	0.55	0.36
PM_{10}	-0.25	-0.23	-0.08	0.01	-0.03

Formatted: Subscript
Formatted: Subscript
Formatted: Subscript
Formatted: Subscript
Formatted: Subscript
Formatted: Subscript
Formatted: Subscript
Formatted: Subscript

Table ~~2~~3. Surface aerosol mass (μg m^{-3}) for different species at Fresno, CA

Species	Cold season						Warm season					
	~~IMPROVE~~OBS	20km ~~20km~~	4km ~~4km~~	4km_D2~~4km_D2~~	20km_D2	20km_P7	~~IMPROVE~~OBS	20km ~~20km~~	4km ~~4km~~	4km_D2~~4km_D2~~	20km_D2	20km_P7
$PM_{2.5}$	16.84	13.71 ~~13.71~~	21.38 ~~21.38~~	22.48 ~~22.48~~	14.90	13.77	8.44	4.914 ~~.91~~	6.29 ~~6.29~~	12.85 ~~12.85~~	10.12	14.85
$PM_{2.5}$_NO_3	5.43	6.366 ~~.36~~	9.549. ~~54~~	9.229 ~~.22~~	6.22	3.16	0.84	0.550 ~~.55~~	0.69 ~~0.69~~	0.790 ~~.79~~	0.66	0.57
$PM_{2.5}$_NH_4	1.42	1.97	2.99	2.88	1.91	0.98	0.40	0.19	0.24	0.20	0.16	0.13
$PM_{2.5}$_OM~~C~~	5.393 ~~.85~~	0.920 ~~.92~~	2.072. ~~07~~	2.072 ~~.07~~	0.93	1.04	2.471 ~~.76~~	0.490 ~~.49~~	0.87 ~~0.87~~	0.870 ~~.87~~	0.50	0.55
$PM_{2.5}$_EC	1.08	0.520 ~~.52~~	1.121. ~~12~~	1.131 ~~.13~~	0.52	0.58	0.32	0.270 ~~.27~~	0.49 ~~0.49~~	0.490 ~~.49~~	0.27	0.30
$PM_{2.5}$_SO_4	0.87	0.530 ~~.53~~	0.820. ~~82~~	0.810 ~~.81~~	0.53	0.46	1.04	0.540 ~~.54~~	0.61 ~~0.61~~	0.600 ~~.60~~	0.53	0.49
$PM_{2.5}$_dust	0.90	0.110 ~~.11~~	0.110. ~~11~~	1.651 ~~.65~~	1.50	4.18	2.08	0.040 ~~.04~~	0.03 ~~0.03~~	6.496 ~~.49~~	5.16	10.05
PM_{10}	31.55	14.93 ~~14.93~~	22.81 ~~22.81~~	28.32 ~~28.32~~	20.10	24.52	34.82	7.087 ~~.08~~	8.69 ~~8.69~~	38.12 ~~38.12~~	30.19	48.02

Formatted: Subscript

Formatted: Subscript

Formatted: Subscript

Formatted: Subscript

Formatted: Subscript

Formatted: Subscript

Formatted: Subscript

Formatted: Subscript

Supplementary Table 1. Correlation with surface observations for meteorological variables at Fresno, CA

	4km_D2	20km_D2	20km_P7
T	0.94	0.94	0.94
RH	0.98	0.98	0.96
Wind	0.83	0.84	0.85
Rain	0.97	0.97	0.97

Supplementary Table 2. Bias for surface meteorological variables at Fresno, CA

	Cold season			Warm season		
	4km_D2	20km_D2	20km_P7	4km_D2	20km_D2	20km_P7
T (K)	3.89	3.56	3.69	2.44	1.50	1.35
RH (%)	-9.78	-14.55	-19.35	-9.48	-9.32	-11.16
Wind (m/s)	-0.67	-1.00	-1.05	0.78	-0.16	-0.49
Rain (mm/day)	-0.15	0.14	-0.03	-0.06	-0.03	-0.04

List of Figures

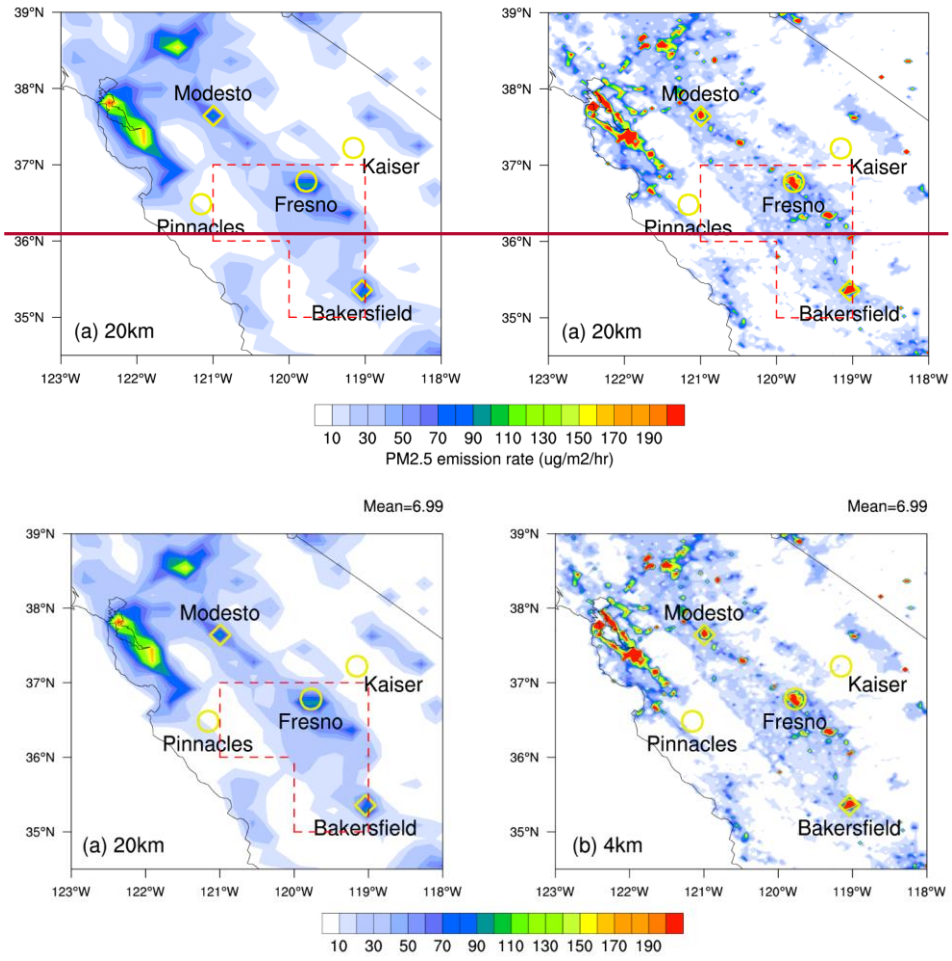

Figure 10~~1~~. Daily mean anthropogenic $PM_{2.5}$ emission rate (μg m^{-2} hrs^{-1}) at (a) 20km and (b) 4km simulation. Domain-averaged emission rate is shown at right corner of each figure. Red dashed lines in Figure 1a represent the region used for the domain averages in the discussions ~~Figure 8 and 9~~. Yellow circle: IMPROVE site; yellow diamond: EPA CSN site. Three urban sites: Fresno, Bakersfield and Modesto; two rural sites: Pinnacles and Kaiser.

Formatted: Subscript

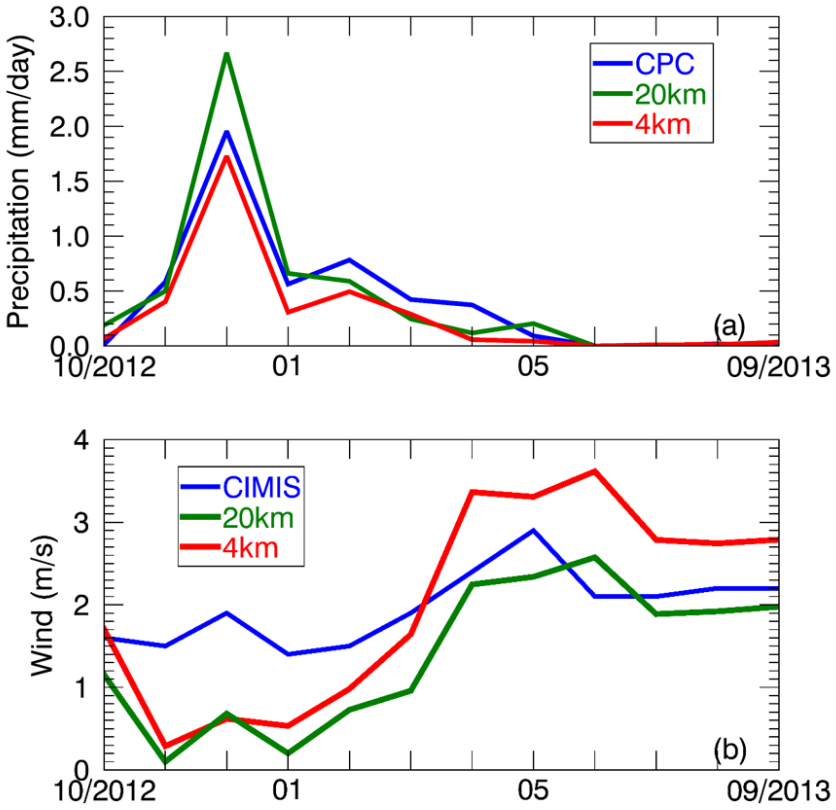

Figure 11. (a) Monthly precipitation (mm/day) from CPC, 20km and 4km; (b) monthly wind speed (m/s) from CIMIS, 20km and 4km. 4km_D2 (not shown) is similar to 4km.

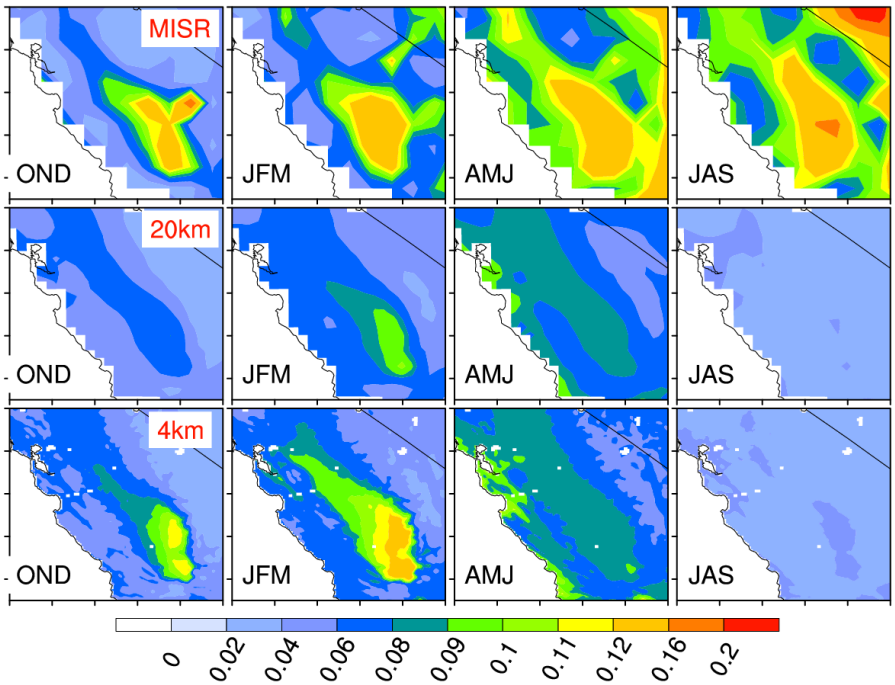

Figure 122. Spatial distribution of seasonal mean 550 nm AOD from MISR and the WRF-Chem (20km and 4km) simulations in WY2013. OND: October, November and December; JFM: January, February and March; AMJ: April, May and June; JAS: July, August and September.

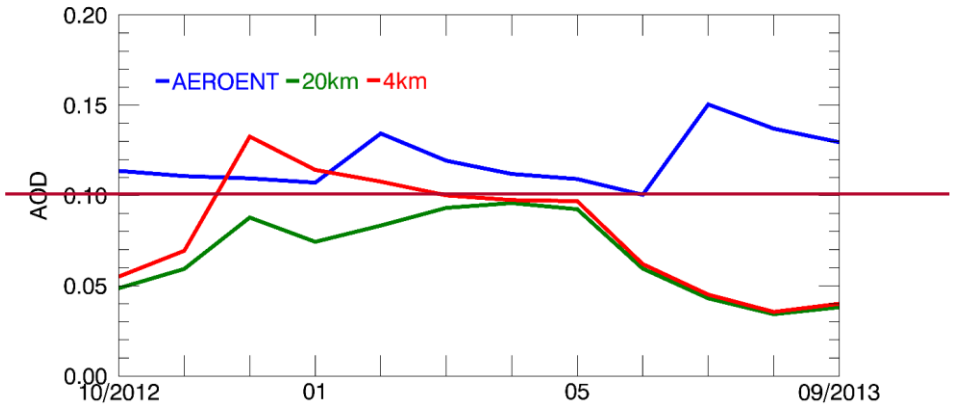

1843

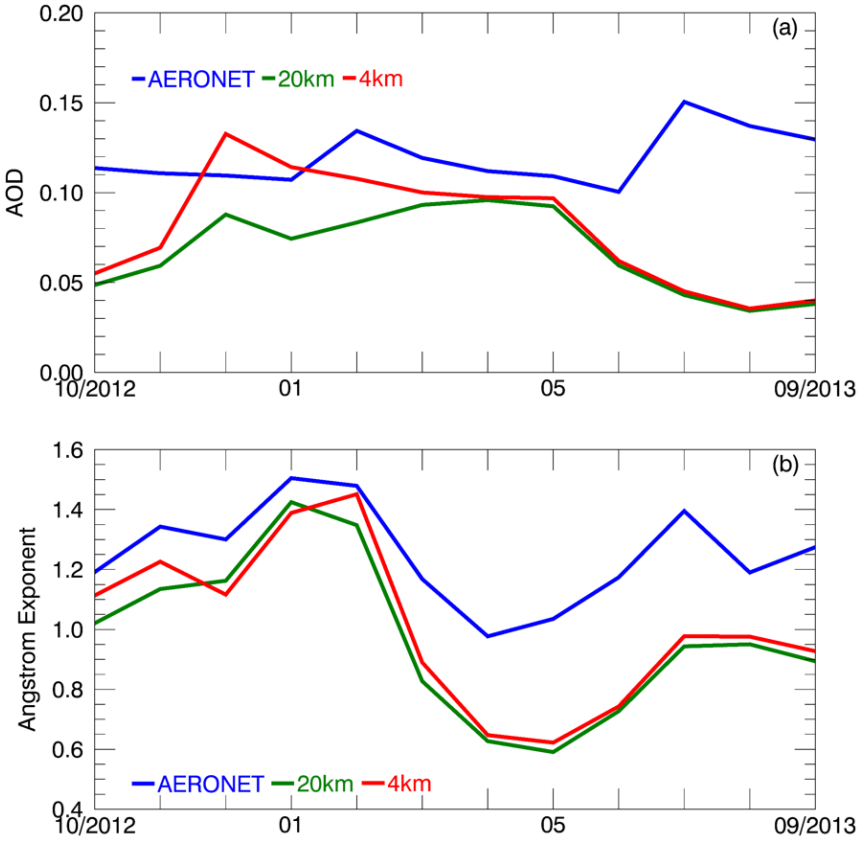

Figure 13~~3~~. (a) Monthly mean 550 nm AOD; (b) monthly mean 400-600 nm Ångström exponent at Fresno, CA from October 2012 to September 2013.

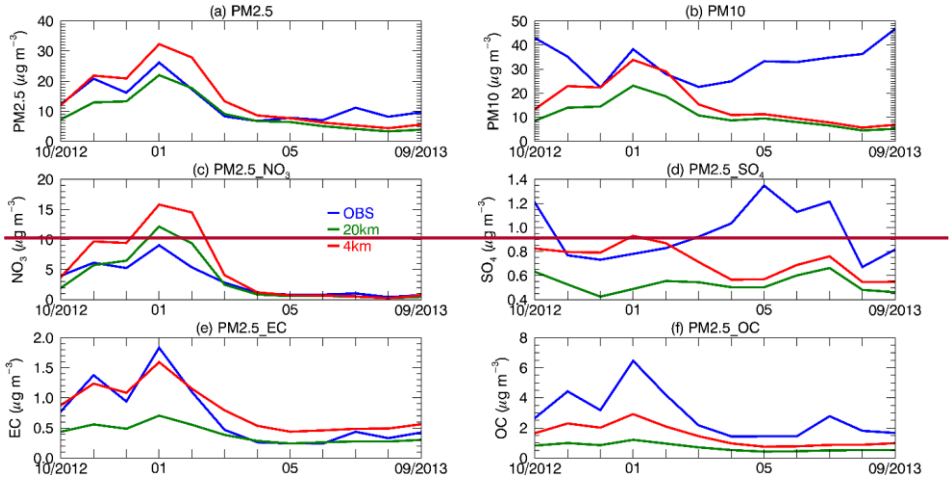
(a) PM2.5
PM2.5 (μg m⁻³)
(b) PM10
PM10 (μg m⁻³)
(c) PM2.5_NO3
NO3 (μg m⁻³)
OBS
20km
4km
(d) PM2.5_SO4
SO4 (μg m⁻³)
(e) PM2.5_EC
EC (μg m⁻³)
(f) PM2.5_OC
OC (μg m⁻³)
10/2012
01
05
09/2013

1847

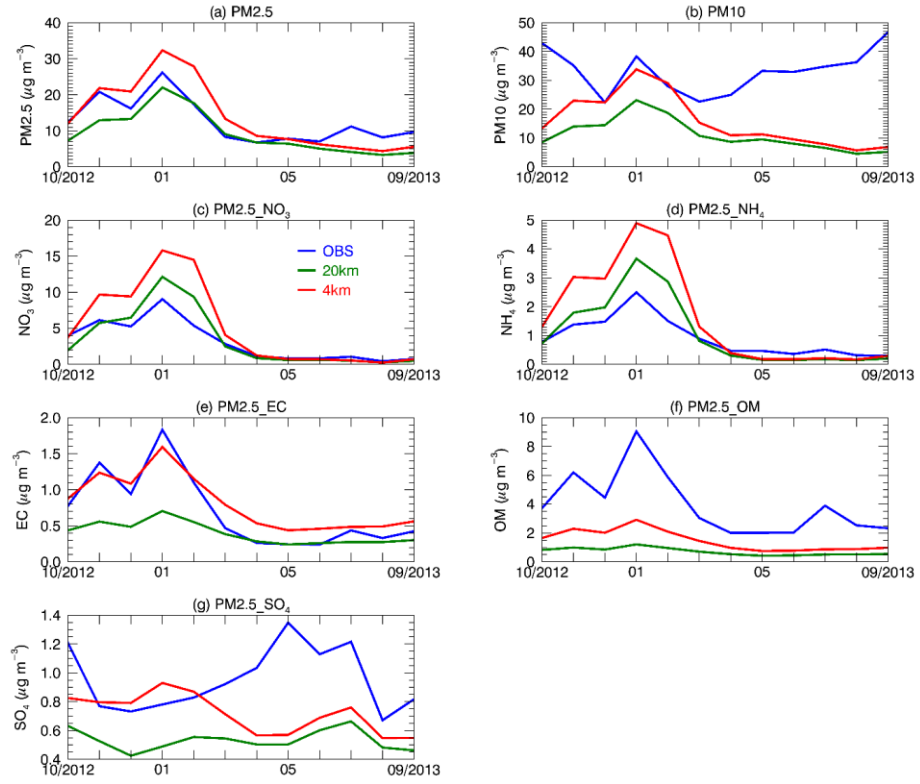
(a) PM2.5
PM2.5 (μg m⁻³)
(b) PM10
PM10 (μg m⁻³)
(c) PM2.5_NO3
NO3 (μg m⁻³)
OBS
20km
4km
(d) PM2.5_NH4
NH4 (μg m⁻³)
(e) PM2.5_EC
EC (μg m⁻³)
(f) PM2.5_OM
OM (μg m⁻³)
(g) PM2.5_SO4
SO4 (μg m⁻³)
10/2012
01
05
09/2013

1848

Figure 14. Aerosol mass (μg m^{-3}) for different species from ~~IMPROVE (~~OBS~~)~~, the 20km and 4km simulations at Fresno, CA. NH_4 observations are from EPA; other observations are from IMPROVE. $PM_{2.5}$ NO_3 represents NO_3 with diameter ≤ 2.5 μm. Similar definition for NH_4~~SO~~$_4$, EC, ~~and~~ OM~~C~~ and SO_4 in the figures.

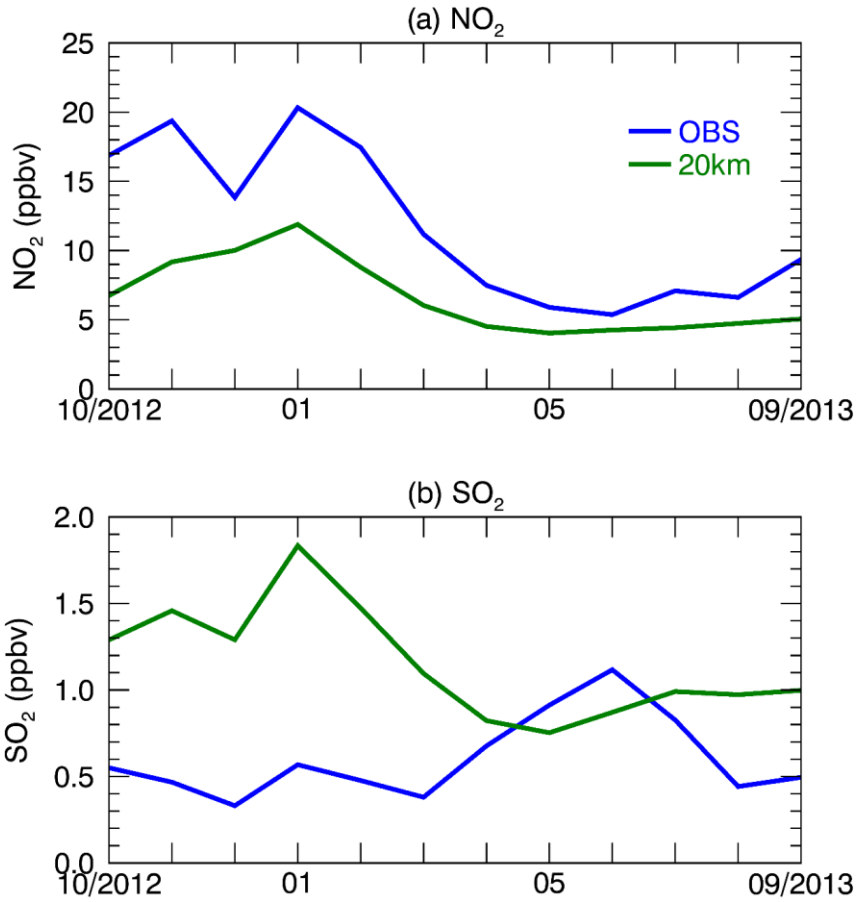

Figure 15. (a) NO_2 and (b) SO_2 from EPA (OBS) and the 20km run at Fresno, CA.

Formatted: Subscript

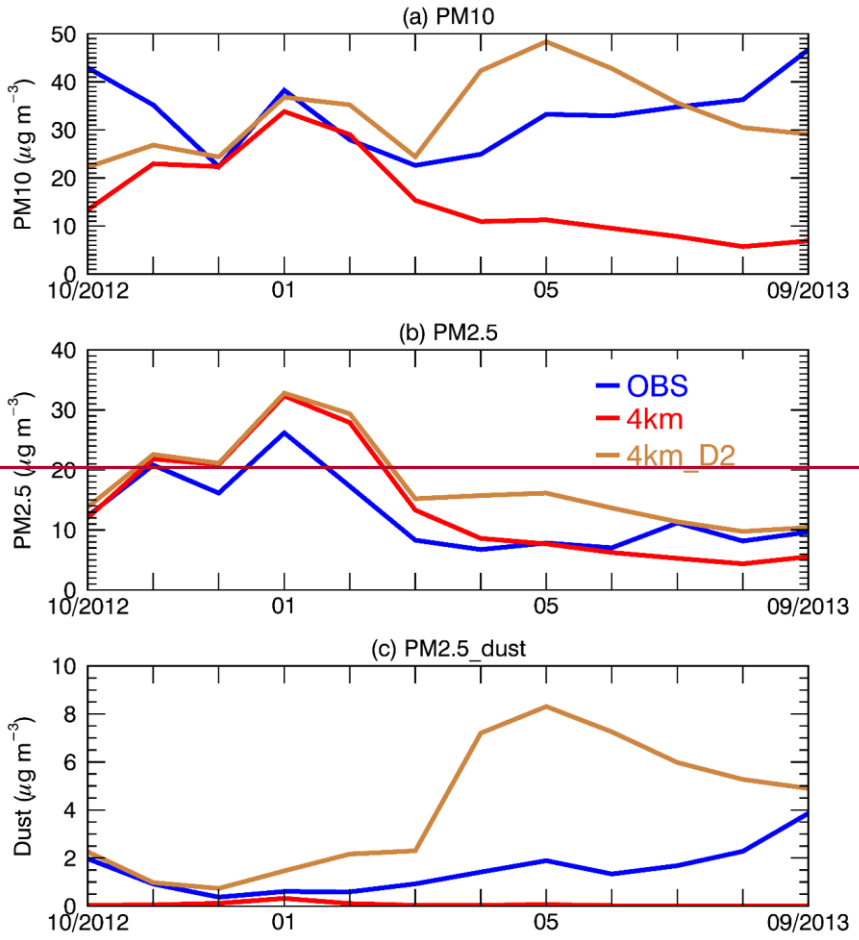
(a) PM10
PM10 (μg m⁻³)
50
40
30
20
10
0
10/2012
01
05
09/2013
(b) PM2.5
PM2.5 (μg m⁻³)
40
30
20
10
0
OBS
4km
4km_D2
10/2012
01
05
09/2013
(c) PM2.5_dust
Dust (μg m⁻³)
10
8
6
4
2
0
10/2012
01
05
09/2013

1856

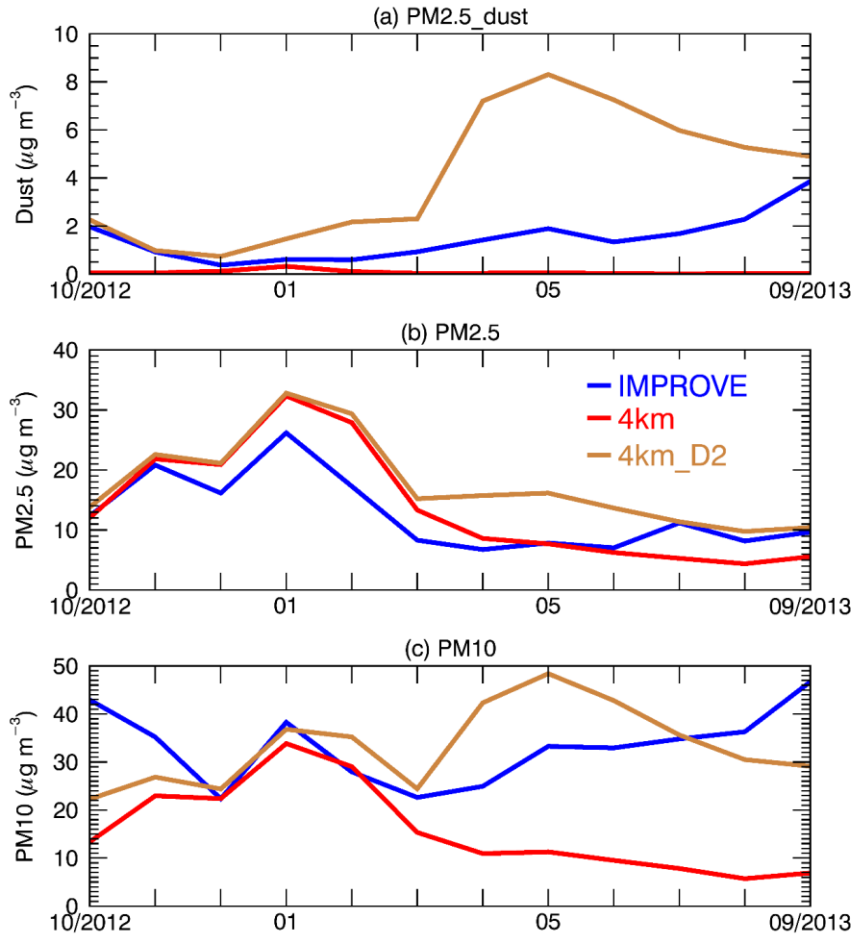

Figure 16~~5~~. (a) $PM_{2.5}$ dust; (b) $PM_{2.5}$; and (c~~a~~) PM_{10}; ~~(b) PM2.5; (c) PM2.5 dust~~ from IMPROVE ~~(OBS)~~, the 4km and 4km_D2 simulations at Fresno, CA.

Formatted: Subscript

Formatted: Subscript

Formatted: Subscript

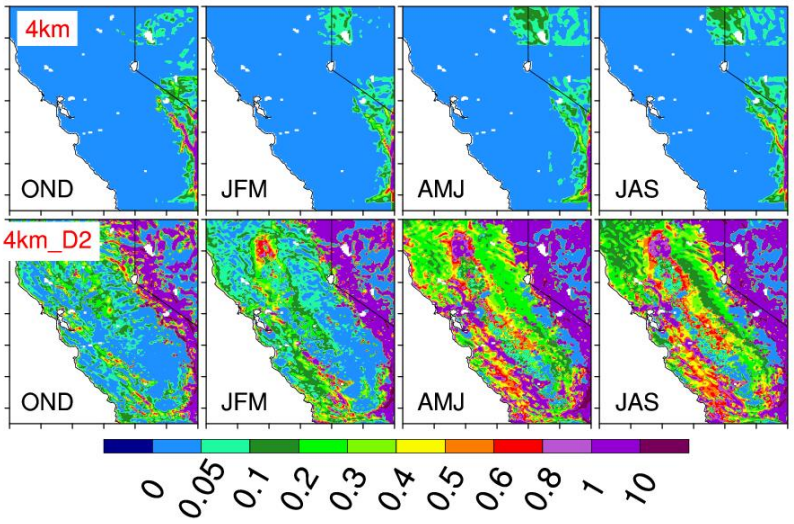

Figure 17. Mean dust emission rate (μg m^{-2} s^{-1}) from the 4km and 4km_D2 runs.

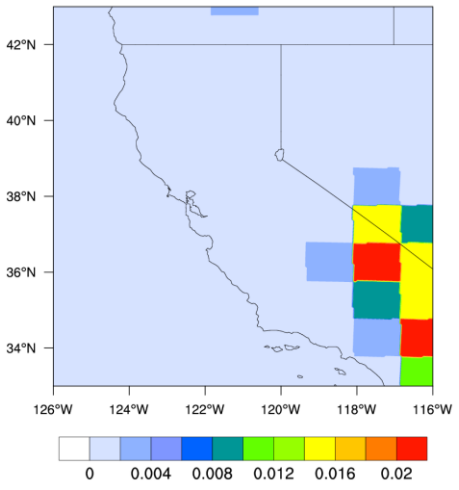

Figure 18. Fraction of erodible surface in the GOCART dataset used in this study.

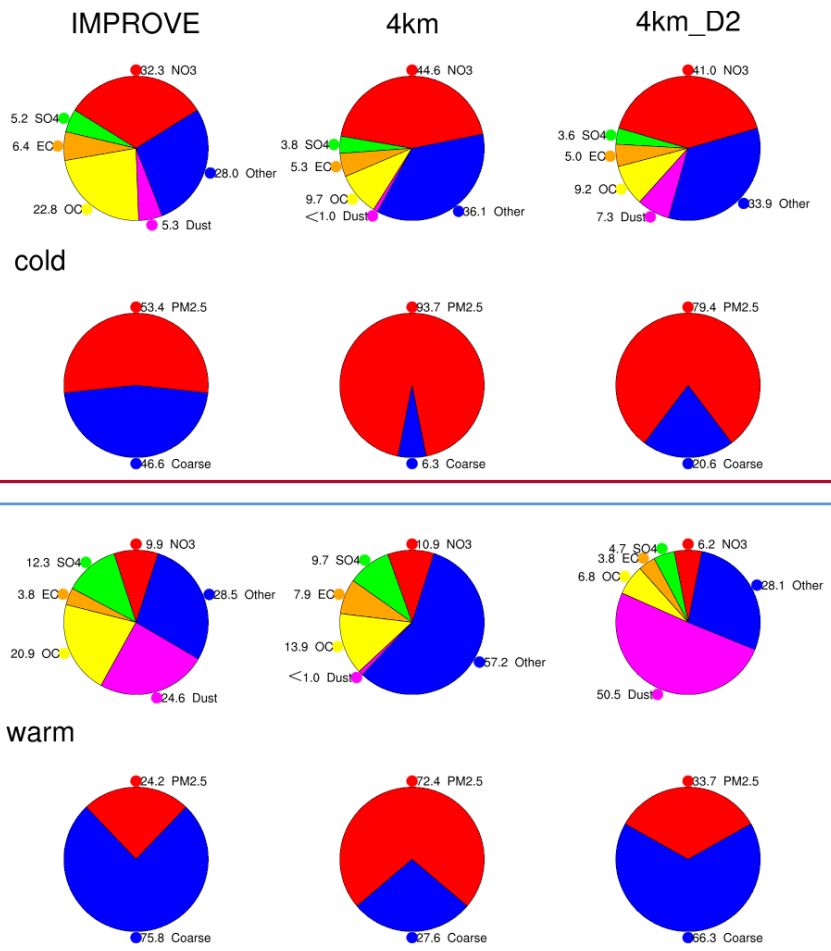
IMPROVE
4km
4km_D2
32.3 NO3
5.2 SO4
6.4 EC
28.0 Other
22.8 OC
5.3 Dust
44.6 NO3
3.8 SO4
5.3 EC
9.7 OC
<1.0 Dust
36.1 Other
41.0 NO3
3.6 SO4
5.0 EC
9.2 OC
7.3 Dust
33.9 Other
cold
53.4 PM2.5
46.6 Coarse
93.7 PM2.5
6.3 Coarse
79.4 PM2.5
20.6 Coarse
9.9 NO3
12.3 SO4
3.8 EC
28.5 Other
20.9 OC
24.6 Dust
10.9 NO3
9.7 SO4
7.9 EC
13.9 OC
<1.0 Dust
57.2 Other
4.7 SO4
3.8 EC
6.2 NO3
6.8 OC
28.1 Other
50.5 Dust
warm
24.2 PM2.5
75.8 Coarse
72.4 PM2.5
27.6 Coarse
33.7 PM2.5
66.3 Coarse

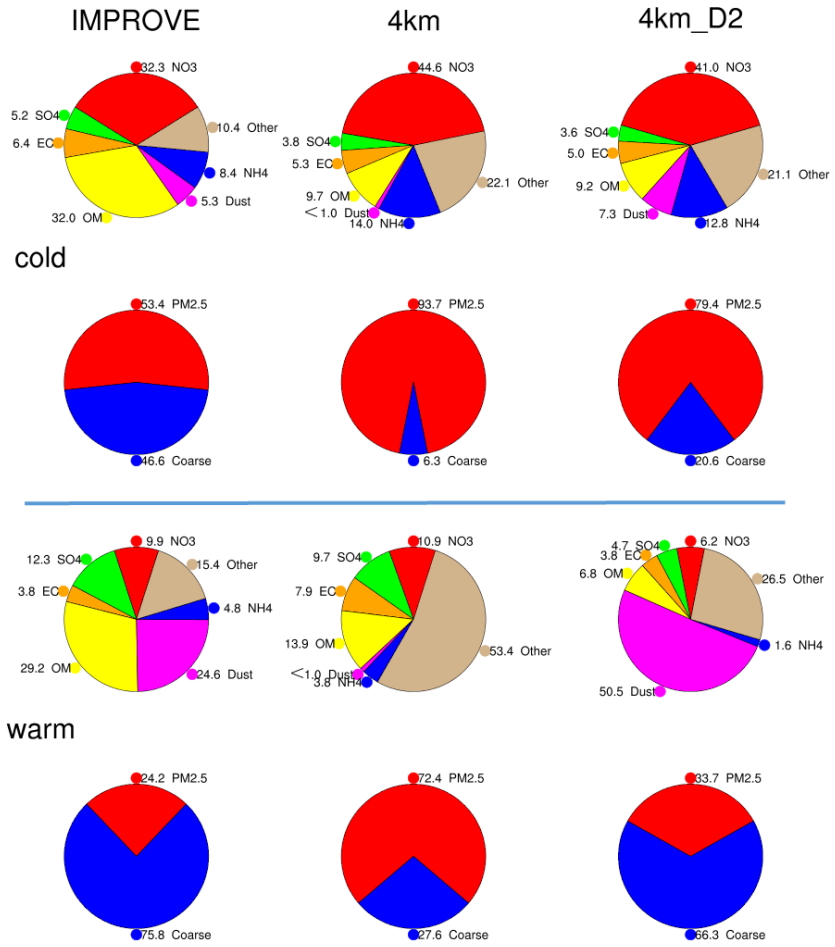

Figure 196. Relative contribution (%) of aerosol species from IMPROVE and the WRF-Chem (4km and 4km_D2) simulations ~~(4km and 4km_D2)~~ at Fresno, CA in WY2013. (Panel 1) Contribution to $PM_{2.5}$ in the cold season; (Panel 2) relative contribution of $PM_{2.5}$ and coarse mass (CM) to PM_{10} in the cold season; (Panel 3) same as Panel 1 but in the warm season; (Panel 4) same as Panel 2 but in the warm season. "Other" refers to the difference of $PM_{2.5}$ total mass and specified $PM_{2.5}$ (NO_3, NH_4, OM, EC, SO_4 and dust).

Formatted: Subscript
Formatted: Subscript
Formatted: Subscript
Formatted: Subscript
Formatted: Subscript

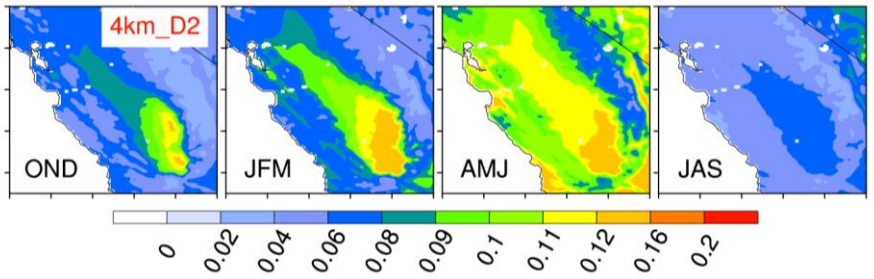

Figure 207. Spatial distribution of seasonal mean 550 nm AOD from the 4km_D2 run in WY2013.

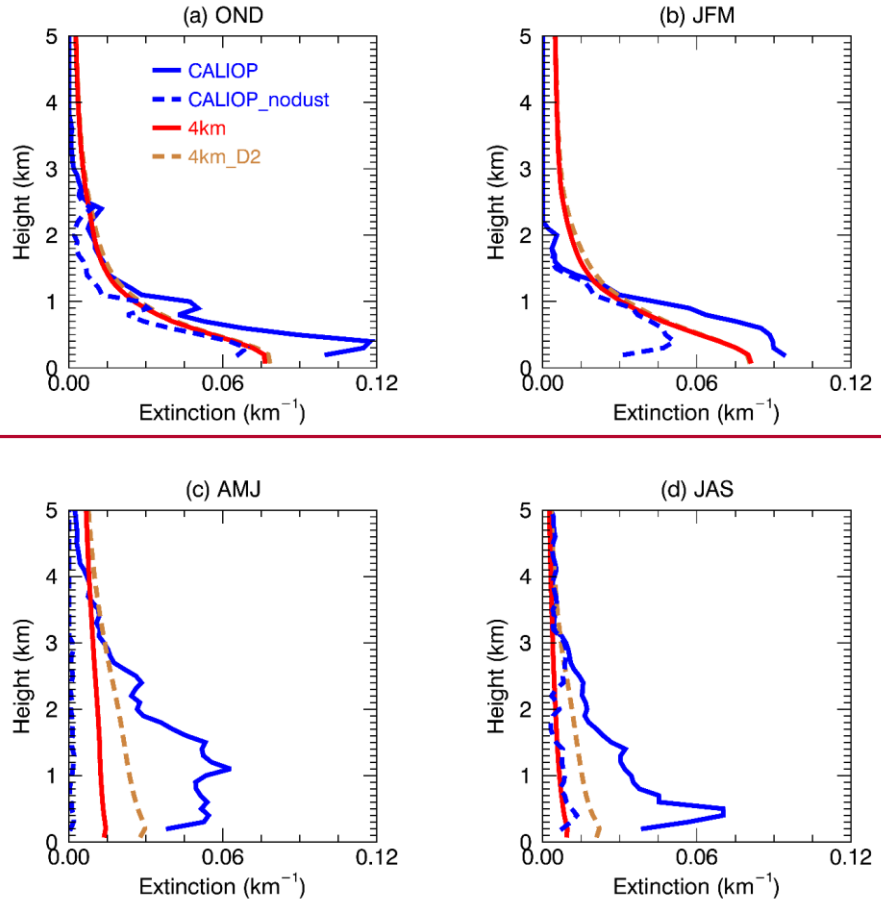
(a) OND
(b) JFM
(c) AMJ
(d) JAS
CALIOP
CALIOP_nodust
4km
4km_D2
Height (km)
Extinction (km^{-1})
0.00
0.06
0.12
0
1
2
3
4
5

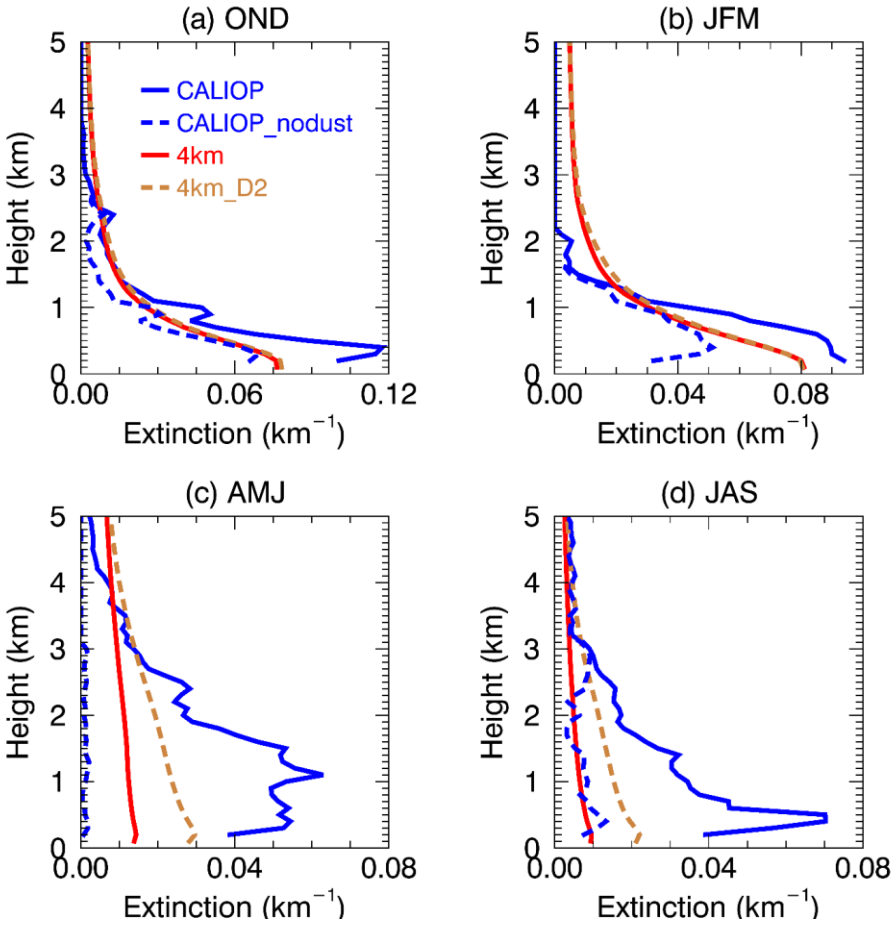

Figure 2~~1~~8. Vertical distribution of seasonal mean 532 nm aerosol extinction coefficient (km^{-1}) from CALIOP (blue) and the WRF-Chem (4km and 4km_D2) simulations over the red box region in ~~Figure~~ Fig. 1a~~)~~ in WY2013. Blue dashed lines (CALIOP_nodust) represent the CALIOP profiles without dust (dust and polluted dust).

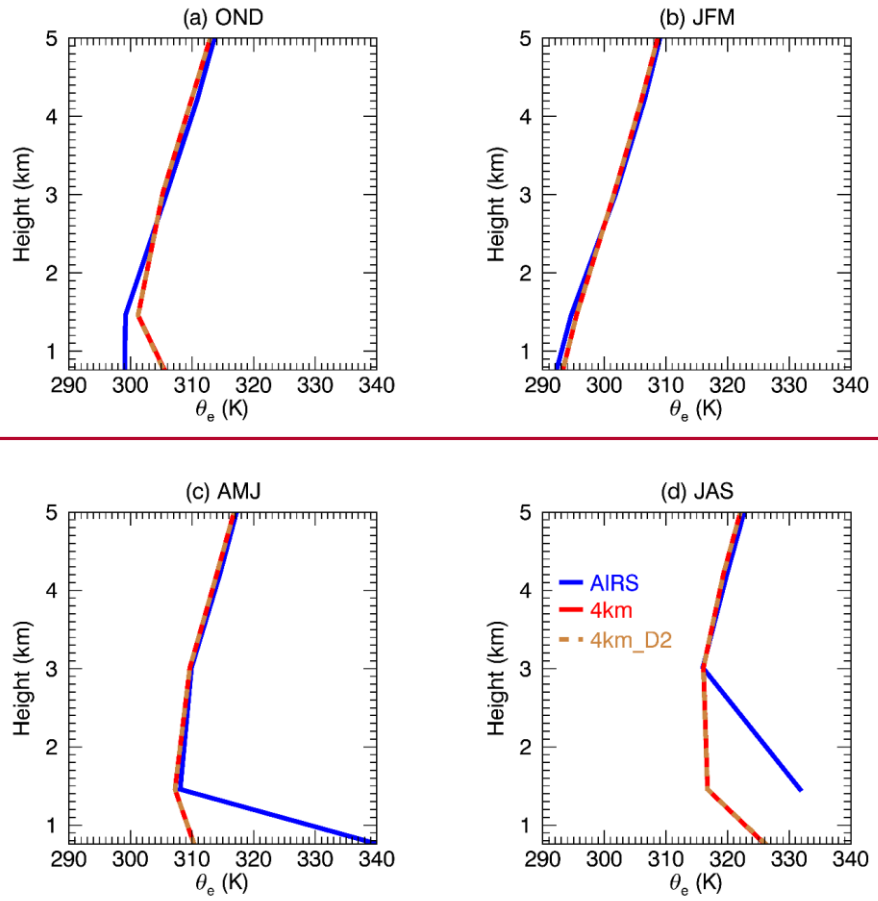

1883

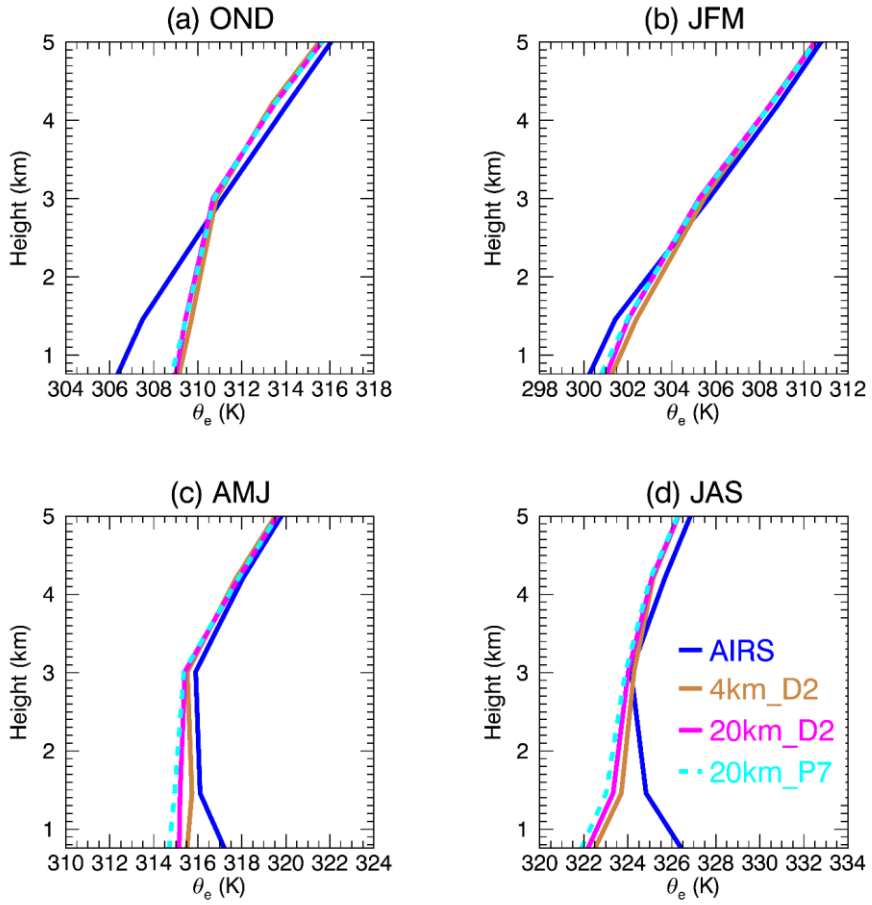

Figure 229. Vertical distribution of season mean equivalent potential temperature (θ_e; K) from AIRS and the WRF-Chem (4km_D2, 20 km_D2 and 204km_P7D2) simulation sover the red box region in Figure Fig. 1a in WY2013. The 4km run (not shown) is similar to the 4km_D2 run.

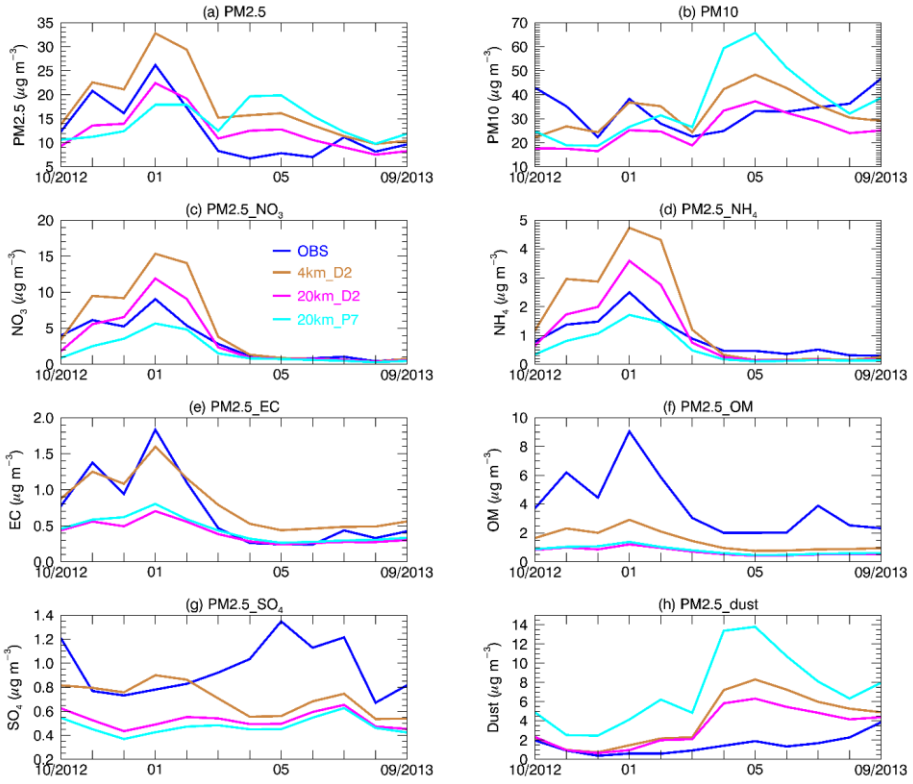

Figure 23. Aerosol mass (μg m^{-3}) for different species from OBS, the 4km_D2, 20km_D2 and 20km_P7 simulations at Fresno, CA. NH_4 observations are from EPA; other observations are from IMPROVE. $PM_{2.5}$_NO_3 represents NO_3 with diameter ≤ 2.5 μm. Similar definition for NH_4, EC, OM, SO_4 and dust in the figures.

Formatted: Subscript

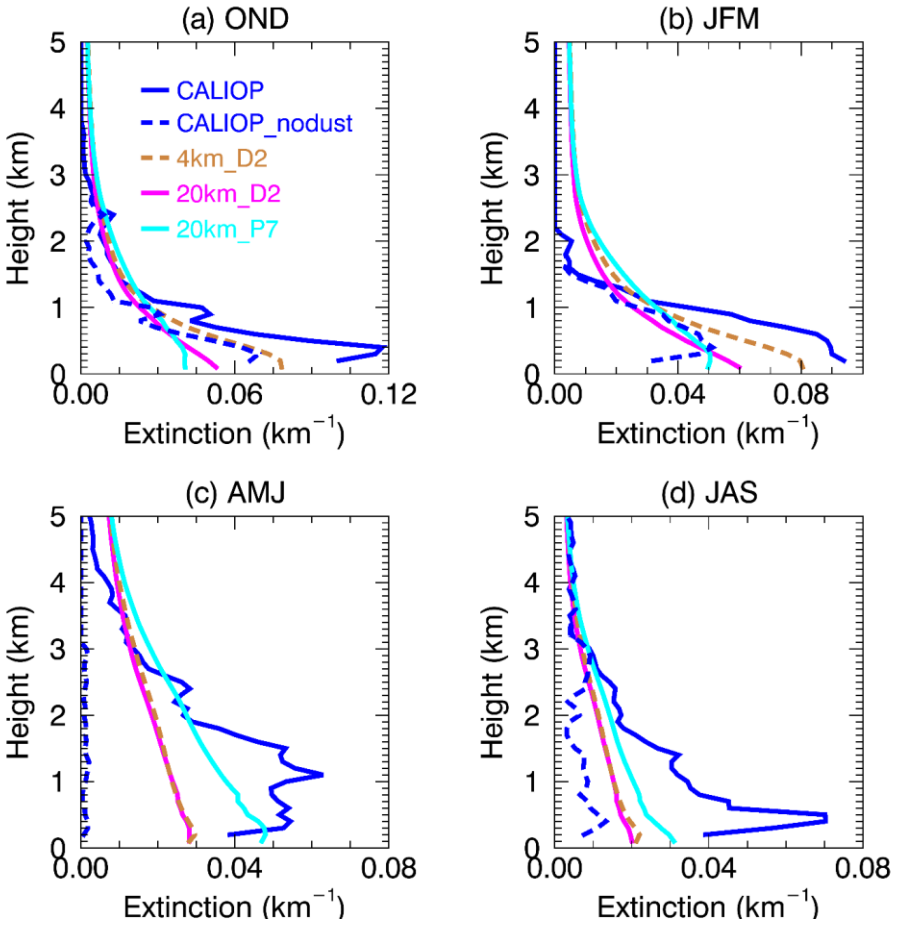

Figure 24. Vertical distribution of seasonal mean 532 nm aerosol extinction coefficient (km^{-1}) from CALIOP, CALIOP_nodust, and the WRF-Chem (4km_D2, 20km_D2 and 20km_P7) simulations over the red box region in Fig. 1a in WY2013.

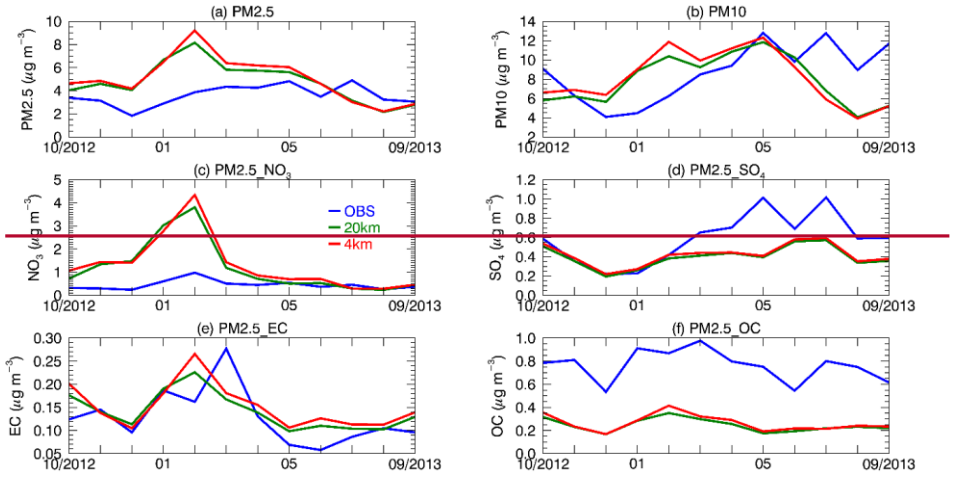
(a) PM2.5
(b) PM10
(c) PM2.5_NO3
(d) PM2.5_SO4
(e) PM2.5_EC
(f) PM2.5_OC
OBS
20km
4km
10/2012
01
05
09/2013

1897

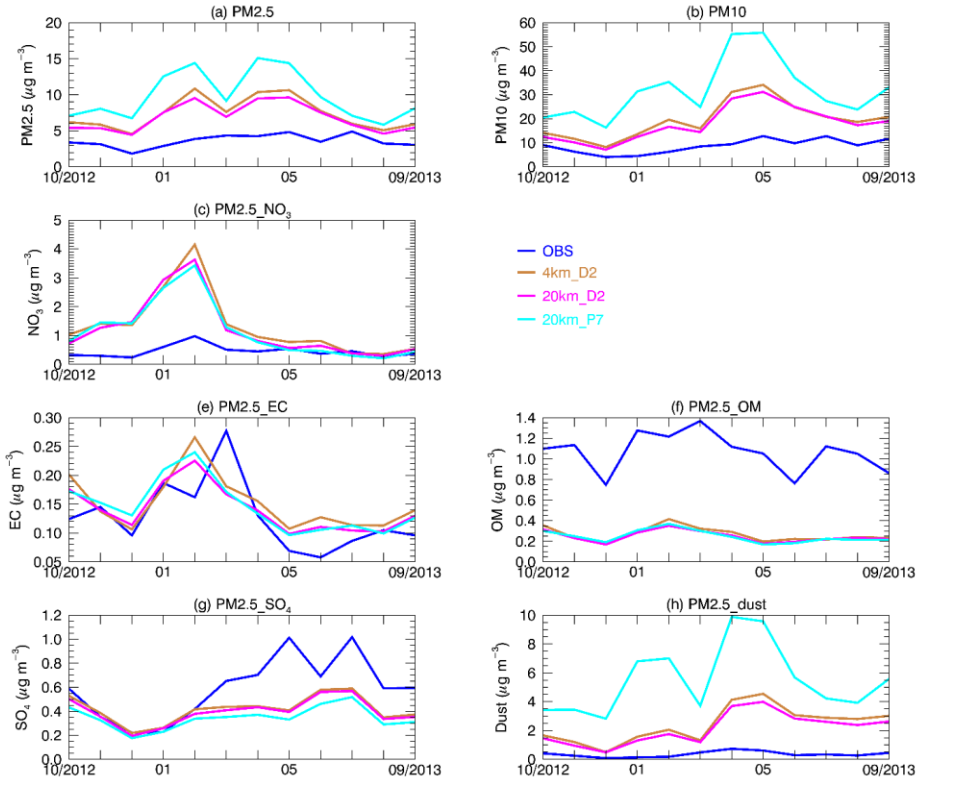
(a) PM2.5
(b) PM10
(c) PM2.5_NO3
(e) PM2.5_EC
(f) PM2.5_OM
(g) PM2.5_SO4
(h) PM2.5_dust
OBS
4km_D2
20km_D2
20km_P7
10/2012
01
05
09/2013

1898

1899 Figure 2510. Aerosol mass (μg m^{-3}) for different species from IMPROVE (OBS), the 420km_D2,
1900 20km_D2 and 204km_P7 simulations at Pinnacles, CA.

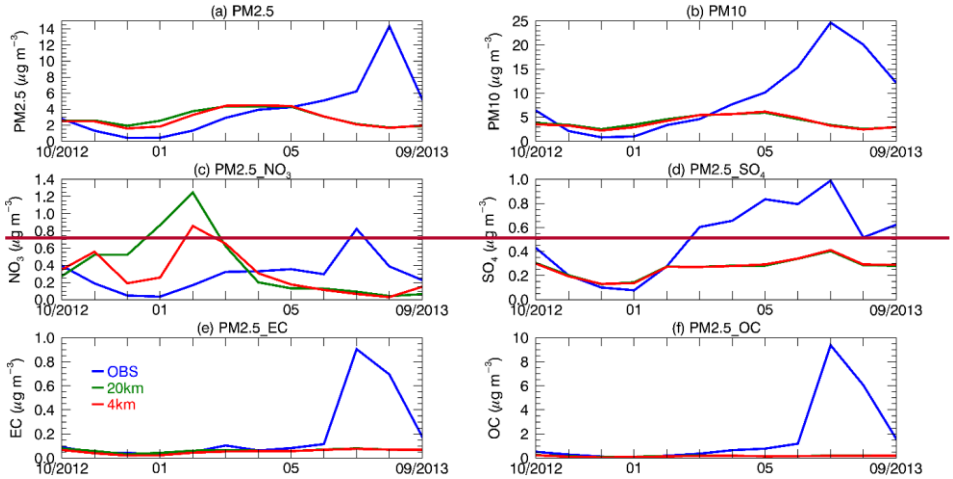
(a) PM2.5
(b) PM10
(c) PM2.5_NO3
(d) PM2.5_SO4
(e) PM2.5_EC
(f) PM2.5_OC
OBS
20km
4km
10/2012
01
05
09/2013

1901

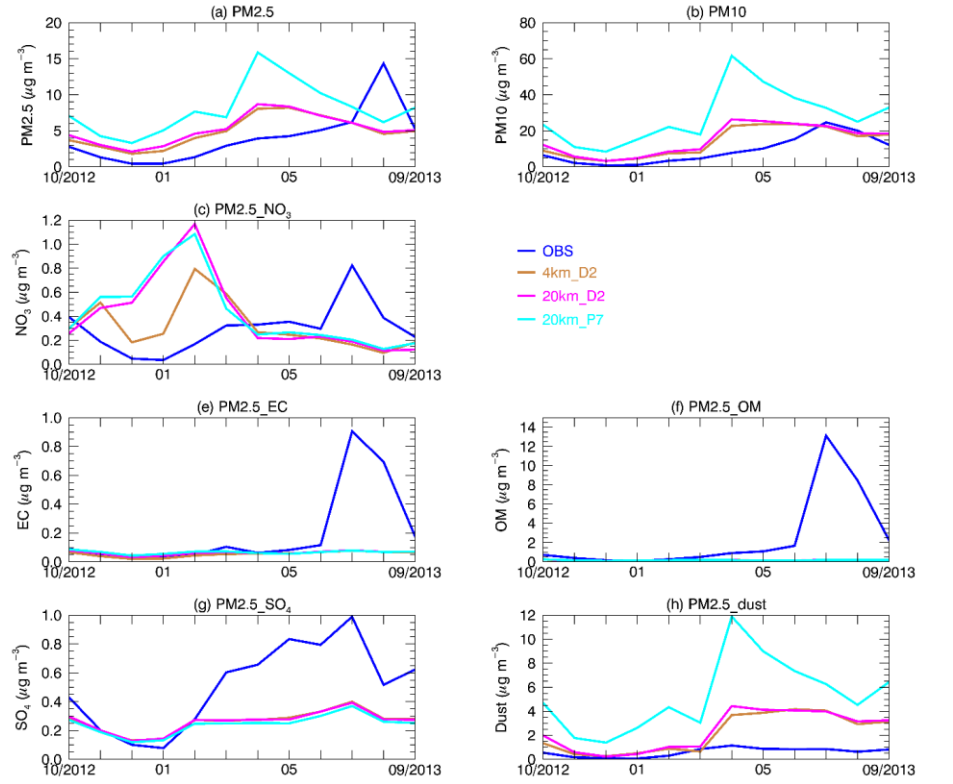
(a) PM2.5
(b) PM10
(c) PM2.5_NO3
(e) PM2.5_EC
(f) PM2.5_OM
(g) PM2.5_SO4
(h) PM2.5_dust
OBS
4km_D2
20km_D2
20km_P7
10/2012
01
05
09/2013

1902

Figure 26~~11~~. Aerosol mass (μg m^{-3}) for different species from IMPROVE (OBS), the ~~20km~~ 4km_D2, 20km_D2 and 20~~4~~km_P7 simulations at Kaiser, CA.

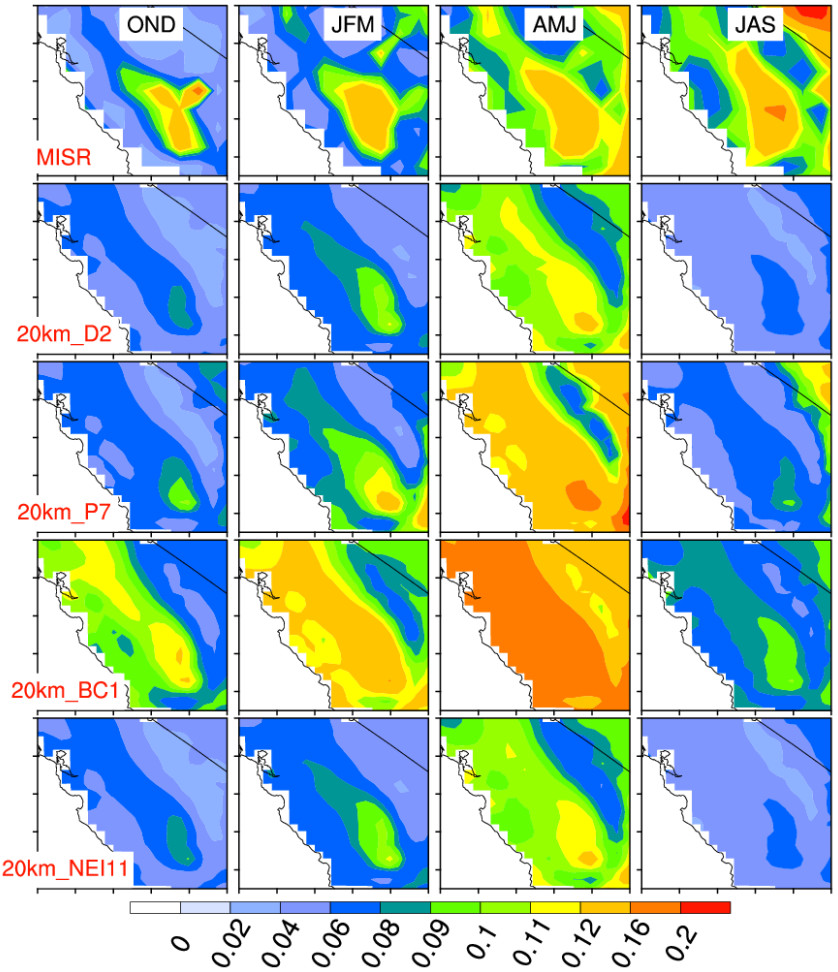

Supplementary Figure 1. Spatial distribution of seasonal mean 550 nm AOD from MISR and the WRF-Chem (20km_D2, 20km_P7, 20km_BC1 and 20km_NEI11) simulations in WY2013. OND: October-November-December; JFM: January-February-March; AMJ: April-May-June; JAS: July-August-September. The 20km_BC1 run is the same as the 20km_D2 run except that chemical boundary conditions use MOZART-4 original data. The 20km_NEI11 run is the same as the 20km_D2 run except with NEI11 anthropogenic emissions.

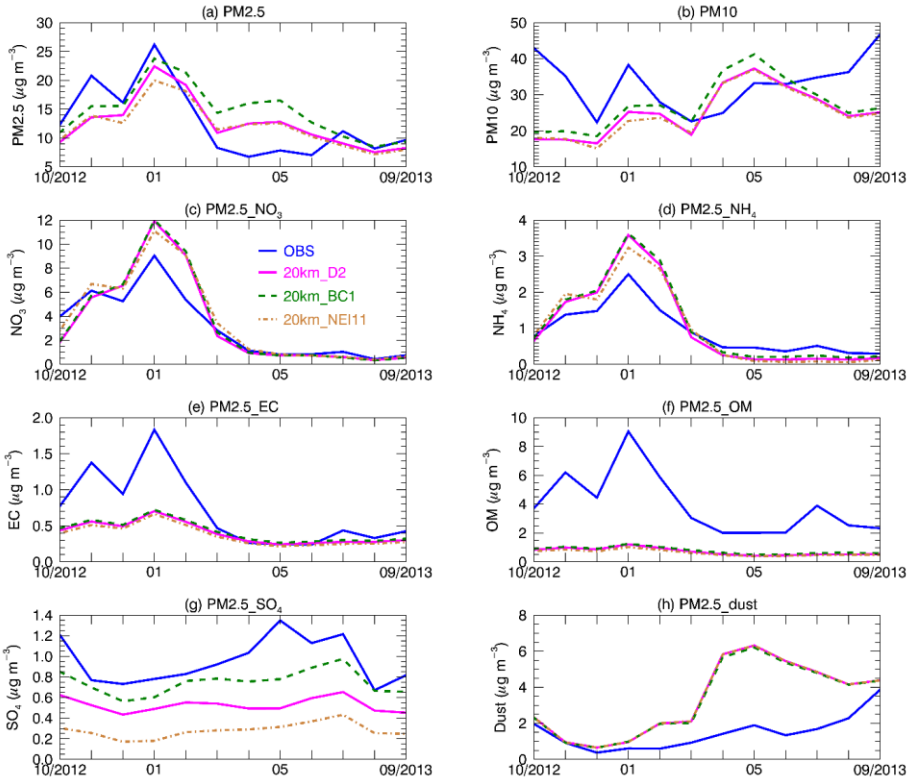

Supplementary Figure 2. Aerosol mass (μg m^{-3}) for different species from OBS, the 20km_D2, 20km_BC1 and 20km_NEI11 simulations at Fresno, CA. NH_4 observations are from EPA; other observations are from IMPROVE. $PM_{2.5}$ NO_3 represents NO_3 with diameter ≤ 2.5 μm. Similar definition for NH_4, EC, OM, SO_4 and dust in the figures.

Formatted: Subscript

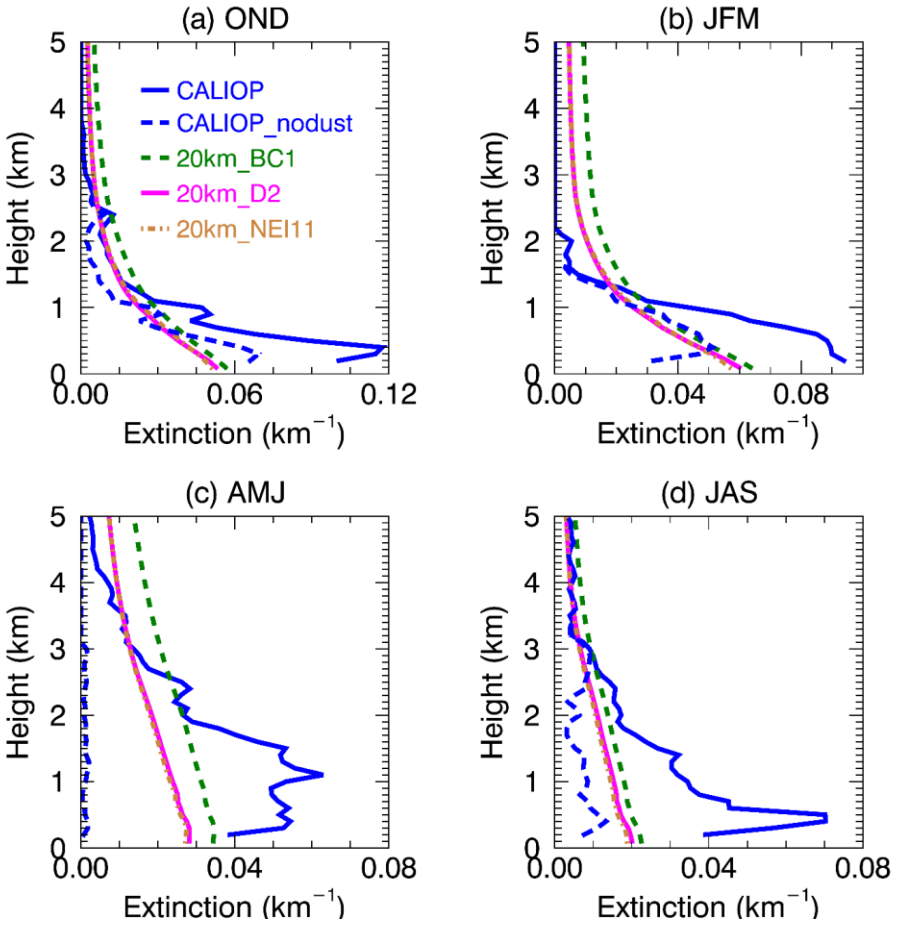

Supplementary Figure 3. Vertical distribution of seasonal mean 532 nm aerosol extinction coefficient (km^{-1}) from CALIOP, CALIOP_nodust, and the WRF-Chem (20km_D2, 20km_BC1 and 20km_NEI11) simulations over the red box region in Fig. 1a in WY2013.

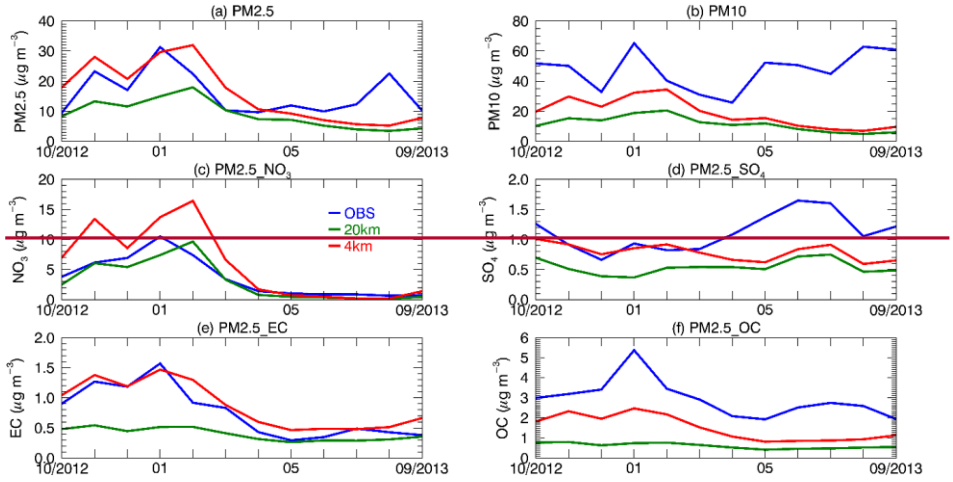
(a) PM2.5
(b) PM10
(c) PM2.5_NO3
(d) PM2.5_SO4
(e) PM2.5_EC
(f) PM2.5_OC
OBS
20km
4km
10/2012
01
05
09/2013

1921

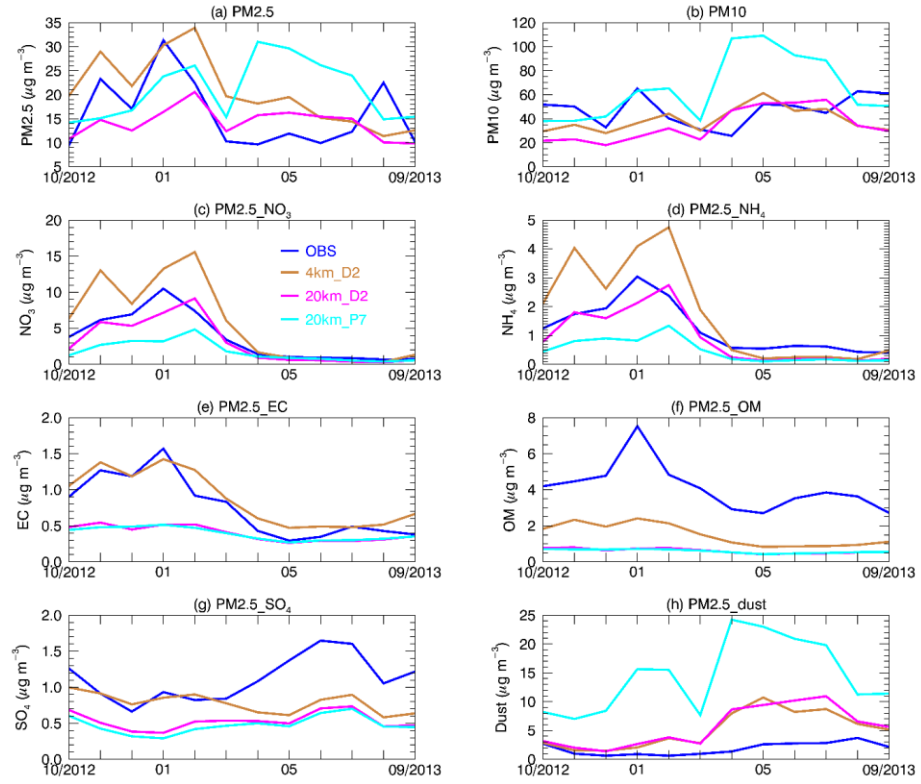
(a) PM2.5
(b) PM10
(c) PM2.5_NO3
(d) PM2.5_NH4
(e) PM2.5_EC
(f) PM2.5_OM
(g) PM2.5_SO4
(h) PM2.5_dust
OBS
4km_D2
20km_D2
20km_P7
10/2012
01
05
09/2013

1922

Supplementary Figure ~~1.~~4. Aerosol mass (μg m^{-3}) for different species from EPA CSN (OBS), the 4~~20~~km_D2, 20km_D2 and 20~~4~~km_P7 simulations at Bakersfield, CA. $PM_{2.5}$_NO_3 represents NO_3 with diameter ≤ 2.5 μm. Similar definition for SO_4, EC ~~and~~, OM~~C~~, NH_4 and dust in the figures.

Formatted: Subscript

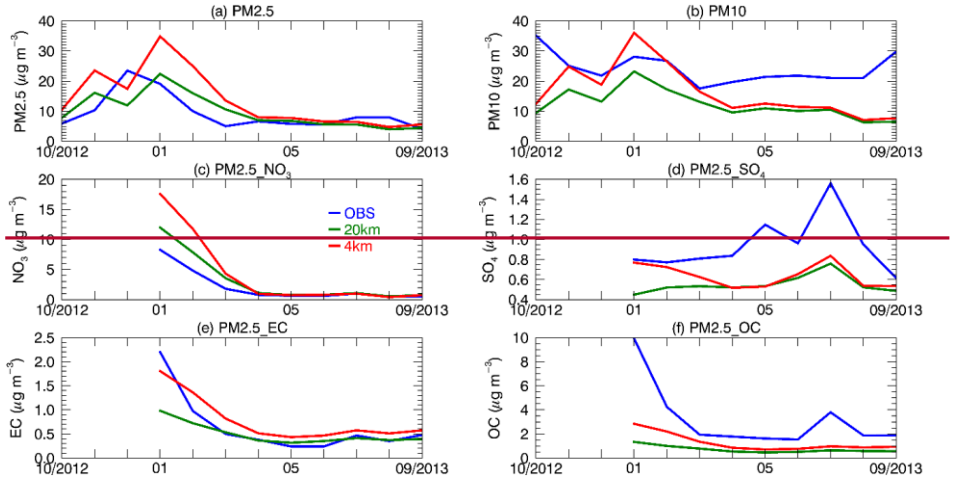
(a) PM2.5
(b) PM10
(c) PM2.5_NO3
(d) PM2.5_SO4
(e) PM2.5_EC
(f) PM2.5_OC
OBS
20km
4km
10/2012
01
05
09/2013

1926

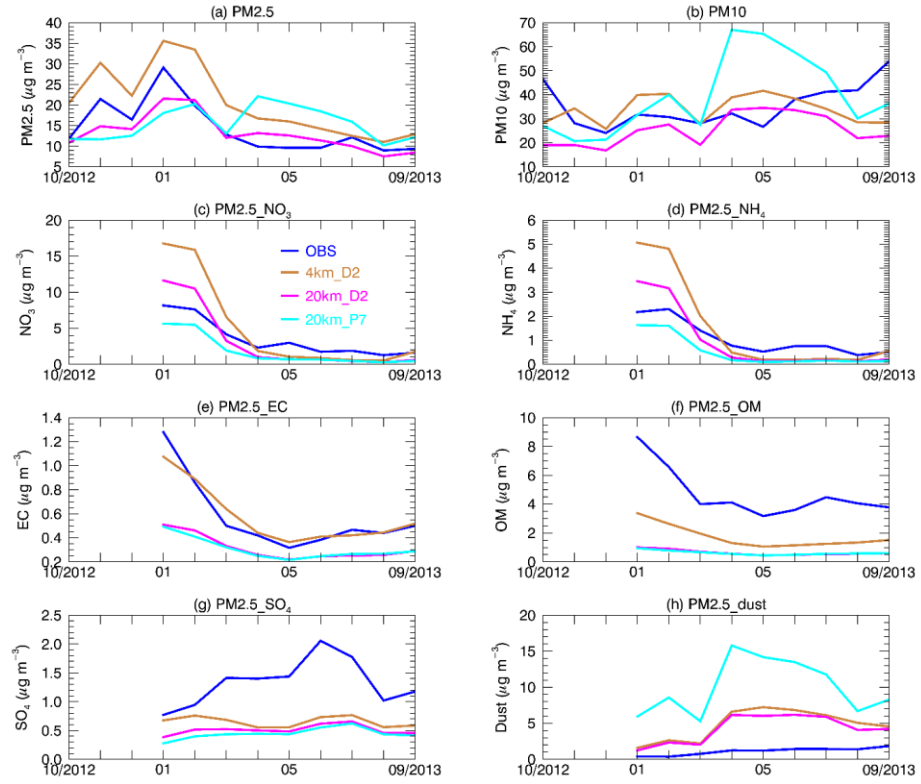
(a) PM2.5
(b) PM10
(c) PM2.5_NO3
(d) PM2.5_NH4
(e) PM2.5_EC
(f) PM2.5_OM
(g) PM2.5_SO4
(h) PM2.5_dust
OBS
4km_D2
20km_D2
20km_P7
10/2012
01
05
09/2013

1927

Supplementary Figure ~~2~~5. Aerosol mass (μg m^{-3}) for different species from EPA CSN (OBS), the ~~20km~~ 4km_D2, 20km_D2 and 20~~4~~km_P7 simulations at Modesto, CA.

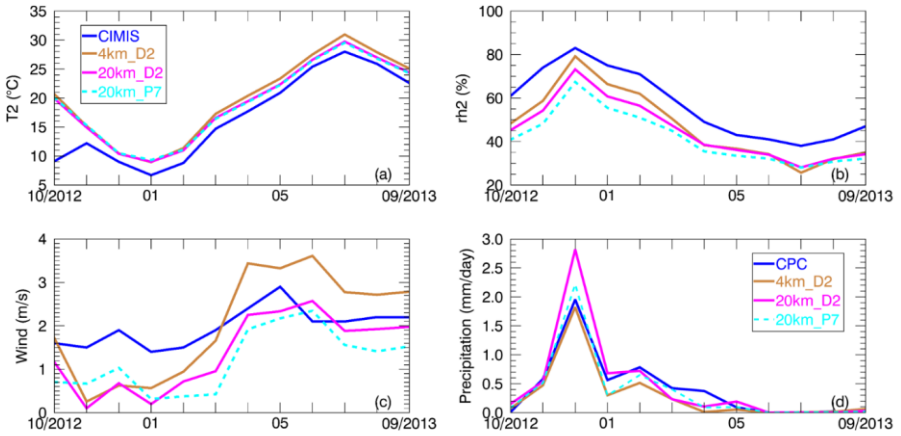

Supplementary Figure 6. Monthly mean of (a) 2-m temperature (℃); (b) 2-m relative humidity (%); (c) 10-m wind speed (m/s); (d) precipitation (mm/day) at Fresno, CA. The 20km (not shown) run is similar to the 20km_D2 run while the 4km (not shown) run is similar to the 4km_D2 run.

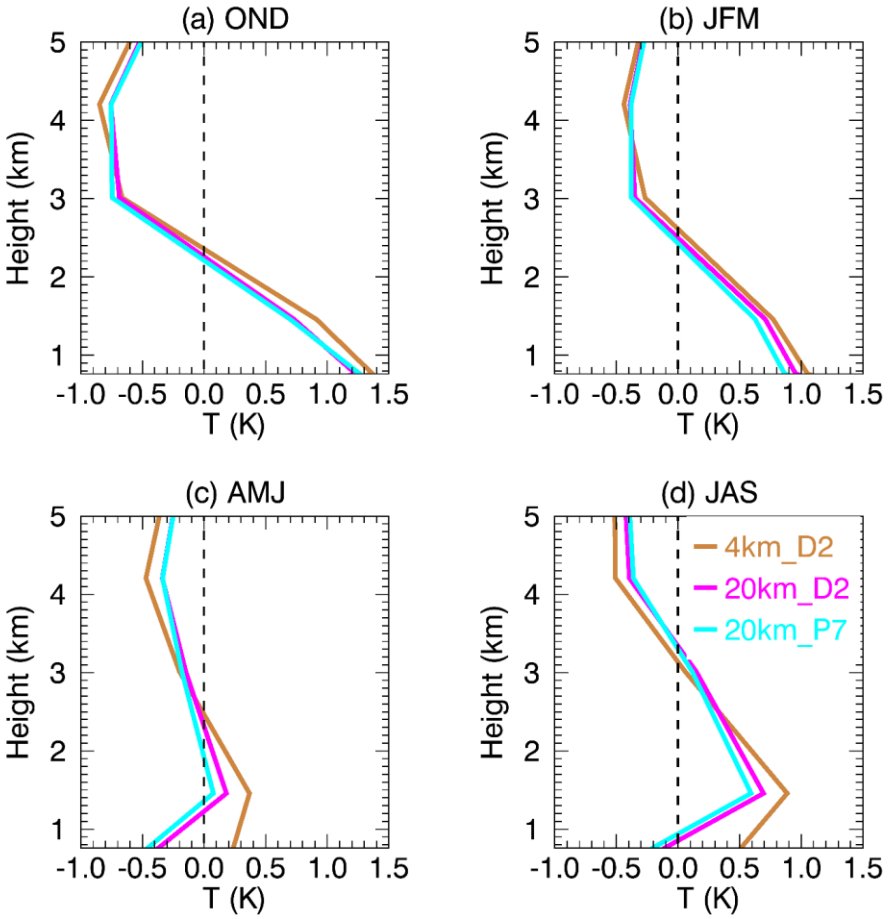

Supplementary Figure 7. Vertical profile of seasonal mean temperature (K) bias in the WRF-Chem simulations comparing to AIRS. The 20km run (not shown) is similar to the 20km_D2 run while the 4km run (not shown) is similar to the 4km_D2 run.

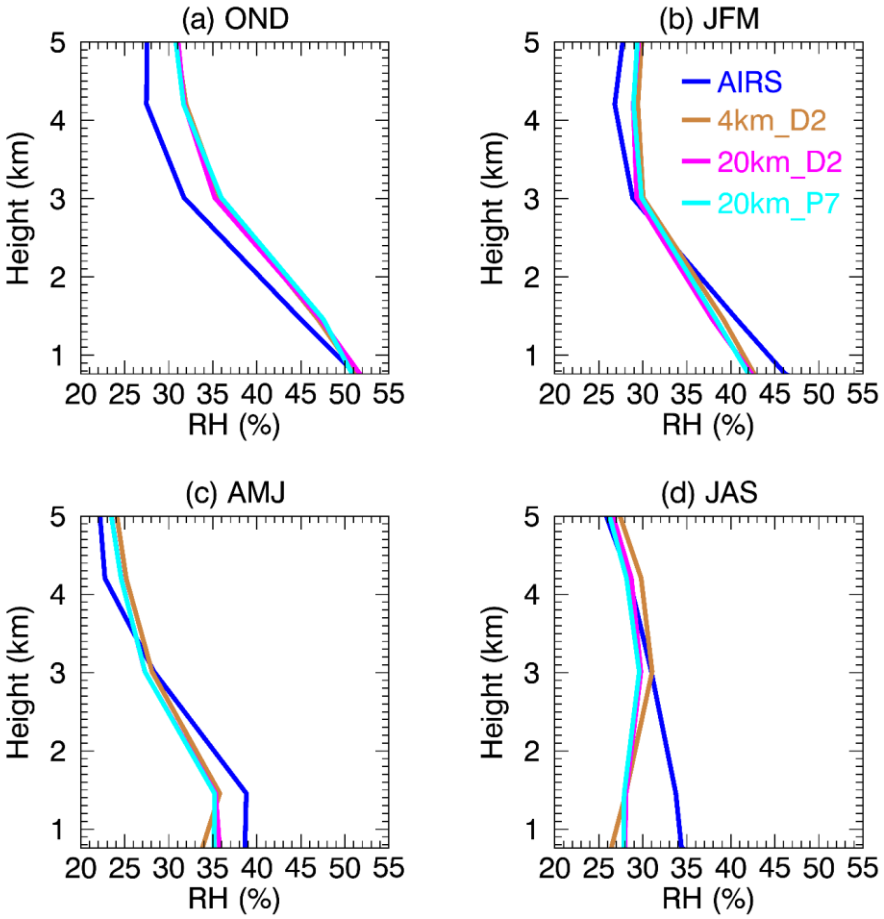

Supplementary Figure 8. Vertical profile of seasonal mean relative humidity (%) in the WRF-Chem simulations comparing to AIRS. The 20km run (not shown) is similar to the 20km_D2 run while the 4km run (not shown) is similar to the 4km_D2 run.